Oxidative Metabolism and Cytochrome P450 Enzyme Inhibition Potential of Creosote Bush and Flaxseed Lignans

A Thesis
Submitted to the College of Graduate Studies and Research
In Partial Fulfillment of the Requirements
for the Degree of Doctor of Philosophy
in the Toxicology Graduate Program
University of Saskatchewan
Saskatoon

By
Jennifer Lynn Billinsky

PERMISSION TO USE

In presenting this thesis in partial fulfillment of the requirements for a Postgraduate degree from the University of Saskatchewan, I agree that the Libraries of this University may make it freely available for inspection. I further agree that permission for copying of this thesis in any manner, in whole or in part, for scholarly purposes may be granted by the professor or professors who supervised my thesis work or, in their absence, by the Head of the Department or the Dean of the College in which my thesis work was done. It is also understood that any copying or publication or use of this thesis or parts thereof for financial gain shall not be allowed without my written permission. It is also understood that due recognition shall be given to me and to the University of Saskatchewan in any scholarly use which may be made of any material in my thesis. Requests for permission to copy or to make other use of material in this thesis in whole or part should be addressed to:

Chair of the Toxicology Graduate Program
Toxicology Centre
University of Saskatchewan
44 Campus Drive
Saskatoon, SK, Canada, S7N 5B3

ABSTRACT

The rising use of natural products creates an imperative need for an enhanced awareness of the safety of current and new products making their way into the marketplace. An important example is natural products containing lignans as the principal active component. Despite their structural similarity the lignan of creosote bush can cause hepato- and renal toxicity while the lignans of flaxseed have no reported serious toxicity. This dissertation aimed to investigate the oxidative metabolism of such lignans to determine whether reversible, competitive interactions and/or bioactivation may explain the differences in their apparent toxicity.

The first objective was to study the metabolism and bioactivation of nordihydroguaiaretic acid (creosote bush) and secoisolariciresinol (flaxseed). Nordihydroguaiaretic acid metabolism in rat liver microsomes led to the production of three glutathione adducts formed via ortho-quinone reactive intermediates. This metabolism was independent of NADPH and thus attributed to autoxidation. Secoisolariciresinol metabolism yielded lariciresinol and no glutathione adducts suggesting an absence of bioactivation to reactive quinone intermediates.

The second objective was to study the autoxidation of nordihydroguaiaretic acid. The major autoxidation product was a unique, stable schisandrin-like cyclolignan which was the result of nordihydroguaiaretic acid cyclization. The half-life of nordihydroguaiaretic acid in aqueous solution, pH 7.4, 37ºC is 3.14 hours suggesting the cyclolignan may be responsible for some of the biological effects of nordihydroguaiaretic acid.

The third objective was to study the inhibition of cytochrome P450 isoforms 1A2, 2B, 2C11 and 3A by lignans derived from creosote bush and flaxseed. None of the lignans caused irreversible inhibition. Both creosote bush and flaxseed lignans caused reversible inhibition of P450 enzyme activity that involved competitive or mixed-type inhibition, however the inhibition was present at nonphysiologically relevant concentrations. Activation of cytochrome P450 isoforms was also observed at low

lignan concentrations. The results suggest that P450-mediated bioactivation or reversible inhibition cannot explain the differences in toxicity noted between the lignans of creosote bush and flaxseed.

This work suggests a minimal risk for drug-lignan interactions at P450 enzymes. Further studies are warranted to determine the presence and biological and toxicological role of the nordihydroguaiaretic acid cyclolignan in herbal preparations.

ACKNOWLEDGEMENTS

To begin with, I want to thank my supervisor, Dr Ed Krol, for all of his help, guidance and compassion over the course of my graduate studies. Next I thank Dr Jane Alcorn, a committee member who went above and beyond and acted more as a co-supervisor to me. A big thank you also to my committee members, Dr Barry Blakley, Dr Brian Bandy and Dr David Janz who helped in guiding me in my graduate studies and to my external examiner, Dr Arno Siraki for finishing the process.

Thank you to Dorota Rogowski in the College of Pharmacy of Nutrition for training me in the use of the fluorescent plate reader in addition to a number of other pieces of equipment in the College. In the Department of Chemistry, many thanks to Keith Brown and Gabriele Schatte for NMR training and discussions on data interpretation and to Ken Thoms for running mass spectrometry samples.

A special thank you to my lab mates who worked with me over the years of graduate studies. Brian, Katie, Erin, Fawzy, Bing, Farah and Chris you were helpful and supportive to me in so many ways both scientifically and socially. Thank you to Erin for being my collaborator for a portion of our studies.

Huge thanks are indebted to my friends and to my family who offered unconditional, constant support to me through my entire journey. I love them for their faith and for believing in me more than I believed in myself.

TABLE OF CONTENTS

LIST OF TABLES

LIST OF FIGURES

LIST OF SCHEMES

LIST OF ABBREVIATIONS

ACN – Acetonitrile

ASECO - Anhydrosecoisolariciresinol

CYP – Cytochrome P450

DEX - Dexamethasone

DMPA – Dimethoxyphenylacetone

DMSO – Dimethylsulfoxide

ED – Enterodiol

EL – Enterolactone

FDA – Food and Drug Administration

FIM – Foundation for Innovation in Medicine

GSH - Glutathione

HPLC – High Performance Liquid Chromatography

IC_{50} – Inhibitor concentration causing 50% inhibition

IGF-1R – Insulin-like growth factor 1 receptor

LOQ – Limit of Quantitation

LOX - Lipoxygenase

MAT - Matairesinol

M-M – Michaelis-Menten (kinetics)

NADPH - Nicotinamide Adenine Dinucleotide Phosphate

NDGA – Nordihydroguaiaretic acid

NHP – Natural Health Product

NHPD – Natural Health Products Directorate

o-Q – *ortho*-Quinone

p-QM – *para*-Quinone Methide

QC – Quality Control

r^2 – Coefficient of Determination

RLM – Rat Liver Microsomes

SD – Sprague-Dawley (rats)

SDG – Secoisolariciresinol Diglucoside

SECO – Secoisolariciresinol

TFA – Trifluoroacetic Acid

v – Enzyme Velocity

1. LITERATURE REVIEW

Concerns are being raised by the general public about the extensive use of pharmaceuticals at the present time. The public scepticism of taking "chemicals" to treat their illnesses has led to an increased interest in the use of herbal preparations and natural products as an alternative to prescription medications as well as over the counter products. The substantial increase in the natural products available on the shelves of pharmacies, health food stores, grocery stores and via the internet has given consumers alternatives for self-treatment of ailments ranging from colds to joint pain to depression. The enhanced availability and use of such products follows from a public expectation of greater safety (with similar efficacy) associated with "medications" from "natural" sources.

Many natural products on the market today have their origins in ancient and traditional medicines which were used in countries all around the world. One example of a traditional medicine with origins in North America is the creosote bush which is native to the southwestern United States and Mexico. The creosote bush has been used traditionally by aboriginal peoples for centuries. Since benefits were found from using the creosote bush in traditional healing, an extract of the plant has now been formulated into a capsule which can be purchased under the name of Chaparral.

Traditional use of the creosote bush by aboriginal peoples for centuries suggests that the creosote bush is an effective natural medicine. While traditional creosote bush use appears to be quite safe, chronic use of Chaparral leads to toxicity. The striking differences in the safety profiles of the two forms of the natural product should serve as a warning to demonstrate that when used out of their proper context, natural products have the same potential for toxicity as pharmaceuticals.

The active ingredient in creosote bush which is believed to be responsible for both the efficacious and toxic properties is the lignan, nordihydroguaiaretic acid

(NDGA). Lignans are a class of compounds found in many plants such as creosote bush, flaxseed, sesame seeds, sunflower seeds, soy beans, garlic and dried fruits[1]. Flaxseed is the highest source of the lignan, secoisolariciresinol diglucoside (SDG). SDG and NDGA show close structural similarities, which is an important observation because we see no toxicity associated with flaxseed use.

Flaxseed use is increasing in popularity both as an added ingredient to breads and nutritional snacks as well as a natural product. Lignans are being extracted and concentrated from flaxseed and sold in capsule (Brevail™) or powder form (Beneflax). In addition to being associated with safety, flaxseed has demonstrated positive effects and is being considered as beneficial for cardiovascular and anti-cancer health.

In this delicate balance, the active lignan component of flaxseed can cause positive biological effects while on the other side the lignan from Chaparral causes negative biological effects. There are only slight variations in the chemical structures of flaxseed and chaparral lignans although they are enough to ultimately tip the balance from safety to toxicity.

My dissertation aims to investigate why the lignan in Chaparral is associated with toxicity while the lignans from flaxseed have limited reported toxicity. My research will specifically focus on attempting to explain the differences in the putative lignan toxicity by determining whether oxidative metabolism of the lignans can lead to bioactivation or cytochrome P450 (450) inhibition and if so, whether bioactivation is mediated through P450 enzyme processes. Furthermore, my research will investigate the possibility of toxicity arising from lignan-mediated inhibition of P450 metabolism either through mechanism-based or reversible inhibition mechanisms. Critically looking at how changes in lignan structure can affect metabolic fate will provide useful information for making predictions about the safety of natural products containing lignans as the principal bioactive components. Natural product wellness and therapeutic value will only be satisfactorily realized with more safety (and efficacy) data. In these terms, my dissertation research will help to fill a significant void in our knowledge of lignan safety.

My dissertation is set up as a paper based format containing three papers which make up chapters four to six of this thesis. Two of the papers have been previously published and the third has been submitted for publication.

1.1 Natural Health Products

The Natural Health Products Directorate (NHPD), a division of Health Canada, defines natural health products (NHP) as vitamins and minerals, herbal remedies, homeopathic medicines, traditional medicines such as traditional Chinese medicines, probiotics, and other products like amino acids and essential fatty acids[2]. Consumers are able to purchase NHP over the counter, without a prescription. The NHP should be both safe and efficacious with customers having the security to self-medicate to treat or prevent disease.

1.1.1 Functional Foods and Nutraceuticals

Health Canada identifies a functional food as being similar in appearance to, or may be a conventional food that is consumed as part of a usual diet, and is demonstrated to have physiological benefits and/or reduce the risk of chronic disease beyond basic nutritional functions, i.e. they contain bioactive compound[3]. An example of a functional food is carrots, which contain beta-carotene that acts as an antioxidant to neutralize free radicals, which can cause damage to cells[4]. Wheat bran is another functional food that can reduce the risk of breast or colorectal cancer due to the insoluble fibre present[5,6].

According to the Agriculture and Agri-Food Canada website, a nutraceutical is a product isolated or purified from foods that is generally sold in medicinal forms not usually associated with foods. A nutraceutical is demonstrated to have a physiological benefit or provide protection against chronic disease[3]. Examples of nutraceuticals are lycopene, from tomatoes, used to reduce the risk of prostate cancer[7] and lutein, from green vegetables used to reduce the risk of macular degeneration[8]. Nutraceuticals are considered to be NHP.

Dr. Stephen L. DeFelice, the founder of the Foundation for Innovation in Medicine (FIM), created the term nutraceutical in 1989 as a comprehensive term which includes foods, dietary supplements (as defined in Dietary Supplementation Health and

Education Act) and medical foods that have a health-medical benefit including the prevention and/or treatment of disease[9].

1.1.2 Regulation of Natural Health Products

Natural health products are regulated in Canada through the NHPD. Starting in January 2004 all NHPs had to comply with the regulations set out by the NHPD[10]. In January 2007, the NHPD published the new natural health products compliance guide to set a precedent for regulatory agencies and industry for ensuring the safety of NHP[10]. The compliance guide outlines a risk based approach followed by an action plan for all NHPs that are not authorized for sale in Canada.

Approval for licensing of a NHP requires that the product meet a series of guidelines, not unlike those set out for a pharmaceutical agent. An overview of these guidelines can be found at http://www.hc-sc.gc.ca/dhp-mps/prodnatur/legislation/docs/index-eng.php[11]. In brief these requirements include: product number, dosage form, recommended dose and route of administration, recommended use, duration of use and the quantity of medicinal ingredient of the natural product[12]. A Drug Identification Number (DIN) or a Natural Product Number (NPN) or DIN-HM, indicates that a NHP has been assessed for quality, safety and efficacy by Health Canada[13]. Other requirements such as adverse reaction reporting are also under the auspices of the NHPD.

1.1.3 Benefits versus Risks of Natural Products

One major area of concern for NHP use is the issue of potential benefits versus risks to health. NHP-drug interactions are possible and may be as common as drug-drug interactions. Since consumers can purchase NHP over the counter without having to speak directly to a pharmacist there is an increased risk of NHP-drug interactions. In addition a lapse in communication with physicians, whether they do not ask about concurrent herbal use or the patient does not relay herbals use to the physician, can potentially result in unfavourable consequences.

The potential benefits of St. John's Wort as an antidepressant for the treatment of mild to moderate depression have been documented[14] however safety issues exist related

to interactions with other drugs due to induction of cytochrome P450 (CYP3A4 and CYP2C9)[15] and P-glycoprotein by preparations with high hyperforin content[16]. In the case of concurrent warfarin use, the induction of CYP2C9 mediated through St. John's Wort can reduce anticoagulant effects by decreasing serum levels of warfarin[17] which would lead to an increased risk of blood clots[18]. However, some reports claim that since herbals such as St. John's Wort do not affect platelet function, that they do not pose a risk for increased risk of bleeding in post-surgical patients[19].

Drug interactions resulting from inhibition of CYP3A activity by bergamottins in grapefruit juice[20] and CYP3A4 and 2C9 inhibition by ginsenoside metabolites from ginseng preparations have also been observed[21]. There are mixed reports in the literature however, claiming that asian ginseng can interfere with blood clotting by inhibiting platelet activating factor[17], which conflict studies that report that ginseng does not appear to affect blood clotting[19].

The active ingredient of the increasingly popular herbal remedy COLD-fX® is an extract containing greater than 80% of polysaccarides from Panax quinquefolis, North American ginseng root[22]. The makers of COLD-fX® warn that those individuals who use warfarin should avoid concurrent use of their product as drug interactions will occur[22].

To make matters confusing for the public taking their product, the additional safety information relating to COLD-fX® states that "In clinical trials and from post-marketing surveillance, COLD-fX has been shown safe and well-tolerated. No known interactions have been found with medications, diseases, or other herbal products. However, as specific clinical trials have not been conducted to investigate these interaction potentials, it is advised that individuals with serious medical conditions or those taking medications consult a health care practitioner prior to use."[22]. The confusion arises when in one breath the manufacturer is telling the consumer that there are no known interactions yet that they should not be taking the product with warfarin medication.

Nonetheless it is important that the makers of COLD-fX® are recommending that consumers consult with their health care providers before use of the NHP. Appropriately labelled NHPs should serve as warnings to consumers that the product

can have the same potential for interactions as concurrent drug therapies might. It is also imperative that health care practitioners, albeit physicians, pharmacists or dentists[17] have complete and thorough background on their patients which would include information about concurrent herbal use.

1.2 Lignans from Creosote Bush and Flaxseed

Lignans are cinnamic acid derivatives that are synthesized from the amino acid phenylalanine via the phenylpropanoid pathway in plants[23]. Lignans are dimers of two C_6C_3 units linked through the β and β' carbons[23]. The basic skeleton structure of a lignan is shown in Figure 1.1. Various substituents can be added at both the aromatic and aliphatic regions of the molecule which will give the lignan different physical and chemical properties.

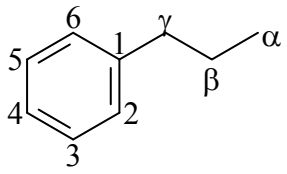

C_6C_3 Lignan subunit

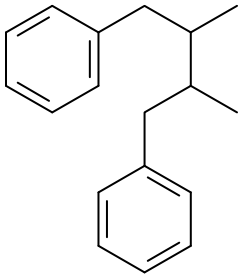

Lignan Skeleton

Figure 1.1: Structures of the basic lignan subunit and the general lignan skeleton.

1.2.1 Creosote Bush Background

Larrea tridentata, commonly known as the creosote bush or Chaparral, is a shrub native to the deserts of the southwestern United States and Northern Mexico. Creosote bush is an ancient shrub estimated to have originated in North America 8.4 to 4.2 million years ago[24]. The catechol lignan, nordihydroguaiaretic acid (NDGA), makes up about 3.8% dry weight of the creosote bush and is believed to be an active component[25]. As it is a polyphenolic catechol, NDGA has lipophilic characteristics (Figure 1.2). Nordihydroguaiaretic acid occurs as the *meso* form in the creosote bush and is a solid at room temperature (mp 185-186). NDGA is found in highest concentrations in the leaves (38.3 mg/g) and green stems (32.5 mg/g) with smaller concentrations found in the

flowers and stems (<5 mm)[25]. In addition to varying concentrations within the creosote bush, NDGA content may vary with respect to geographical location and season[26]. Being a secondary plant metabolite, it is likely that NDGA serves to protect the creosote bush from herbivorous predators[27]. The lambda-max for NDGA is 282 nm, which could infer protection against UV-radiation.

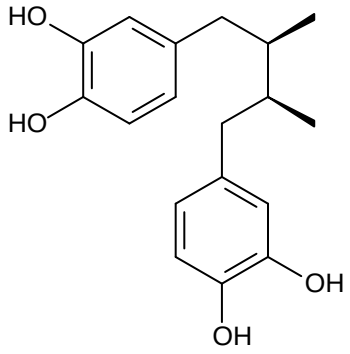

Figure 1.2: Structure of nordihydroguaiaretic acid

1.2.1.1 Historical uses of Creosote Bush

Due to its lengthy history, the creosote bush has been used by various peoples including Mexicans and Native American peoples, including the Pima Bajo, Seri and Tohono O'odham[28]. Traditional use of the creosote bush by Native Americans includes treatment of ailments such as arthritis, cancer, tuberculosis and rheumatism[29]. The Tohono O'odham make a tea from the leaves and stems of the creosote bush to drink after long spiritual walks to help ease aching muscles (author's personal communication with Terrol Dew Johnson). Creosote bush leaves and stems can also be boiled and then reduced down to an oil which is combined with Vaseline, to be used as an ointment for diaper rash or HIV lesions. Branches from the creosote bush are burned during rituals and funeral rites.

Due to its lipophilic structure and antioxidant properties as a result of its polyphenolic groups, NDGA was used as a food additive for fats and oils[30]. Studies performed in 1968 by the Canadian Food and Drug Directorate using a rat model for toxicity found that NDGA caused cystic nephrotoxicity, leading to the banning of NDGA as a food preservative[31].

1.2.1.2 Present uses of Creosote Bush

Nordihydroguaiaretic acid can be purchased in the form of an herbal tablet called Chaparral, which is prepared from the leaves of the creosote bush. Numerous examples document that the chronic use of Chaparral tablets has led to hepatotoxicity[32-35]. The Canadian Food Inspection Agency issued a warning in 2005 stating that Chaparral sold as food in bulk and in any size package under any brand should not be consumed due to risk of liver and kidney problems[36]. Chaparral is not currently available in Canada; however tablets can be purchased over the internet from various sources in the USA (author's personal observations).

There are many online websites that tout the use of Chaparral. One site which sells Chaparral claims "The plant is known to act against free radicals and thus may be effective in preventing degenerative disease associated with aging. This plant is of particular interest to us in cleansing the lymph system, an important part of rejuvenation. It is anti-inflammatory and non-toxic. Chaparral is a strong antioxidant, pain-killer and antiseptic."[37]. The fact that the authors claim that Chaparral is non-toxic is contrary to scientific findings and could potentially be detrimental to unsuspecting or unquestioning consumers. Other websites claim that Chaparral can be used to detoxify the body from industrial chemicals, has blood purifying properties and that it is anti-bacterial and anti-fungal[38].

Some online sources do suggest using caution when taking Chaparral although the caution is to varying degrees. An example is seen with Rose Mountain Herbs, where they warn that at one point Chaparral was banned by the American Herbal Products Association due to issues relating to hepatitis. Therefore they advise that consumers should watch out for detrimental symptoms[39]. Yet another site advises potential users of Chaparral that there have been negative liver effects seen with use; however, that the studies were perhaps flawed and that the blame was irresponsibly placed on Chaparral and not the other medications that were being concurrently taken[40]. The aforementioned website was written with an air of self-righteousness but does, perhaps unintentionally, allude to the fact that there is the potential for herb-drug interactions.

Arteaga *et al*[27] recently reviewed the literature and found many traditional medicinal uses of the creosote bush. Some examples, from a list of over 30 uses,

included treatment of acne, psoriasis, allergic problems, anemia, bronchitis, burns, cramping, menstrual pains, kidney pain and cystitis, sterility ulcer and weight loss. Despite these various pharmacological claims adequate *in vivo* results are lacking.

The pharmacological properties of NDGA with respect to benefits related to cancer chemoprevention, cancer therapy, antimicrobial, fertility and hypoglycaemic effects, both *in vitro* studies and *in vivo* animal studies and human clinical trials, have been reviewed by Lambert *et al*[41].

Today NDGA and methylated analogues of NDGA are being studied for potential use as anti-viral agents against human immunodeficiency virus[42], herpes simplex virus[43], and growth inhibition of various tumours[44-46]. Methylated analogues of NDGA are being investigated to reduce the toxicity that has been associated with NDGA.

An NDGA formulation called Actinex® (Chemex Pharmaceuticals, Denver, CO), developed for the topical treatment of actinic keratoses, was approved by the FDA. However Actinex® was withdrawn from the market once it was established that it caused skin hypersensitivity[47]. The skin hypersensitivity of NDGA and possible antimicrobial properties have resulted in the topical use of NDGA in the treatment of warts[48]. NDGA has also been proposed for the treatment of corns, calluses and warts (US Patent 5702694). In addition, NDGA can be found in commercially available formulations for the treatment of acne and muscle aches, such as the LaKOTA™ joint care system, which lists Chaparral among the ingredients.

1.2.2 Flaxseed Background

Linum usitatissimum, commonly known as flaxseed, is an ancient crop first cultivated in 3000 BC and now grown worldwide. Flaxseed is an important crop with 40% of the world's total production grown in Canada and 85% of Canada's total crop grown in Saskatchewan[49]. The flax plant has small blue flowers that eventually fall off the plant and yield a small pod containing small, flat, oval brown flaxseeds[49]. According to the Flax Council of Canada, flaxseed's many uses include human and animal consumption, processing into Linseed oil to be used for wood protection and as a strengthener for concrete and the production of Linoleum[50]. Flaxseed contains 41% fat,

28% dietary fiber, and 21% protein by weight and is a rich source of the essential omega-3 fatty acid, alpha-linolenic acid[49]. Flaxseed is a functional food which can be consumed in its whole form, ground or as an oil.

1.2.2.1 Flaxseed Lignans

Flaxseed contains a number of lignans which are similar in structure to NDGA. Like NDGA, the lignans in flaxseed may serve to protect the plant against herbivores[51]. The principle flaxseed lignan is secoisolariciresinol diglucoside (SDG), which is present as a 3-hydroxy-3-methylglutaryl (HMG) – SDG polymer in the plant[52]. Detectable levels of matairesinol (MAT), the oxidized lactone analogue of SECO, can be also be found in flaxseed[53]. MAT may also be formed via oxidation of SECO *in vivo* as will be discussed in section 1.2.2.2. A known by-product of isolation of SECO from flaxseed-derived SDG is the hydrolysis product anhydrosecoisolariciresinol (ASECO), which will be further discussed in section 1.2.2.2.2.

1.2.2.2 Metabolism of Flaxseed Lignans

The metabolism of flaxseed lignans is summarized in Figure 1.3 below. The two glucose moieties of SDG can be cleaved by β-glucosidase and β-glucuronidase enzymes in the intestinal microflora to form the aglycone SECO[54]. Secoisolariciresinol can then be converted to MAT, lariciresinol and the mammalian lignans, enterodiol (ED) and enterolactone (EL)[55,56]. Secoisolariciresinol conversion to MAT takes place in the large intestine and is the result of closure of the aliphatic hydroxyl groups to a lactone ring[56,57]. Intestinal microflora also directly convert SECO to the mammalian lignans, ED and EL[56]. Enterodiol may be oxidized to EL by the microflora in an analogous manner to how SECO is converted to MAT[57]. Alternatively, EL may be produced from MAT[55].

In addition to intestinal metabolism, SECO and MAT are also oxidized in the liver by cytochrome P450 (P450) enzymes, however P450 metabolism is only a minor pathway for lignan elimination[58]. SECO is converted to lariciresinol, isolariciresinol, two hydroxylated aliphatic metabolites and three aromatic hydroxylated metabolites in rat liver microsomes (RLM)[58]. It should be noted however that the formation of

isolariciresinol may be due to acidic concentration of lariciresinol and may therefore be an analytical artefact. Matairesinol was converted by RLM to a number of hydroxylated metabolites, both aliphatic and aromatic, in addition to demethylated metabolites[58].

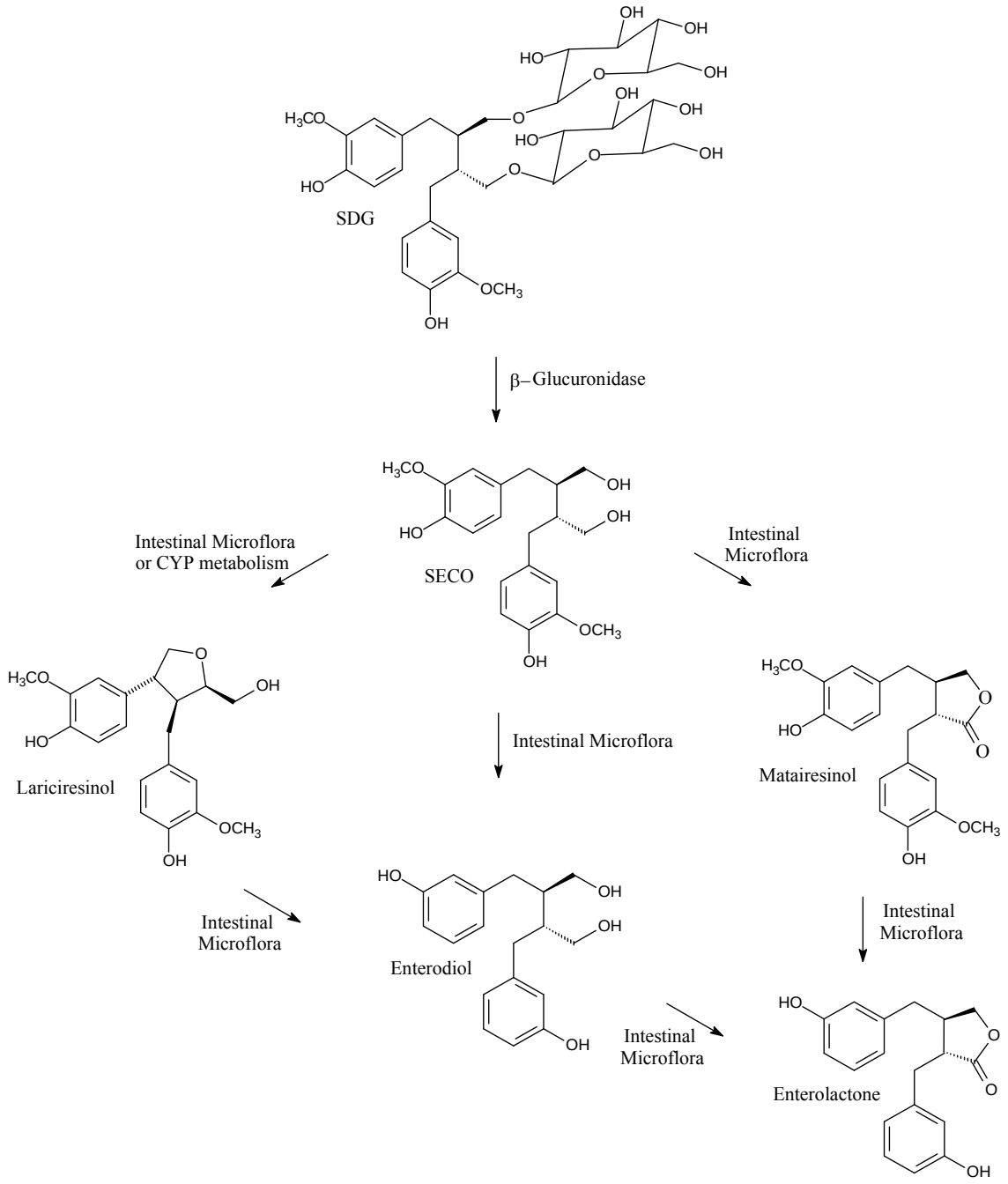

Figure 1.3: Flaxseed lignan metabolism of secoisolariciresinol diglucoside (SDG) to secoisolariciresinol (SECO), matairesinol, lariciresinol and the mammalian lignans enterodiol and enterolactone

1.2.2.2.1 Secoisolariciresinol

Secoisolariciresinol is of importance to investigate as it is the major lignan found in flaxseed as part of the diglucoside complex SDG[59]. The form of SECO found in the plant is (R, R)[53] and it is a yellow solid at room temp (mp 114ºC)[60]. The lambda max for SECO is 280 nm, which is very similar to that of NDGA (282 nm). While NDGA is a catechol, SECO varies slightly in that it is a phenolic compound. The presence of the aliphatic hydroxyl groups on SECO make it more water soluble than NDGA.

1.2.2.2.2 Anhydrosecoisolariciresinol

Anhydrosecoisolariciresinol shown in Figure 1.4, is also referred to in the literature as Shonanin[61]. Several reports state that ASECO can be found in flaxseed[61,62], although the actual presence of ASECO in the plant is disputed as the process to hydrolyze flaxseed for analysis also converts SECO to ASECO[61]. Acid hydrolysis of SECO will result in the loss of a water molecule and the cyclization of the aliphatic moieties to form a tetrahydrofuran ring. It should be noted that the furan ring of ASECO is distinct from the more hydrophilic lactone ring of MAT.

Although it is still unclear as to whether or not ASECO is actually found in flaxseed, we have chosen to investigate it for the purposes of this dissertation. Firstly, we believe that it is possible that oral ingestion of SECO could lead to the formation of ASECO in the acidic stomach environment. Secondly, the structure of ASECO is intermediate to that of SECO and NDGA. ASECO is similar to SECO in the aromatic regions but is missing the aliphatic hydroxyl groups, whereas the chain portion of ASECO is more similar to NDGA.

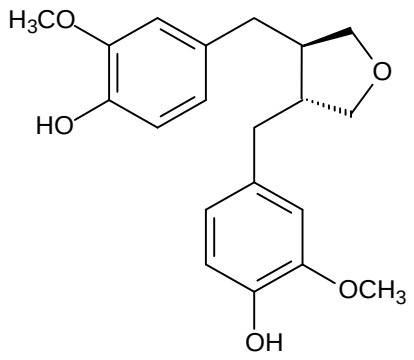

Figure 1.4: Structure of anhydrosecoisolariciresinol

1.2.2.2.3 Mammalian Lignans Enterodiol and Enterolactone

The mammalian lignans enterodiol (ED) and enterolactone (EL) are products of the microbial metabolism of plant lignans and have been observed in human plasma and urine[63]. Enterodiol and EL are derived from numerous lignans including SECO[55], sesamin[64], matairesinol, 7-hydroxymatairesinol, pinoresinol, isolariciresinol, and lariciresinol [65]. Numerous epidemiological studies have investigated the relationship between ED/EL and disease states. Serum EL levels were inversely correlated to acute coronary events[28] and breast cancer risk[66,67], and plasma EL levels were inversely related to F(2) isoprostane levels, a marker of *in vivo* lipid peroxidation[68]. However studies on prostate cancer risk[69] and a subsequent study on serum EL and breast cancer risk[70] have shown no relationship. Studies performed *in vitro* have demonstrated that ED and EL inhibit the growth of four estrogen-independent colon-tumour cell lines [71] and three human prostate cancer cell lines[72], inhibit aromatase activity[73]and increase growth of MCF-7 and T47D human breast cancer cell lines[74]. Enterodiol and EL have also been determined to be antioxidants *in vitro*[75-77].

Enterodiol and EL undergo hepatic metabolism to glucuronide conjugates in rhesus monkeys[78] and by cytochrome P450 to a mixture of hydroxylated metabolites in hepatic microsomes from rat, pig and human [79]; these metabolites have been found in urine from humans[80], rats[81] and rhesus monkeys[78]. Jacobs and Metzler[79] studied ED and EL metabolism in human, pig and rat liver microsomes and determined that both enterolignans undergo hydroxylation at various aliphatic and aromatic positions in mammalian microsomes, however they found that in uninduced microsomes, aliphatic hydroxylation predominated over aromatic. Further investigations of enterolignan metabolites in human urine samples yielded aromatic hydroxylation products but not aliphatic hydroxylation metabolites[80].

1.2.2.3 Present uses of Flaxseed

Flaxseed and the defatted flaxseed polymer are under study for the treatment of a number of disease states including hypercholesterolemia, diabetes and benign prostatic hyperplasia. Flaxseed has been shown to decrease cholesterol in animal models including rats[82] and rabbits[83] and flaxseed reduced LDL and total cholesterol in post-

menopausal women [84,85]. Studies on chronic flaxseed consumption in healthy humans however found no change in cholesterol [86]. Defatted flaxseed polymer decreased cholesterol in rabbits[87] and humans[88]. Flaxseed improved glucose tolerance in humans[89] and flaxseed lignan complex improved glycemic control in type 2 diabetes patients[90]. Decreased prostate-specific antigen levels and proliferation rates were seen in benign prostatic hyperplasia patients treated with flaxseed[91]. Flaxseed was also shown to increase gamma-glutamyltranspeptidase in rats suggesting a potential hepatoprotective effect[92-94].

Fairly new to the market is the flaxseed product, Brevail®, which is being advertised for its benefits for breast health[95]. Brevail® is composed of defatted flaxseed which provides up to a 35% increase in lignan content as opposed to consuming flaxseed alone. The Brevail® website educates the general public by explaining that their product contains lignans which are natural plant compounds which would be a part of a vegetarian or plant based diet and claims that a vegetarian diet would provide small amounts of lignan to the body whereas Brevail® is a concentrated form of lignan and if taken on a regular basis it would provide an exact dose of lignan, much like a pharmaceutical product[95]. Brevail® describes the lignan in their product (SDG) as having a chemical structure which is very similar to estrogen and thus it can competitively block excess estrogen for binding to the estrogen-binding receptor, allowing the body to eliminate the excess estrogen, thus improving breast health. The website claims "excessive or "bad" forms of estrogen that are left unchecked may have adverse effects in the body" [95].

1.3 Lignan Toxicology

1.3.1 Nordihydroguaiaretic Acid Toxicity

Although NDGA is now considered toxic, it was once utilized for its antioxidant properties[30,96,97] as a food preservative in oil based products beginning as early as 1948[30]. Studies confirming that NDGA caused nephrotoxicity in rats resulted in the removal of NDGA from the registry of compounds which have generally recognised as safe status[31,98]. Feeding rats a diet of 0.5% or 1.0% NDGA resulted in cystic reticuloendotheliosis of the paracaecal lymph nodes and vacuolation of kidney

epithelium[31]. *ortho*-quinone (o-Q) intermediates of NDGA were found in kidney extracts and in the lower one third of the ileum and caecum in rats fed a diet of 2% NDGA[31], suggesting that an o-Q intermediate may be the cause of toxicity.

The antioxidant properties of NDGA have demonstrated benefit *in vivo* in rat alveolar macrophages at a concentration of less than 10 μM[99]. There appears to be a fine balance though as concentrations of NDGA from 20 to 100 μM caused prooxidant effects in clone-9 rat hepatocyte cultures[100].

The LD_{50} of NDGA in rats is 75 mg/kg and dosing causes a time and dose-dependant increase in levels of serum alanine transferase, a marker for liver damage[101]. A potential mechanism suggested for liver damage was P450 inhibition.

In rat epidermal and hepatic microsomes NDGA caused a concentration dependant inhibition of CYP1A2 and P450 enzymes affected by aryl hydrocarbon hydroxylase activities[102]. The inhibition by NDGA manifested itself as type I binding difference spectrum[102]. Type I binding difference spectrum refers to the interaction of the inhibitor with the heme portion of the P450 enzyme and results in a shift in iron(III) spin equilibrium from a low-spin to a high-spin which can have an effect on the redox state which thus affects the rate and extent of substrate turnover[103]. This type of inhibition differs from a Type II binding spectrum which infers that the inhibitor binds to the heme portion of the P450 indicating an irreversible type of enzyme inhibition[103]. It is believed that the hydroxyl groups are important for the inhibition of P450[102] as when the catechol was converted to an *ortho*-methoxy derivative, the inhibition ceased[104]. NDGA has also demonstrated an ability to induce astroglial death by glutathione depletion[105] which may be due to metabolism to reactive intermediates by P450.

There are numerous case reports of Chaparral induced hepatotoxicity in humans[32,33,35,106,107] which are believed to be due to NDGA as it comprises the majority of the dry weight of the creosote bush[29]. The symptoms of NDGA toxicity ranged from nausea and anorexia[32] to hepatomegaly and jaundice[107] and hepatotoxicity was confirmed by liver biopsies. Biopsies were consistent with injury caused by necrosis and periportal inflammation and bile duct proliferation[33,35,107]. Symptoms began on average 3 months after beginning Chaparral treatment and subsided with cessation of

Chaparral use[35,106]. If Chaparral use was reinitiated, the symptoms of hepatotoxicity returned.

1.3.1.1 Apoptosis and Lipoxygenase Inhibition

The toxic properties of NDGA are being utilized as a potential therapy for cancer treatment. There are currently a variety of mechanisms reported as the means by which NDGA can induce apoptosis. The mechanism of apoptosis is being studied by a number of groups in murine pro-B lymphocytes and has still not yet been fully elucidated, although it is believed to be triggered by a combination of factors such as glutathione depletion[108,109], mitochondrial depolarization and oxidative processes[109].

In contrast to the above studies, NDGA has demonstrated anti-apoptotic activity in murine fibroblasts[110]. Nordihydroguaiaretic acid blocked apoptosis by inhibiting tumour necrosis factor induced apoptosis by blocking caspase cleavage, mitochondrial inactivation, externalization of phosphatidylserine, ^{51}Cr-release in addition to preventing intracellular calcium levels from increasing to allow phosphorylation of cytosolic phospholipase A_2.

Insulin-like growth factor 1 receptor (IGF-1R) is another target for apoptosis for which NDGA has demonstrated positive effects[111-113]. NDGA inhibited the phosphorylation and activation of IGF-1R in breast cancer cells by inhibiting tyrosine kinase activity[111].

As NDGA has shown promise in a potential treatment for cancers, analogues of NDGA are also being examined. While investigating NDGA inhibitory potency against IGF-1R kinase and an alternative target, 15-lipoxygenase (LOX), Blecha *et al*[113] determined that altering the structure of NDGA had a greater effect on the inhibition of LOX. A cyclic form of NDGA resulted in similar inhibition of IGF-1R kinase as NDGA however the inhibition of LOX was 10-fold weaker, a promising result as LOX may play a role in suppressing tumours in breast cancer.

Lipoxygenase enzymes are part of the arachidonic acid pathway which results in hydroxyeicosatetraenoic acids and leukotriene production. Products of the lipoxygenase pathway have been associated with regulating apoptosis[41,114]. Leukotrienes are connected with inflammation and its associated conditions such as pain and asthma.

Nordihydroguaiaretic acid is a known lipoxygenase inhibitor and has been used as a control compound in studies involving lipoxygenase inhibition[115,116]. Part of NDGA's ability to induce apoptosis is believed to be due to its ability to inhibit lipoxygenase[115,117]. The lipoxygenase inhibiting properties have also been attributed to NDGA being an inhibitor of ovulation in rats[118].

1.3.1.2 Activation of Nordihydroguaiaretic Acid

There are reports in the literature of NDGA undergoing activation in the presence of molecular oxygen. Prevention of the oxidation of NDGA during extraction from plant sources is a major concern[119]. Nordihydroguaiaretic acid can be activated in two distinct manners, one of which is activation to a quinone species[31,120], which will be subsequently discussed in Section 1.3.3.

The second method of NDGA activation is one which has been less studied. Wagner *et al* (1980) reported that an activated form of NDGA could interact with DNA[121]. The authors noted that two hours after NDGA was dissolved in buffer, the λ_{max} shifted from 280nm to 285nm to produce what was termed an "activated" NDGA which could bind with the major or minor grooves of DNA[121]. If NDGA was left to sit in buffer alone, after 72 hours the clear solution changed colour to a red brown colour which absorbed at 460nm. Interestingly Grice *et al* found that rats fed a diet enriched with NDGA had a red brown coloured material in lymph node cysts[31], suggesting that perhaps they too had observed the formation of an "activated" NDGA. It should be noted that the structure of the "activated" NDGA had not been identified by either researchers.

1.3.2 Flaxseed Toxicity

Flaxseed is a relatively safe natural product. The small toxicity that is associated with flaxseed is due to the fibre content rather than the lignan content. Fibre intake in excess of 60 to 70 g per day can cause dehydration and intestinal discomfort or gas[122]. The fibre of flaxseed contains cyanogenic glycosides which can release cyanide upon autolysis, however the levels of cyanide produced are below the limits which would be

toxic to humans[123] and incorporation of flaxseed up to 28% in baked products have shown no harmful effects[123,124].

Kulling, *et al*[125] studied SECO, MAT, ED and EL and concluded that all four lignans are devoid of genotoxicity after investigating their anueploidogenic, clastogenic and mutagenic potential. No information is available on the genotoxic potential of the oxidative metabolites of the mammalian lignans[125].

Because of the estrogenic effects associated with flaxseed, gestational feeding studies have been performed to examine the effect of flaxseed in rats[126,127]. Hemmings *et al*[126] found that a 10% flax chow had no long-term effect on growth, development and behaviour. Long term feeding studies on the rats showed that gamma-glutamyltranspeptidase levels were increased in the livers after puberty with males showing a greater increase, 4-fold, in levels compared to females, 1.38-fold. The authors state that the increase in the gamma-glutamyltranspeptidase levels however were not out of the ordinary when compared to changes that can occur in adult rats[126]. Collins *et al* used higher levels of flaxseed in their studies, flaxseed added at 20 or 40% and also defatted flaxseed meal 13 or 26% of the total diet[127]. Fetal development was not affected by the incorporation of flaxseed into the dam diet. Whole flaxseed had no effect however defatted flaxseed delayed puberty in F1 males. No differences in the age or weight at the time of onset of puberty was observed in female pups; however, both flaxseed diets caused irregular oestrus cycles in F1 females. The levels of flaxseed studies were quite high though, levels which would not be consumed in humans.

1.3.3 Formation of Quinone Species

Quinones are reactive, electrophilic oxidants which are coloured compounds[128] and contain extended pi-conjugated systems. Based on their structure, the lignans NDGA and SECO may undergo oxidation to one or two types of chemically reactive quinone species, either an *ortho*-quinone (o-Q) or a *para*-quinone methide (p-QM). Documented evidence already exists of NDGA o-Q formation[31,120]. Figure 1.5 shows the basic skeleton structures of the o-Q and the p-QM. The two types of quinones will be presently discussed in sections 1.3.3.1 and 1.3.3.2.

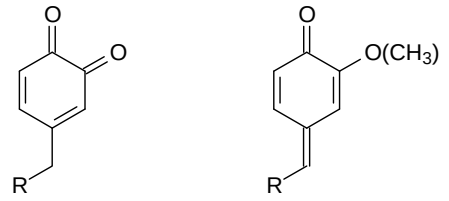

ortho-quinone *para*-quinone methide

Figure 1.5: Structures of *ortho*-quinone and *para*-quinone methide skeletons.

Catechols such as NDGA can be oxidized to either an *ortho*-quinone or a *para*-quinone methide[129]. The presence of the methoxy groups on SECO's aromatic rings prevents the formation of an *ortho*-quinone but will allow the formation of a *para*-quinone methide. Figure 1.6 depicts how NDGA and SECO could be oxidized to quinones.

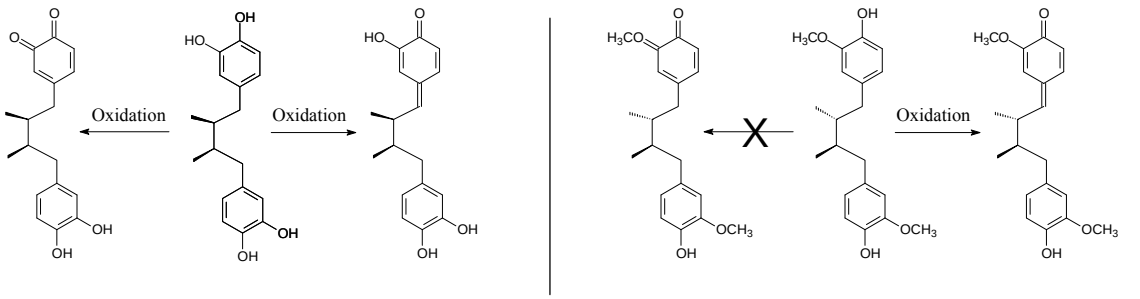

ortho-quinone NDGA *para*-quinone methide *ortho*-quinone SECO *para*-quinone methide

Figure 1.6: Oxidation of Nordihydroguaiaretic acid (NDGA) and Secoisolariciresinol (SECO) to quinones.

Given their inherent reactivity, quinones cannot be stably isolated from biological systems. Nucleophilic trapping agents, such as glutathione (GSH) are required to trap the quinone as a stable adduct[130]. Addition of GSH to o-Q molecules results in GSH addition on the aromatic ring whereas addition to p-QM results in addition at the benzylic position[130].

1.3.3.1 Ortho-Quinones and Reactive Oxygen Species

Ortho-quinones are formed *in vivo* by oxidative processes such as P450 enzyme systems and form by the abstraction of a proton and electron to first form a semi-quinone radical which can then be further oxidized to the quinone[131]. The damage caused by o-Q is due to oxidative stress created by the redox cycling process (Figure 1.7) in which oxygen (O_2) can react with the semi-quinone radical to form superoxide

(O_2^-) and the o-Q, which can then be reduced back to the semi-quinone radical by reductases[84,85]. Superoxide may cause damage on its own or lead to the formation of hydrogen peroxide, singlet oxygen and the hydroxyl radical[128].

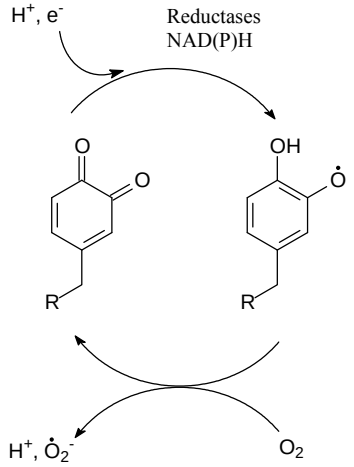

Figure 1.7: Redox cycling of ortho-quinones.

ortho-quinones are intermediate in toxicity between *meta*- and *para*-quinones[128,132]. Moridani *et al* determined that in rat hepatocytes, 3-hydroxyanisole was more toxic than 2-hydroxyanisole which was more toxic than 4-hydroxyanisole, which corresponded to *meta*-, *ortho*-, and *para*-quinones (p-Q), respectively[132]. The reason that o-Q are more toxic than p-Q is that they are more polarized due to a lack of symmetry in their structure[128]. The increased polarization makes the carbon atom of the carbonyl group more electron deficient and thus more likely to seek out cellular nucleophiles[128]. Quinone methides (QM) however are even more polarized than o-Q and p-Q which makes them much more chemically reactive. Isomerization of o-Q to p-QM can add complexity to the damage which can be caused by quinones.

1.3.3.2 Para-Quinone Methides and Adduct Formation

A requirement for the ability of o-Q to isomerize to p-QM is that there must be at least one benzylic proton available for abstraction[131] (Figure 1.8). Bolton *et al* determined that 4-allyl-*o*-quinones can spontaneously rearrange to p-QM[129]. The conclusions were drawn based on microsomal experiments where o-Q was formed only in the presence of GSH during the oxidation of safrole. If GSH was added 10 minutes after the initial incubation period, then a mixture of o-Q and p-QM was formed. The

rate of isomerization of o-Q to p-QM is enhanced when there is extended π-conjugation at the *para* or 4-position of the catechol molecule[130] and when the acidity of the benzylic proton is increased[133].

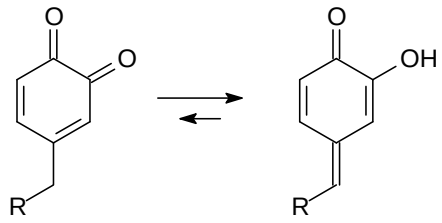

ortho-quinone *para*-quinone methide

Figure 1.8: Isomerization of ortho-quinone to para-quinone methide.

Quinone methides differ from o-Q in that one of the carbonyl oxygen molecules is replaced by a methylene group[131], thus catechols like NDGA can be converted to either an o-Q or a p-QM however phenols like SECO can only be converted to p-QM (see Figure 1.6). The p-QM are more electrophilic at the benzylic carbon and more reactive than the o-Q which makes them more likely to undergo adduction to cellular nucleophilic macromolecules such as DNA and proteins[134-136]. Quinone methides, like o-Q may also be formed via P450 oxidation[137]. Figure 1.9 depicts the position at which nucleophiles would form adducts with the electrophilic p-QM.

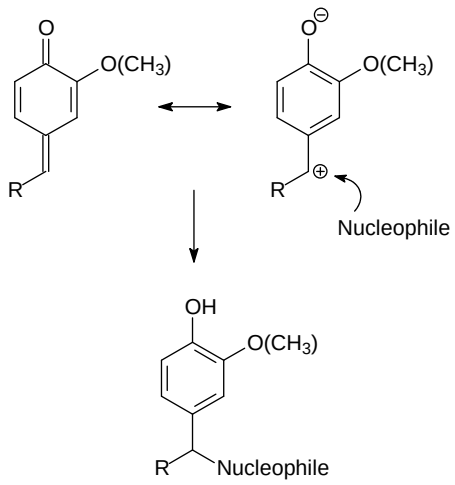

Figure 1.9: Nucleophilic addition to para-quinone methides.

1.4 Xenobiotic Metabolism and Cytochrome P450 Enzymes

The cytochrome P450 enzymes are a family of Phase I enzymes responsible for the metabolism of the majority of xenobiotics, including drugs, toxicants, natural

products and environmental contaminants, encountered by the body. Cytochrome P450 enzymes are heme centred and known as monooxygenase or mixed-function oxidase enzymes. Although the majority of P450 reactions take place within the liver, P450 enzymes are also located throughout the body in the small intestine, kidney, skin, lungs and brain.

In humans, CYP1A2, CYP2C9/19 and CYP3A4/5 comprise 13%, 19% and 34% or the isoforms present in liver, respectively[138]. The majority of clinically relevant drugs are metabolized by CYP2C and CYP3A and CYP2C9/19, and CYP2D6 account for the most frequent metabolically-relevant polymorphisms[138]. The majority of the bioactivation reactions observed are due to metabolic activation by CYP1A[138].

Phase I P450 enzymes function to increase the water solubility of xenobiotics by hydroxylation, dealkylation, and double bond oxidation, in order to enhance excretion however in the process sometimes compounds can become bioactivated[138]. Bioactivation results in the production of an electron deficient molecule which can react with electron rich cellular macromolecules, such as proteins, and result in enzyme inhibition and/or organ toxicity[139-141].

1.4.1 Cytochrome P450 Inhibition

Interactions of xenobiotics with P450 can be a mechanism of toxicity and may result in inhibition of P450 enzymes by either reversible or irreversible mechanisms[142,143].

Irreversible, mechanism-based inhibition occurs when a xenobiotic goes through the catalytic cycle of the P450 and is bioactivated to a reactive intermediate which covalently binds with the heme or apoprotein portion of the enzyme resulting in cessation of further P450 activity[144,145]. Irreversible inhibitors are identified in microsomal incubations by a decrease in substrate formation in a time and concentration-dependant manner. Mechanism-based inhibition can also result in covalent binding of the newly bioactivated, electron deficient molecule to electron rich proteins or nucleic acids which can lead to either inactivation or hapten formation which can illicit an immune response[144,146]. If the bioactivated compound binds to P450 the

only way to restore function is *de novo* synthesis of enzyme. Reversible inhibition on the other hand does not result in destruction or loss of P450 function.

1.4.1.1 Mechanisms of Reversible Enzyme Inhibition

Reversible inhibition is generally categorized into three types: Competitive, Non-competitive, and Uncompetitive[147]. Competitive inhibition is characterized by an inhibitor which binds to the same active site[145] as the substrate for the enzyme resulting in an increase in the K_M of the enzyme while the V_{Max} remains consistant[148]. Uncompetitive inhibition occurs when an inhibitor binds to an allosteric site of the enzyme-substrate complex which results in a decrease in both K_M and V_{Max} of the enzyme[148]. Non-competitive inhibition is the result of allosteric binding to either the enzyme or the enzyme-substrate complex which results in a decrease in V_{Max} of the enzyme while K_M is unchanged [148]. Mixed type inhibition can also occur and is similar to non-competitive binding however it is believed that the inhibitor binds to the enzyme and the enzyme-substrate complex with differing affinities[147].

1.4.1.2 Inhibition of Cytochrome P450 by Natural Products

The literature cites many examples of natural compounds that can inhibit P450 by irreversible mechanisms. A classic example is the inhibition of intestinal CYP3A by bergamottin, a furanocoumarin found in grapefruit juice[149]. Bergamottin causes irreversible inhibition by binding to the CYP3A4 apoprotein and can also inhibit CYP1A2, 2A6, 2C9, 2C19, 2D6 and 2E1 [149]. Another non heme-mediated inhibition of CYP3A4 is observed with glabridin, an isoflavan isolated from licorice root[44]. Mechanism-based inhibition also occurs by methylenedioxyphenyl-containing lignans which are present in the spice *Piper cubeba*[150].

In the case of capsaicin metabolism by CYP2E1, peroxy radicals are generated which react directly with the CYP enzyme in addition to tissue macromolecules[151]. Interestingly the inactivation of P450 seems to be semi-protective in this instance, as toxic capsaicin metabolite formation is thus prevented by the loss in enzyme activity.

Damage may also occur when inhibition is the result of reversible mechanisms and bioactivation does not necessarily lead to irreversible inhibition. The dietary

supplement kava is known to cause hepatotoxicity in humans[152]. Analysis of an extract of kava in human hepatic microsomes identified the formation of several quinoid metabolites which were not reactive with the nucleophile GSH[152]. Interactions between natural products causing P450 inhibition and concurrent pharmaceutical drug treatment is also of concern and is becoming increasingly common[18,153,154]. Thus it is imperative that natural products are investigated for their potential to undergo bioactivation so as to minimize toxicities and interactions[155].

1.5 Structure Activity Relationships

Few studies have investigated the relationship between lignan structure and activity. Akiyama *et al* examined various analogues of MAT and a compound the authors called Lio[156]. Lio is similar in structure to MAT, except that it contains a furan ring in the aliphatic portion of the molecule whereas MAT contains a lactone ring. It appears that the compound that Akiyama *et al*[156] are calling Lio is actually ASECO. The authors found that while stereochemistry did seem to play an important role in antimicrobial activity of the various lignans, there was no direct relationship which could be established[156]. The main finding was that a higher oxidation degree at the two benzylic positions resulted in higher antimicrobial capacity of the lignans. The most antimicrobial action was seen when there were two carbonyl groups at the benzylic position.

Eugenol and eugenol-related compounds have been studied for associated toxicity towards human submandibular gland carcinoma[157]. Although eugenol is not a lignan, it resembles the structure of one half of a lignan molecule and contains a phenol ring with an *ortho*-methoxy substituent which makes it resemble SECO. The compounds analyzed were all ones which could be converted to QM. The results of the investigations suggest logP and redox potential as having the greatest correlation to toxicity for quantitative structure activity relationships[157]. Toxicity was associated with the production of phenoxy radicals, however the homolytic bond dissociation energy (of the phenol oxygen and hydrogen) could not be used to accurately predict the toxicity of all of the molecules studied. The bond dissociation energy could be predicted for mono-phenols but not dimer-phenols.

Lastly, Moridani *et al* looked at a number of catechols, including NDGA, to determine quantitative structure activity relationships for toxicity in freshly isolated rat hepatocytes[158]. The authors found that lipophilicity and pKa were important determinants in associating toxicity with structure. An increased lipophilicity and lower degree of ionization and higher pKa (which would essentially dictate the degree of ionization in a physiological system) were associated with increased toxicity to hepatocytes. LogP alone was also examined as a possible determinant however it appeared to be a less predictable measure of cytotoxicity.

The few available studies on lignan structure-activity relationships justifies further investigations in the area. The literature clearly shows that toxicity is associated with catechols and phenols through convertsion to o-Q and p-QM, respectively. However, little evidence exists in the literature for toxicity associated with flaxseed phenolic lignans. Our efforts will be focused on reversible P450 enzyme inhibition and bioactivation with possible subsequent P450 inhibition (as a result of bioactivation) as potential determinants of lignan toxicity.

1.6 Perspectives

I knew that the creosote bush lignan NDGA caused toxicity however the structurally similar flaxseed lignan SECO had limited toxicity. I was interested in studying this dichotomy of different lignan safety profiles. In order to gain clearer insight into the division between lignan safety and toxicity I studied the oxidative metabolism of various lignans to determine whether or not bioactivation may be the key factor in the differences in lignan safety profiles. Investigating the potential of lignans to inhibit P450 enzymes as a result of bioactivation or reversible mechanisms was also of importance in determining whether lignans in creosote bush or flaxseed would have the potential to interact with concurrently used medications. Given that natural product use is on the rise, my studies should provide valuable information about lignan safety.

2. PURPOSE OF PROJECT

2.1 Rationale

There is a growing popularity and availability of herbal products on the market today, with an increased need for regulation and rigorous chemical testing performed on these products. To add to the issue, the public has been given the impression that because herbals are natural, they must be safe. An example of adverse effects from herbals is illustrated in the hepatotoxicity that is associated with the intake of the lignan nordihydroguaiaretic acid (NDGA), a compound found in the creosote bush and in the herbal remedy, Chaparral. The lignan secoisolariciresinol (SECO), found in flaxseed, is not hepatotoxic despite being structurally similar to NDGA. Studying the oxidative metabolism of NDGA and SECO will help to provide insight into how lignan structure and functional groups may influence natural product safety. In addition, studying the ability of the lignans NDGA, SECO, secoisolariciresinol diglucoside (SDG), anhydosecoisolariciresinol (ASECO), enterodiol (ED), enterolactone (EL) and a nordihydroguaiaretic acid dibenzocyclooctadiene to inhibit the cytochrome P450 1A2, 2B, 2C11, and 3A enzymes will provide insight into whether toxicity is mediated through bioactivation resulting in mechanism-based or reversible inhibition mechanisms. The aims of this project will be accomplished by the following objectives:

2.2 Objectives

2.2.1 Objective 1

Study the oxidative metabolism and bioactivation of NDGA and SECO.

2.2.1.1 Specific Aims for Objective 1

- Develop a high performance liquid chromatography (HPLC) method to separate and purify metabolites.

- Perform rat hepatic microsomal incubation experiments using NDGA and GSH, and SECO and GSH.
- Identify products in microsomal incubations using nuclear magnetic resonance and mass spectroscopy.

2.2.2 Objective 2

Study the autoxidation of NDGA.

2.2.2.1 Specific Aims for Objective 2

- Develop an isocratic HPLC method to allow quantification of an NDGA autoxidation product.
- Perform oxidation studies on NDGA at various pH levels.

2.2.3 Objective 3

Study the inhibition of CYP isoforms 1A2, 2B, 2C11 and 3A by lignans.

2.2.3.1 Specific Aims for Objective 3

- Develop an HPLC method to separate and quantify metabolites of testosterone metabolism.
- Develop a fluorescence plate reader method to quantify resorufin methyl ether metabolism.
- Determine the type and extent of CYP inhibition.

2.3 Hypotheses

1. NDGA and SECO can be oxidized to quinones in rat microsomal systems.
2. Lignans inhibit rat hepatic cytochrome P450 enzymes.

3. Oxidative Metabolism of NDGA and SECO

The first objective was to study the oxidative metabolism and bioactivation of NDGA and SECO. Given that NDGA has toxicity reported with its use and SECO is comparatively safe I postulated that the toxicity associated with NDGA was linked to bioactivation. The catechol structure of NDGA could give rise to an *ortho*-quinone (o-Q) or a *para*-quinone methide (p-QM) intermediate formed *in vivo* which could potentially be the cause of hepatotoxicity[129]. With one hydroxy substituent per phenol ring, SECO has the potential to undergo conversion to a *para*-quinone methide.

To accomplish the first objective, NDGA and SECO were incubated in rat liver microsomes (RLM) in the presence and absence of the nucleophilic trapping agent glutathione (GSH). The metabolites produced were separated by HPLC and the structures identified using NMR and mass spectroscopy.

3.1 Materials and Methods

Preparation of Hepatic Microsomes

Rats (n=4) were anesthetized with isoflurane and a midline incision made to expose the abdominal cavity. A 20*g* 1 ¼" Terumo Surflo I.V. catheter was inserted into the portal vein, the vena cava was nicked to allow outflow, and the livers were perfused with room temperature phosphate buffered saline (PBS) for about 3 minutes to clear the liver of blood. Livers were excised, rinsed in PBS, and 6 g pieces were immediately flash frozen in liquid nitrogen and stored at -80°C until microsomal preparation.

Hepatic microsomes were prepared according to the method of Iba *et al*[159]. Briefly, 0.5 g of liver was homogenized in 2 mL cold homogenization buffer (50 mM Tris buffer, 150 mM KCl, 0.1 mM dithiothreitol, 1 mM ethylenediamine tetracetic acid, 20% glycerol and 0.1 mM phenylmethylsulfonylfluoride) using potter-elvehjem pestle and sleeve. The homogenate was transferred to a Beckman (Beckman Coulter Canada, Inc. Mississauga, ON) ultracentrifuge tube and spun in a Beckman L8-55

Ultracentrifuge at 9000×*g* for 30 minutes at 4°C. The supernatant was transferred into clean ultracentrifuge tubes and spun at 100 000×*g* for 30 minutes at 4°C. The pellet was washed with 2 mL 150 mM KCl then similarly spun for an additional 30 minutes at 4°C. The pellet was resuspended in 2 mL of 0.25 M sucrose solution and passed through a syringe with a 25×*g* needle. Microsomes were pooled (n = 4), partitioned into 500 µL aliquots in cryogenic microcentrifuge tubes (1.5 mL) and stored at -80°C until use.

Microsomal protein content was determined by the method of Lowry *et al*[160] using bovine serum albumin as the standard. Analysis was carried out on an Agilent 8453E UV-visible spectrophotometer using Chemstation software (Palo Alto, CA, USA). Absorbance was measured at 750 nm.

Hepatic Microsomal Incubation Experiments to Assess Formation of Reactive Intermediates

Microsomal incubation mixtures (1 mL) consisted of cytochrome P450 (1 nmol), $MgCl_2$ (5.0 mM), and 50 mM sodium phosphate buffer (pH 7.4). NDGA or SECO dissolved in DMSO was added to achieve a final concentration of 0.5 mM (final concentration of DMSO was <0.1%) and GSH dissolved in phosphate buffer was added to a final concentration of 1.0 mM or 5.0 mM. The mixture was pre-incubated in a shaking water bath set to 37°C for 5 min. NADPH (1 mM) was added to initiate the reaction. Control incubations included samples with no NADPH, heat-inactivated (95°C for 5 min) microsomes or no GSH. Incubations were carried out at 37°C in uncapped 12×75 mm glass culture tubes in a shaking water bath for 60 min. The reaction was terminated by chilling in an ice bath followed by subsequent addition of 50 µL of acetonitrile containing internal standard (2mM salicylamide). Samples were centrifuged at 20,000×*g* for 10 min on a Micromax Thermo IEC microcentrifuge. Aliquots of the supernatant (150 µL) were analyzed directly by HPLC (NDGA, SECO).

NMR

NMR data was obtained on a Bruker AVANCE DPX-500 (Dept of Chemistry, University of Saskatchewan) operating at 500 MHz and 125 MHz for proton and carbon, respectively and the data analyzed using XWIN-NMR version 3.0. CD_3OD, ME_2SO-d_6 and CD_3CN were used as solvent. Residual signals from CD_3OD (3.30 ppm (^1H) and 49.0 ppm (^{13}C)), ME_2SO-d_6 (2.50 ppm (^1H) and 39.5 ppm (^{13}C)) and CD_3CN (1.94 ppm

(^{1}H) and 118.7ppm (^{13}C)) served as internal standards. Programs for 2-D experiments were available from the software package XWINNMR, provided by Bruker. COSY, HMQC and HMBC experiments were performed with gradient pulses. The Distortionless Enhancement by Polarization Transfer (DEPT) experiment together with 2-dimentional-NMR (2D-NMR) experiments including: Correlation Spectroscopy (COSY), Heteronuclear Multiple Quantum Correlation (HMQC), Heteronuclear Multiple Bond Correlation (HMBC) and Nuclear Overhauser Effect Spectroscopy (NOESY) experiments were performed with gradient pulses.

3.2 Results and Discussion

Incubation of NDGA in rat liver microsomes resulted in the production of three GSH adduct metabolites which were consistent with the formation of o-Q intermediates. There was no evidence of p-QM formation in RLM. HPLC chromatograms for the incubations can be found in Chapter 4, Figure 2, page 37 of this thesis and NMR results can be found in Chapter 4, NMR Materials and Methods, page 36. One NGDA-GSH and two NDGA-GSH_2 metabolites were formed, however both control experiments (no NADPH added and heat inactivated microsomes) also generated the same metabolites in similar quantities, suggesting that cytochrome P450 enzymes are only partially contributing to the metabolism of NDGA. It appears that autoxidation is the main mechanism for NDGA oxidation in RLM[161]. Autoxidation of NDGA could be visualized over time as the initially clear NDGA solution turned to a reddish-brown solution. Chapter 5 of this thesis details the experiments studying the autoxidation of NDGA.

When SECO was incubated in RLM in both the presence and absence of GSH, SECO underwent conversion to lariciresinol without formation of a stable reactive quinone intermediate. Lariciresinol was confirmed by comparison with authentic standard by HPLC and the result is in agreement with the literature[58]. Lariciresinol is formed by intramolecular cyclization of the aliphatic hydroxyl group on SECO with the distal benzylic carbon. The intramolecular cyclization of SECO to lariciresinol is believed to occur sufficiently rapidly, such that it out competes the formation of an intermolecular adduction between SECO and GSH. It is possible that lariciresinol

formation is either the result of oxidation to a quinone methide intermediate or the result of a radical mediated process although further studies would have to be done to confirm this mechanism.

There was no visual colour change observed over time of SECO in buffered solution. In addition, no lariciresinol formation was observed in the RLM control experiments (no NADPH added and heat inactivated microsomes), further suggesting that SECO does not autoxidize to any appreciable extent under our conditions. Thus the lack of formation of a reactive intermediate capable of interacting with biological nucleophiles via either autoxidation or microsomal oxidation of SECO agrees with the lack of toxicity observed with SECO.

4. Oxidation of the Lignan Nordihydroguaiaretic Acid

Jennifer L. Billinsky, Michelle R. Marcoux and Ed S. Krol

Chemical Research in Toxicology, 2007, *20* (9), pp 1352–1358

Publication Date (Web): August 3, 2007 (Article)

DOI: 10.1021/tx700205j

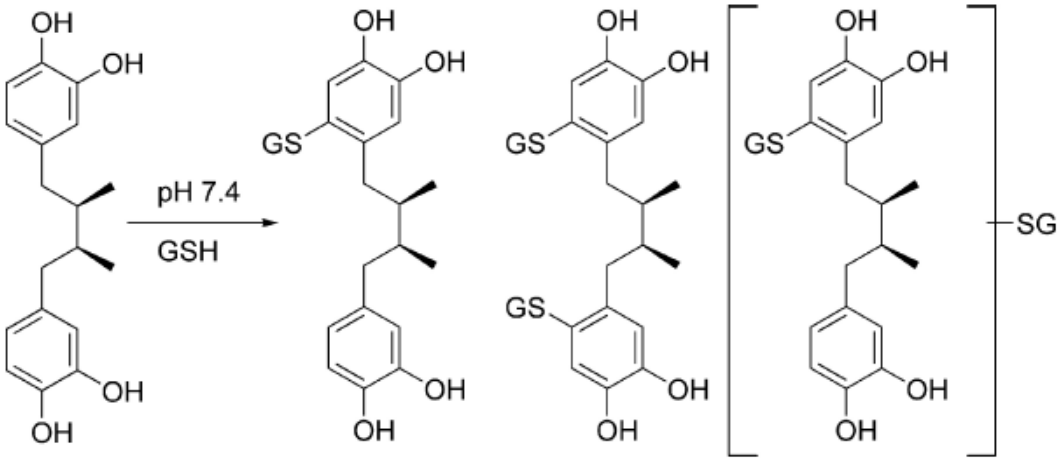

Oxidation of the Lignan Nordihydroguaiaretic Acid

Jennifer L. Billinsky,[†] Michelle R. Marcoux,[‡] and Ed S. Krol*[,‡]

Graduate Toxicology Program and College of Pharmacy and Nutrition, University of Saskatchewan, 110 Science Place, Saskatoon, SK S7N 5C9 Canada

Received June 7, 2007

The naturally occurring antioxidant lignan nordihydroguaiaretic acid has been used in traditional medicine to treat a variety of conditions and more recently has been investigated for its anticancer and antimicrobial properties. Nordihydroguaiaretic acid has also been shown to cause kidney toxicity in rats and there is evidence to suggest that chronic nordihydroguaiaretic acid consumption may cause liver toxicity in humans. Nordihydroguaiaretic acid likely undergoes biotransformation to a reactive quinone species, either an *ortho*-quinone or a *para*-quinone methide, which is responsible for its toxicity. In an effort to probe the toxicity of nordihydroguaiaretic acid, we oxidized nordihydroguaiaretic acid with both chemical and enzymatic systems and trapped the resultant products with glutathione. The nordihydroguaiaretic acid–glutathione adducts were compared with the products found when nordihydroguaiaretic acid was incubated in rat hepatic microsomes in the presence of glutathione. Glutathione metabolites consistent with *ortho*-quinone formation were the only oxidation products observed. Control experiments in microsomes however suggested that a majority of the nordihydroguaiaretic acid *ortho*-quinone glutathione adducts were formed as the result of nordihydroguaiaretic acid autoxidation. We measured the rate of this autoxidation process over a range of pH values and determined that the autoxidation reaction is base-catalyzed. We suggest that caution must be exercised when using nordihydroguaiaretic acid in experiments above pH 7.4 as relatively little of the parent compound may be left in incubations longer than 3 h.

Introduction

The naturally occurring lignan, nordihydroguaiaretic acid (NDGA[1]) (Figure 1) is found in the creosote bush (*Larrea tridentata*), a native plant in the southwest United States. Creosote was originally used in traditional medicine for treatment of skin irritations and pain relief (*1*). NDGA is known to inhibit lipoxygenase activity (*2, 3*), transactivation of c-fos and AP-1 (*4*), estradiol binding to sex steroid binding protein (*5*), DNA synthesis in a rat model (*6*), amyloid fibril formation *in vitro* (*7*), Ca^{2+}-ATPase (*8*) and cytochrome P450 (*9*). It has also been shown to have cancer chemopreventive properties (*10–12*), to stabilize microtubules *in vitro* (*13*), to be antigenotoxic in methyl methanesulfonate-induced sister-chromatid exchange in lymphocytes, (*14, 15*) and it can induce apoptosis and mitochondrial depolarization in a murine hematopoietic cell line (*16, 17*). It is also an estrogen receptor (ER) α agonist and ERβ mixed agonist/antagonist (*18*). NDGA was licensed in the United States for use as a topical treatment for actinic keratosis under the name Actinex (Chemex Pharmaceuticals, Denver, CO) but has seen limited use due to skin hypersensitivity.

NDGA is also a well-known lipophilic antioxidant (*19–23*) that has found use in the polymer industry (*24*) and was incorporated into oil-based foods as a preservative (*25*). NDGA was later withdrawn from use as a food preservative when it was shown that NDGA caused nephrotoxicity in rats (*25, 26*). More recently, NDGA was found to be hepatotoxic to rats as determined by increased serum alanine aminotranferase levels and had an LD_{50} of 75 mg/kg (*27*). NDGA is the active ingredient in the herbal product Chaparral, prepared from the creosote bush (*28*) and chronic use has been associated with hepatotoxicity (*28–32*). *In vitro* studies suggest that NDGA undergoes *in vivo* biotransformation to a reactive intermediate which is responsible for its toxicity (*26*). The reactive intermediate was suggested to be a di-*ortho*-quinone, based on a derivative formed from reaction with *ortho*-phenylenediamine and the lack of hydroxyl groups seen by IR and NMR. In another study an activated NDGA species formed a noncovalent, reversible complex with DNA, although the activated species was not identified (*33*).

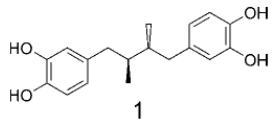

1

Figure 1. *meso*-Nordihydroguaiaretic acid (NDGA).

Catechols such as NDGA are known to be oxidized directly to either *ortho*-quinones or *para*-quinone methides (Scheme 1) (*34, 35*). These transformations appear to occur via formation of an initial semi-quinone radical which undergoes subsequent oxidation by P450 or other oxidases (*36*). Alternatively an *ortho*-quinone may also isomerize to form a *para*-quinone methide, provided that at least one benzyl proton is present. *ortho*-Quinones contribute to cytotoxicity mainly via an increase in oxidative stress from processes such as redox cycling as depicted in Scheme 1, where an initially formed semi-quinone radical can react with O_2 to form superoxide (O_2^{-}) and the *ortho*-quinone may be reduced to the catechol by endogenous reductases (*37–39*). The more electrophilic *para*-quinone me-

* To whom correspondence should be addressed. Phone: (306) 966-2011. Fax: (306) 966-6377. E-mail: ed.krol@usask.ca.
[†] Graduate Toxicology Program.
[‡] College of Pharmacy and Nutrition.

[1] Abbreviations: NDGA, Nordihydroguaiaretic acid; ESI–MS, electrospray ionization–mass spectrometry; ER, estrogen receptor; DMPA, 3,4-dimethoxyphenylacetone; TFA, trifluoroacetic acid.

10.1021/tx700205j CCC: $37.00
Published on Web 08/03/2007

Scheme 1. Proposed Oxidation of NDGA to Quinones

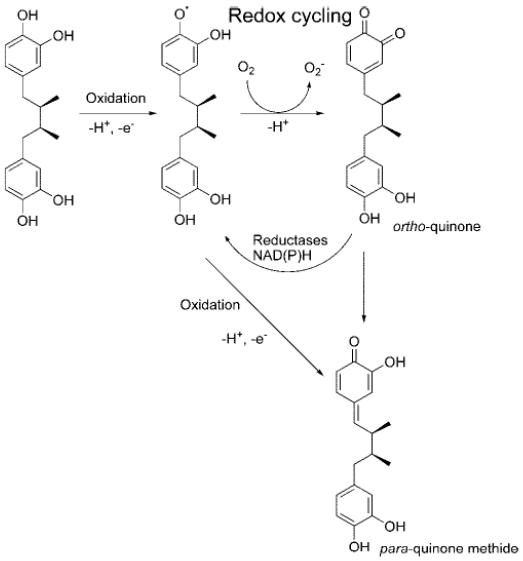

thides typically cause cytotoxicity via alkylation of cellular nucleophiles producing adducts *in vivo* (*40*). Isomerization of the *ortho*-quinone to the *para*-quinone methide is hindered by substituents at the benzyl position, suggesting that an *ortho*-quinone of NDGA would isomerize very slowly to a quinone methide (*35*). In addition, *ortho*-quinones which isomerize very slowly to *para*-quinone methides have been observed to correlate well with cytotoxicity (*41*). NDGA can increase oxidized glutathione (GSSG) and lipid peroxidation levels in murine hematopoietic cells (*16*), suggesting an increase in oxidative stress consistent with the formation of an *ortho*-quinone.

There are reports that NDGA can be unstable in aqueous media, undergoing conversion to "activated NDGA" (*33*), or a quinone (*42*). This process of autoxidation appears to be pH dependent, with the greatest conversion occurring at elevated pH. Since the precise identity of the quinone has not been confirmed, we were interested in determining whether both the *ortho*-quinone and the *para*-quinone methide of NDGA are produced in aqueous solution or with NADP(H) and rat hepatic microsomes. The *ortho*-quinone and the *para*-quinone methide can be distinguished by reacting the quinone intermediates with the thiol-reactive trapping agent glutathione (GSH) (*35*). GSH typically forms ring adducts with *ortho*-quinones (Scheme 2a) while GSH adds to the exocyclic benzyl carbon of *para*-quinone methides (Scheme 2b) (*35*). Further to this, we wanted to determine whether cytochrome P450-catalyzed oxidation of NDGA contributes to the observed toxicity, so we measured the formation of NDGA–GSH adducts catalyzed by rat liver microsomes and NADP(H). Since studies on the biological properties of NDGA are performed in aqueous solution, we thought it important to determine the stability of NDGA in aqueous solution. Our results suggest that the *ortho*-quinone of NDGA is formed at pH 7.4 and that cytochrome P450 makes only a small contribution to its formation. In addition, the pH-rate profile for NDGA autoxidation suggests that in many of the previous biological studies of NDGA, *ortho*-quinone formation may contribute to biological activity in addition to toxicity.

Experimental Procedures

Materials. Caution. *The following chemicals are hazardous and should be handled carefully: NDGA. meso*-Nordihydroguiairetic acid (NDGA)) from *Larrea Tridentata*, reduced glutathione (GSH), trifluoroacetic acid (TFA), tyrosinase from mushroom (EC1.14.18.1), dimethylsulfoxide (ME_2SO), NADP(H), 3,4-dimethoxyphenylacetone (DMPA), and silver oxide were purchased from Sigma-Aldrich Co. (Madison, WI). Citric acid and K_2HPO_4 were purchased from Fisher Scientific (Ottawa, ON). Perchloric acid was purchased from G. Frederick Smith Chemical Co. (Columbus, OH). All solvents were HPLC grade. Water was purified via a Millipore (Mississauga, ON) Milli-Q system with a Quantum EX Cartridge.

Mushroom Tyrosinase-Catalyzed Synthesis of NDGA–GSH_2 (5). A mixture of NDGA (0.5 mM), GSH (1 mM), and tyrosinase (945 U) in 10 mL of sodium phosphate buffer (50 mM, pH 6.0) was vortexed for 60 min at 22 °C. The reaction was quenched by the addition of 250 μL of perchloric acid and the reaction mixture was concentrated under vacuum.

Mushroom Tyrosinase-Catalyzed Synthesis of NDGA–GSH (4). The NDGA–GSH adduct was prepared using the same procedure used to prepare the NDGA–GSH_2 adduct but with a different ratio of reagents (NDGA (1 mM), GSH (5 mM), and tyrosinase (472.6 U) in 10 mL of sodium phosphate buffer (50 mM, pH 6.0)).

Semi-Preparative HPLC Purification of GSH Adducts of NDGA *ortho*-Quinones. Aliquots of 200 μL of combined oxidative products were injected onto a 10 × 300 mm Alltech ODS-2, 5 μ, C-18 column using a Waters 2695 Separations module with autosampler and gradient controller, and the peaks were detected with a Waters 2996 Photodiode array detector set at 280 nm. Peaks were integrated using Waters Empower software. Peaks of interest were collected using a Waters Fraction Collector III. The mobile phase consisted of A, acetonitrile with 0.1% trifluoroacetic acid (TFA); and B, 0.01% TFA in water. For semi-preparative collection a flow rate of 5.0 mL/min was used. Peaks were eluted with 5% A for 2 min, increased to 20% A over 16 min, isocratic for 2 min, increased to 65% A over 16 min, increased to 90% A over 3 min, and then held isocratic for 3 min.

Scheme 2. Proposed GSH Adducts of (a) NDGA *ortho*-Quinone, and (b) NDGA *para*-Quinone Methide

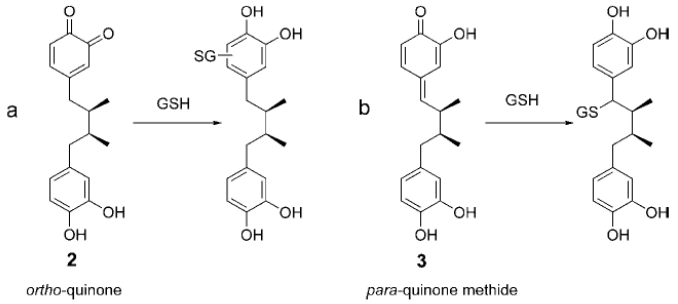

Microsomal Incubations. Microsomes were prepared from the livers of male Sprague–Dawley rats in accordance with University of Saskatchewan Animal Care Guidelines. Protein (*43*) and P450 (*44*) levels were determined using literature procedures. Incubations containing 1.0 nmol P450 were conducted for 60 min in 50 mM sodium phosphate buffer (pH 7.4, 1 mL final volume). NDGA was added in Me_2SO (final concentration of Me_2SO was <1%) and GSH was added in sodium phosphate buffer to achieve final concentrations of 0.5 and 1.0 mM, respectively. $MgCl_2$ was added to a final concentration of 5.0 mM. The mixture was preincubated in a shaking water bath set to 37 °C for 5 min. NADP(H) (1.0 mM final concentration) was added to initiate the reaction. Control incubations contained no NADP(H). The reaction was terminated by chilling in an ice bath followed by subsequent addition of 50 μL of ice cold acetonitrile containing 2.0 mM salicylamide as an internal standard. The incubates were centrifuged at 13,000 rpm for 10 min on a Micromax Thermo IEC microcentrifuge. Aliquots of the supernatant (150 μL) were analyzed directly by analytical HPLC.

HPLC Analysis of Microsomal Incubations of NDGA. For analysis of the microsomal incubations, a 250 × 4.6 mm Alltech ODS-2, 5 μ, C-18 analytical column was used at a flow rate of 1.5 mL/min. The same mobile phases that were used for semi-preparative HPLC were employed. A gradient of 5% A for 3 min, increased to 20% A over 4 min, isocratic for 3 min, increased to 35% A over 16 min, increased to 90% A over 5 min, and then held isocratic for 4 min was used.

NMR. NMR data was obtained on a Bruker AVANCE DPX-500 (Dept. of Chemistry, University of Saskatchewan) operating at 500 MHz and 125 MHz for proton and carbon, respectively, and the data were analyzed using XWIN-NMR version 3.0. CD_3OD and CD_3CN were used as solvents. Residual signals from CD_3OD (3.30 ppm (^{1}H) and 49.0 ppm (^{13}C)) and CD_3CN (1.94 ppm (^{1}H) and 118.7 ppm (^{13}C)) served as internal standards. Programs for 2-D experiments were available from the software package XWIN-NMR, provided by Bruker. COSY, HMQC, and HMBC experiments were performed with gradient pulses. The distortionless enhancement by polarization transfer (DEPT) experiment together with 2-dimensional-NMR (2D-NMR) experiments, including correlation spectroscopy (COSY), heteronuclear multiple quantum correlation (HMQC), heteronuclear multiple bond correlation (HMBC), and nuclear Overhauser effect spectroscopy (NOESY) experiments, were performed with gradient pulses.

1-(3,4-dihydroxyphenyl-6-*S*-glutathionyl)-4-(3,4-dihydroxyphenyl)-2,3-dimethylbutane (**4**, Rt = 27 min). ^{1}H NMR (CD_3OD): δ 0.83 (d, *J* = 5.4 Hz, 6 H, CH_3-2, CH_3-3), 1.70 (m, 2 H, CH-2, CH-3), 2.18 (m, 4 H, CH_2-1a, CH_2-4a, Glu-β), 2.53 (m, 2 H, Glu-γ), 2.66 (m, 2 H, CH_2-1b, CH_2-4b), 3.08 (m, 1 H, Cys-β), 3.35 (m, 1 H, Cys-β), 3.87 (s, 2 H, Gly-α), 3.95 (t, *J* = 6.3 Hz, 1 H, Glu-α), 4.49 (m, 1 H, Cys-α), 6.47 (dd, *J* = 5.8 Hz, 2.3 Hz, 1 H, ArH-6′), 6.60 (d, *J* = 2.0 Hz, 2 H, ArH-2, ArH-2′), 6.67 (dd, *J* = 6.3 Hz, 1.3 Hz, 1 H, ArH-5′), 6.68 (dd, *J* = 6.3 Hz, 1.3 Hz, 1 H, ArH-5); UV 255, 286 nm; positive ion electrospray-MS (80% acetonitrile with 0.1% formic acid), *m/z* 608 ($M + H^+$).

^{13}C NMR (CD_3OD) δ: 15.54 (CH_3-3), 15.60 (CH_3-3), 15.66 (CH_3-2), 15.71 (CH_3-2), 26.16 (Glu-β), 31.54 (Glu-γ), 36.21 (Cys-β), 36.29 (Cys-β), 38.34 (CH_2-4), 38.44 (CH_2-4), 38.60 (CH_2-1), 38.71 (CH_2-1), 39.21 (CH-3), 39.33 (CH-3), 39.47 (CH-2), 39.58 (CH-2), 40.83 (Gly-α), 40.88 (Gly-α), 53.01 (Glu-α), 53.53 (Cys-α), 115.22 (Ar-5′), 116.22 (Ar-2′), 116.46 (Ar-2), 119.40 (Ar-SG), 120.45 (Ar-6′), 125.23 (Ar-5), 125.36 (Ar-5), 133.75 (Ar-1′), 134.11 (Ar-1), 143.11 (Ar-4′), 143.70 (Ar-4), 143.73 (Ar-4), 144.95 (Ar-3′), 145.31 (Ar-3), 145.33 (Ar-3), 171.04 (C=O), 171.70 (C=O), 171.99 (C=O), 173.55 (C=O).

1,4-Bis(3,4-dihydroxyphenyl-6-S-glutathionyl)-2,3-dimethylbutane (**5**, Rt = 18 min). ^{1}H NMR (CD_3OD) δ: 0.83 (t, *J* = 6.3 Hz, 6 H, CH_3-2, CH_3-3), 1.70 (m, 2 H, CH-2, CH-3), 2.18 (m, 6 H, CH_2-1a, CH_2-4a, Glu-β, Glu-β'), 2.53 (m, 4 H, Glu-γ, Glu-γ'), 2.63 (m, 2 H, CH_2-1b, CH_2-4b), 3.08 (m, 2 H, Cys-β, Cys-β′), 3.35 (m, 2 H, Cys-β, Cys-β′), 3.87 (s, 4 H, Gly-α, Gly-α′), 3.95 (t, *J* = 6.2 Hz, 2 H, Glu-α), 4.50 (m, 2 H, Cys-α, Cys-α′), 6.59 (dd, *J* = 1.5, 4.2 Hz, 2 H, ArH-2, ArH-2′), 6.68 (dd, *J* = 5.7 Hz, 1.3 Hz, 2 H, ArH-5, ArH-5′); UV 255, 293 nm; positive ion electrospray-MS (80% acetonitrile with 0.1% formic acid), *m/z* 457 ($M + 2H^+$).

^{13}C NMR (CD_3OD) δ: 15.73 (CH_3-2, CH_3-3), 26.17 (Glu-β), 31.53 (Glu-γ), 36.29 (Cys-β), 38.40 (CH_2-1, CH_2-4), 39.21 (CH-2, CH-3), 48.84 (Gly-α), 53.55 (Glu-α), 53.55 (Cys-α), 116.54 (Ar-2, Ar-2′), 119.47 (Ar-SG), 125.31 (Ar-5, Ar-5′), 134.04 (Ar-1, Ar-1′), 143.73 (Ar-4, Ar-4′), 145.32 (Ar-3, Ar-3′), 171.12 (C=O), 171.76 (C=O), 172.01 (C=O), 173.56 (C=O).

NDGA-SG_2 (**6**, Rt = 18.5 min). ^{1}H NMR (CD_3OD) δ: 0.81 (t, *J* = 18.4 Hz, 6 H, CH_3-2, CH_3-3), 1.74 (m, 2 H, CH-2, CH-3), 2.19 (m, 6 H, CH_2-1a, CH_2-4a, Glu-β, Glu-β′), 2.57 (m, 4 H, Glu-γ, Glu-γ′), 2.76 (m, 2 H, CH_2-1b, CH_2-4b), 2.98 (m, 2 H, Cys-β, Cys-β′), 3.36 (m, 2 H, Cys-β, Cys-β′), 3.90 (s, 4 H, Gly-α, Gly-α′), 4.00 (s, 2 H, Glu-α), 4.48 (m, 2 H, Cys-α, Cys-α′), 6.51 (m, 4.2 Hz, 1 H, Ar), 6.64 (m, 4.2 Hz, 1 H, Ar), 6.69 (m, 1 H, Ar), 6.81 (m, 1 H, Ar); UV 275 nm; positive ion electrospray-MS (80% acetonitrile with 0.1% formic acid), *m/z* 457 ($M + 2H^+$).

Electrospray Mass Spectroscopy. Positive and negative electrospray mass spectra were obtained using either a Micromass Quattro LC instrument with a Waters Alliance HPLC (Saskatoon Research Centre) or an API Qstar XL with an Agilent 1100 HPLC (Saskatchewan Structural Sciences Centre).

Kinetics of NDGA Autoxidation. NDGA in acetonitrile (20 mM) was added to 25 mL of 0.5 M phosphate-citric acid buffer (*45*) pre-equilibrated to 37 °C to give a final NDGA concentration of 0.1 mM. Aliquots (1 mL) were removed at various intervals (t_i) and added to a solution containing DMPA as an internal standard (0.2 mM final concentration), and HCl was added to stop the reaction by acidification to pH 1.25–1.50. Samples (30 μL) were injected directly onto an Alltech ODS-2, 250 mm × 4.6 mm column using 60:40 H_2O/acetonitrile containing 0.1% TFA as mobile phase at a flow rate of 1 mL min^{-1}. NDGA (Rt = 12.1 min) and DMPA (Rt = 5.9 min) were monitored at 282 nm. A ratio of peak area for NDGA vs. DMPA was used to follow the loss of NDGA. Pseudo-first-order reaction rates (k_{obs}) were determined by plotting ln(peak area(t_0) − peak area(t_i)) vs. time, where the slope = k_{obs}. All experiments were performed in triplicate. The linear range and limits of detection and quantitation for NDGA were determined by performing serial dilutions of NDGA–DMPA and analyzing by HPLC.

NDGA Stability Studies. A mixture of NDGA (0.1 mM) and DMPA (0.2 mM), pH 1.50, was stored in an HPLC autosampler vial at 25 °C or −5 °C for 6 days. Samples were analyzed at 0, 12, 24, 48, and 144 h by comparison with freshly prepared samples using the same HPLC conditions used for the kinetics studies.

Results

Preparation of NDGA–GSH Adducts. Substituted catechols can be oxidized to either an *ortho*-quinone or a quinone methide (*34*). These quinones can be distinguished via trapping with a sulfur nucleophile such as GSH, since the *ortho*-quinone predominantly forms ring adducts, whereas the quinone methide predominantly forms exocyclic GSH adducts.

NDGA was oxidized with tyrosinase to the *ortho*-quinone in the presence of the trapping agent GSH and analyzed by HPLC. Three GSH-containing NDGA adducts were isolated by semi-preparative HPLC and identified by MS and NMR. However, if NDGA was incubated with tyrosinase in the absence of GSH and the trapping agent was added after starting material was depleted, no GSH reactive products were observed. ESI-MS (+) data for the three adducts obtained correspond to NDGA with the addition of one GSH molecule (Rt = 27 min, *m/z* 608 [$M + H^+]^+$, **4**) and NDGA with the addition of two molecules of GSH (Rt = 18 min, *m/z* 457 [$M + 2H^+]^{2+}$, **5**; Rt = 18.5 min, *m/z* 457 [$M + 2H^+]^{2+}$, **6**). The ^{1}H and ^{13}C NMR for NDGA only display signals for one phenyl propanoid unit as NDGA

Scheme 3. Reaction Scheme for the Formation of NDGA–GSH Adducts 4, 5, and 6

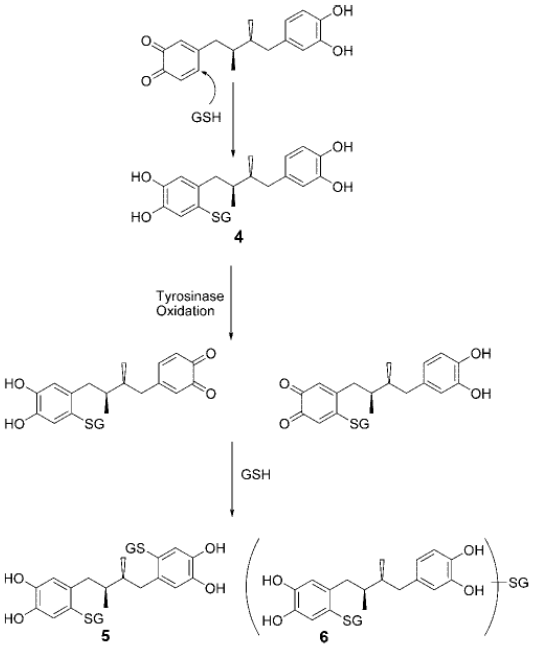

is C_2 symmetrical; substitution of GSH on one half of the molecule or at two different positions would result in loss of symmetry and a more complex NMR spectrum. ^{1}H and ^{13}C and HMQC NMR studies for compound **4** indicate that the catechol ring is substituted with GSH at the 6′-position (Scheme 3). This was confirmed by the expected loss of symmetry, a 15 ppm downfield shift of the 6′ carbon attached to GSH and the loss of the 6′ ^{1}H signal. Compound **5** (Scheme 3) was determined to be substituted with GSH at the 6′ positions of both aromatic rings. The ^{1}H, ^{13}C, and HMQC NMR showed that no loss of symmetry was observed, the 6′ ^{1}H signal was absent, and a 15 ppm downfield shift was observed for the 6′ carbon attached to GSH. Compound **6** was also substituted with two GSH molecules. Due to a poorly resolved NMR we were unable to definitively assign the position of the GSH adducts in compound **6**, however, the proton splitting pattern in the aromatic region suggests that both molecules of GSH are substituted on different aromatic rings.

We saw no evidence of GSH adducts derived from a *para*-quinone methide of NDGA under the tyrosinase-catalyzed conditions. Attempts to oxidize NDGA directly to a *para*-quinone methide with silver oxide resulted in a decrease in the NDGA absorbance at 282 nm, an increase in absorbance at 386 nm, and the appearance of a yellow color to the solution, all of which were consistent with the formation of a quinone (*41*). Upon addition of GSH to trap any reactive intermediates, we found no major products corresponding to *para*-quinone methide-derived adducts. Rather, we observed the formation of a complex mixture of products which formed independently of GSH. Silver-oxide-catalyzed oxidation of NDGA in CD_3CN and analysis by ^{1}H NMR also yielded a mixture of products which did not include a *para*-quinone methide (data not shown).

Microsomal Incubations. Microsomal incubations were performed with NDGA in hepatic microsomes isolated from male Sprague–Dawley rats. NDGA, in the presence of GSH, was preincubated in rat hepatic microsomes for 5 min prior to initiation with NADP(H) and then incubated for 60 min. HPLC analysis revealed a mixture of unreacted NDGA and **4** and **6** as major products, in addition to a small amount of **5** (Figure 2a). Control microsomal incubations of NDGA conducted in either the absence of NADP(H) (Figure 2b) or using heat-inactivated microsomes (Figure 2c) provided similar results. This suggested that NDGA could be oxidized to an *ortho*-quinone in the absence of P450.

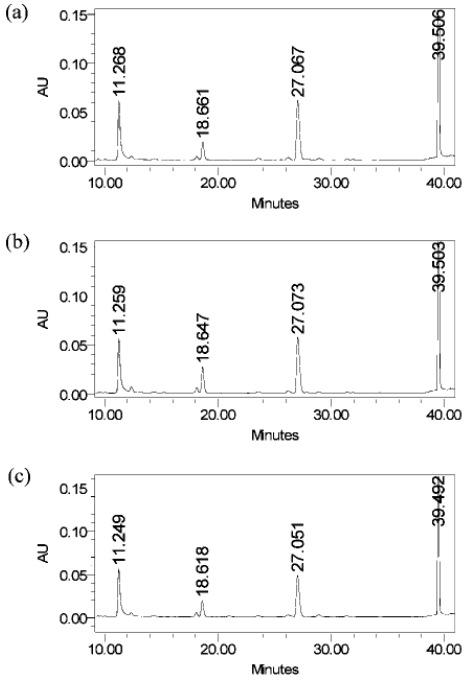

Figure 2. HPLC chromatograms (analytical column, see Experimental Procedures) of 60 min incubations of NDGA (0.5 mM) with GSH (1.0 mM) in rat liver microsomes (1 nmol P450, pH 7.4, 50 mM sodium phosphate buffer, 37 °C). NDGA was preincubated for 5 min prior to addition of NADP(H): (a) incubation performed in the presence of NADP(H) (1.0 mM), (b) incubation performed in the absence of NADP(H), and (c) incubation performed using heat-inactivated microsomes with NADP(H). Compounds in the chromatograms were identified as follows: Rt = 11.3 min (salicylamide), Rt = 18.0 min (**6**), Rt = 18.6 min (**5**), Rt = 27.1 min (**4**), Rt = 39.5 min (**NDGA**).

NDGA Autoxidation Kinetics. A control incubation of NDGA in pH 7.4 buffer with GSH and analysis by LC–MS resulted in a mixture of **4**, **5**, and **6** comparable to the microsomal incubations. The rate of NDGA autoxidation was measured by following the loss of NDGA via isocratic HPLC analysis (60:40, H_2O/acetonitrile mobile phase) over the pH range 6.0–9.0. A pH rate profile for the autoxidation of NDGA is shown in Figure 3; half-lives for NDGA autoxidation were calculated from $t_{1/2} = 0.693/k_{obs}$ and are summarized in Table 1. A limit of quantitation of 0.039 ± 0.002 mM was determined for NDGA and all values reported were within the linear range. NDGA was determined to be stable at 25 °C, pH 1.5 for at least 48 h; all samples were analyzed within 24 h. From the pH rate profile in Figure 3 it may be seen that NDGA autoxidation is a base-catalyzed process from pH 6.0 to 9.0. The half-life of NDGA at pH 7.4 is 3.1 h in 0.5 M phosphate-citric acid buffer. Moreover, in the physiologically relevant range (pH 7.0–8.0),

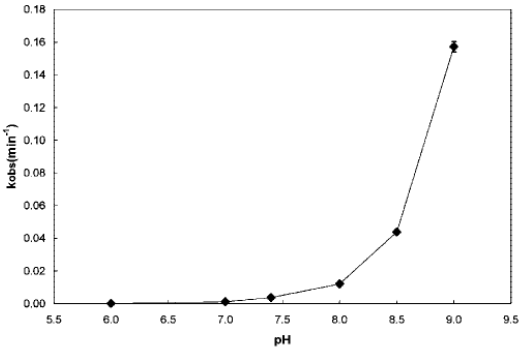

Figure 3. pH Rate profile for NDGA autoxidation. Pseudo-first-order rates were determined for NDGA (0.1 mM) in K_2HPO_4/citric acid buffer (0.5 mM) at 37 °C. Experiments were performed in triplicate at each pH value. Data points indicate the mean of three replicates, and error bars represent standard deviation from the mean.

Table 1. Rate of NDGA Autoxidation in 0.5 M Phosphate-Citric Acid Buffer at 37 °C[a]

pH	k_{obs} (s^{-1})	$t_{1/2}$ (h)
9.0	2.62×10^{-3}	0.07
8.5	7.31×10^{-4}	0.26
8.0	2.01×10^{-4}	0.95
7.4	6.1×10^{-5}	3.12
7.0	2.1×10^{-5}	8.88
6.0	3.3×10^{-6}	57.75

[a] NDGA autoxidation was determined by following the loss of NDGA (0.1 mM) via HPLC as described in Experimental Procedures.

the half-life of NDGA decreased by 65% from pH 7.0 (8.88 h) to pH 7.4 (3.1 h) and by 69% from pH 7.4 (3.1 h) to pH 8.0 (0.95 h).

Discussion

The *in vivo* biotransformation of phenols and catechols to quinones has been described for a variety of compounds (*36*). Oxidation of catechols can lead to either an *ortho*-quinone (*34*) or, if the catechol has a *para*- or *ortho*-methyl substituent, a quinone methide (*35*). These quinone species are implicated in the toxicity of many catechols as both compounds are capable of reacting with biological nucleophiles with the resultant formation of DNA adducts (*46*). *ortho*-Quinones can also be involved in an increase in oxidative stress as a result of redox cycling (*39*). It has been suggested that NDGA, a di-catechol lignan, exerts its nephro- and hepatotoxic effects via an *ortho*-quinone species (*25, 26*). The major urinary metabolites from rats given NDGA were the mono- and the diglucuronide conjugates; no mercapturic acids were reported (*27*). NDGA is capable of forming both an *ortho*-quinone and a *para*-quinone methide (Scheme 1), and, as it is a symmetrical molecule with two catechol groups, both catechols could potentially be oxidized to quinones as suggested by Grice (*26*). Isomerization of an NDGA *ortho*-quinone to a *para*-quinone methide however, would be predicted to be very slow as a result of substitution at the benzylic position (4-propylcatechol *ortho*-quinone isomerization $t_{1/2}$ > 89 min, pH 6.0, 25 °C) (*35*), thus the *ortho*-quinone would be expected to be the major product.

Tyrosinase-catalyzed oxidation of catechols in the presence of GSH is a well-documented method for preparation and trapping of *ortho*-quinones (*34*). In agreement with earlier studies (*26*) we confirmed that NDGA can be oxidized to an *ortho*-quinone, and we have now identified mono- and di-substituted GSH adducts of NDGA from our tyrosinase catalyzed oxidations (Scheme 3). Reaction of GSH with 4′-alkyl *ortho*-quinones is known to produce 6′-substituted ring adducts, which agrees with our findings of 6′-substituted NDGA adducts (**4** and **5**). The structure of the second NDGA–SG_2 adduct (*6*) could not be determined. Compounds **5** and **6** are the result of a tyrosinase catalyzed oxidation of compound **4** to an *ortho*-quinone followed by substitution by a second molecule of GSH (Scheme 3). Hydroquinone–GSH adducts are known to be readily oxidized to quinones which can form further GSH adducts (*38*), and catechol–SG_2 adducts have also been previously reported (*34*). Oxidation of the NDGA–SG adduct (*4*) would be expected to contribute further to oxidative stress by also leading to the production of superoxide.

Our inability to synthesize an NDGA *para*-quinone methide and the absence of isomerization products from the *ortho*-quinone suggests that *para*-quinone methide formation is unlikely to occur for NDGA. Oxidation of NDGA with silver oxide produced a UV absorbance peak consistent with formation of a *para*-quinone methide, however the products in the reaction mixture were not GSH reactive. In addition, we observed that the *ortho*-quinone is not appreciably stable at neutral pH since the addition of GSH immediately after oxidation did not result in the formation of GSH adducts, rather a mixture of non-GSH reactive products was observed. It is likely that oxidized NDGA undergoes dimerization or polymerization under these conditions in the absence of GSH (*47–49*).

The *ortho*-quinone GSH standards were used to identify the products of a microsomal incubation of NDGA (Figure 2). NDGA metabolite formation was independent of NADP(H)-dependent processes such as P450-catalysis, instead autoxidation was rapid and seemed to predominate. The autoxidation of NDGA has been noted previously (*3, 26, 33, 42*) and has been exploited in the cross-linking polymerization of NDGA for the development of tendon mimics (*49*). Catechol autoxidation has been observed previously (*50–52*) and is related to pK_a of the catechol, so that the ionized form of the catechol undergoes autoxidation more rapidly than the un-ionized form (*51*), which is consistent with studies utilizing NDGA in formulations for topical skin application (*42*). To confirm that autoxidation of NDGA occurs more rapidly as pH increases, we determined the rate of NDGA autoxidation from pH 6.0 to 9.0 and constructed a pH–rate profile. Figure 3 shows that NDGA autoxidation is a base-catalyzed process with nearly an order of magnitude increase in the rate of autoxidation from pH 7.0 to 8.0 and a half-life of 3.1 h at pH 7.4, 37 °C, the conditions under which many biological assays are performed.

Rates of autoxidation of 4′-alkyl-substituted catechols vary considerably. The autoxidation of NDGA at pH 7.4 (6.1×10^{-5} s^{-1}) is faster than that observed for catechol (2.3×10^{-8} s^{-1}, 25 °C (*53*); 5.3×10^{-10} s^{-1}, 37 °C (*54*)), dopamine (3.19×10^{-6} s^{-1}, 25 °C (*50*)), pyrogallol (7.4×10^{-8} s^{-1}, pH 7.4, 0.1 mM, 37 °C (*54*)), and catechin (2.1×10^{-10} s^{-1}, 0.1 mM, 37 °C (*54*)), but is slower than that of epinephrine (1.5×10^{-4} s^{-1} (*55*)), 5,6,6a,11b-tetrahydro-3,9,10-trihydroxybenzo[c]fluorene (6×10^{-4} s^{-1}, pH 7.8 (*56*)), and 4-hydroxyequilenin (1.9×10^{-2} s^{-1}, 25 °C (*52*)). One study of catechol toxicity suggested that a weak association existed between catechol pK_a and hepatocyte toxicity, where toxicity increased with decreasing ionization for a series of compounds including NDGA, catechol, and pyrogallol (*57*). NDGA displayed toxicity 8 times greater than catechol and 14 times greater than pyrogallol, even though NDGA and catechol have the same pK_a (9.30) and pyrogallol

has a pK_a of 8.94. On the basis of our results we speculate that the rate of autoxidation and *ortho*-quinone formation may have a greater influence on catechol toxicity than pK_a. Additional factors such as the stability and reactivity of the *ortho*-quinone will also influence catechol toxicity (*41*). It is interesting that the rate of NDGA autoxidation does not seem to be solely dependent on pK_a, as catechol and NDGA have markedly different rates of autoxidation, but the same pK_a (*57*). One possibility is that the more rapid autoxidation of NDGA is due to intramolecular hydrogen-bonding between the catechol rings of NDGA which may lead to a greater degree of ionization, although this would require further investigation.

In our own microsomal incubations NDGA is preincubated for 5 min followed by a 60 min incubation which is sufficient for measurable NDGA autoxidation to occur. NDGA is a known antioxidant (*19*), a lipoxygenase inhibitor (*3*), and has also been shown to inhibit P450 (*9*). All of these systems use NDGA at or near pH 7.4 and frequently include preincubations, suggesting that the *ortho*-quinone contributes to the biological activity of NDGA. The use of NDGA as a topical agent for the treatment of actinic keratosis has been plagued by a high incidence of contact hypersensitivity, which is frequently associated with the formation of reactive intermediates (*58, 59*). Toxicity mediated through the formation of a reactive NDGA *ortho*-quinone is consistent with previous reports of nephro- (*25, 26*) and hepatotoxicity (*27–32*) associated with consumption of NDGA.

In summary, our work confirmed that NDGA can be oxidized to an *ortho*-quinone which can form adducts with GSH and this reactive intermediate is responsible for the observed cytotoxicity. In rat liver microsomes the mono-GSH adduct **4** and the di-GSH adduct **6** are the major products. The *ortho*-quinone of NDGA however does not isomerize to a *para*-quinone methide and furthermore we were unable to isolate NDGA *para*-quinone methides via oxidation with silver oxide. Instead, formation of a mixture of polymeric materials seems to predominate. We have observed similar difficulties preparing *para*-quinone methides from other lignan analogs and are presently pursuing this observation in our lab. Finally, NDGA undergoes autoxidation to an *ortho*-quinone species through a base-catalyzed process. As a result of this autoxidation process at physiological pH, it seems likely that at least some of the observed properties of NDGA, such as lipoxygenase inhibition (*3*), are due to formation of the *ortho*-quinone in the *in vitro* or *in vivo* system under study.

Acknowledgment. This work was funded by HSURC and NSERC. M.R.M. was supported by a NSERC USFA and J.L.B. was supported by a NSERC PGSM and PGSD.

References

(1) Arteaga, S., Andrade-Cetto, A., and Cardenas, R. (2005) *Larrea tridentata* (Creosote bush), an abundant plant of Mexican and US-American deserts and its metabolite nordihydroguaiaretic acid. *J. Ethnopharmacol. 98*, 231–239.

(2) Tong, W., Ding, X., and Adrian, T. E. (2002) The mechanisms of lipoxygenase inhibitor-induced apoptosis in human breast cancer cells. *Biochem. Biophys. Res. Commun. 296*, 942–948.

(3) Yasumoto, K., Yamamoto, A., and Mitsuda, H. (1970) Studies on Soybean Lipoxygenase. 4. Effect of Phenolic Antioxidants on Lipoxygenase Reaction. *Agric. Biol. Chem. 34*, 1162–1168.

(4) Gonzales, M., and Bowden, G. T. (2002) Nordihydroguaiaretic acid-mediated inhibition of ultraviolet B-induced activator protein-1 activation in human keratinocytes. *Mol. Carcinog. 34*, 102–111.

(5) Martin, M. E., Haourigui, M., Pelissero, C., Benassayag, C., and Nunez, E. A. (1996) Interactions between phytoestrogens and human sex steroid binding protein. *Life Sci. 58*, 429–436.

(6) Wong, W. S., and McLean, A. E. M. (1999) Effects of phenolic antioxidants and flavonoids on DNA synthesis in rat liver, spleen, and testis in vitro. *Toxicology 139*, 243–253.

(7) Naiki, H., Hasegawa, K., Yamaguchi, I., Nakamura, H., Gejyo, F., and Nakakuki, K. (1998) Apolipoprotein E and antioxidants have different mechanisms of inhibiting Alzheimer's beta-amyloid fibril formation in vitro. *Biochemistry 37*, 17882–17889.

(8) Barata, H., Cardoso, C. M., Wolosker, H., and de Meis, L. (1999) Modulation of the low affinity Ca^{2+}-binding sites of skeletal muscle and blood platelets Ca^{2+}-ATPase by nordihydroguaiaretic acid. *Mol. Cell. Biochem. 195*, 227–233.

(9) Agarwal, R., Wang, Z. Y., Bik, D. P., and Mukhtar, H. (1991) Nordihydroguaiaretic acid, an inhibitor of lipoxygenase, also inhibits cytochrome P-450-mediated monooxygenase activity in rat epidermal and hepatic microsomes. *Drug Metab. Dispos. 19*, 620–624.

(10) Athar, M., Raza, H., Bickers, D. R., and Mukhtar, H. (1990) Inhibition of benzoyl peroxide-mediated tumor promotion in 7,12-dimethylbenz (a)anthracene-initiated skin of Sencar mice by antioxidants nordihydroguaiaretic acid and diallyl sulfide. *J. Invest. Dermatol. 94*, 162–165.

(11) Moody, T. W., Leyton, J., Martinez, A., Hong, S., Malkinson, A., and Mulshine, J. L. (1998) Lipoxygenase inhibitors prevent lung carcinogenesis and inhibit non-small cell lung cancer growth. *Exp. Lung Res. 24*, 617–628.

(12) Nakadate, T., Yamamoto, S., Aizu, E., and Kato, R. (1989) Inhibition by lipoxygenase inhibitors of 7-bromomethylbenz[a]anthracene-caused epidermal ornithine decarboxylase induction and skin tumor promotion in mice. *Carcinogenesis 10*, 2053–2057.

(13) Nakamura, M., Nakazawa, J., Usui, T., Osada, H., Kono, Y., and Takatsuki, A. (2003) Nordihydroguaiaretic acid, of a new family of microtubule-stabilizing agents, shows effects differentiated from paclitaxel. *Biosci. Biotechnol. Biochem. 67*, 151–157.

(14) Madrigal-Bujaidar, E., Barriga, S. D., Cassani, M., Márquez, P., and Revuelta, P. (1998) In vivo and in vitro antigenotoxic effect of nordihydroguaiaretic acid against SCEs induced by methyl methanesulfonate. *Mutat. Res. 419*, 163–168.

(15) Barriga, S. D., Madrigal-Bujaidar, E., and Márquez, P. (1999) Inhibitory effect of nordihydroguaiaretic acid on the frequency of micronuclei induced by methyl methanesulfonate in vivo. *Mutat. Res. 441*, 53–58.

(16) Biswal, S. S., Datta, K., Shaw, S. D., Feng, X., Robertson, J. D., and Kehrer, J. P. (2000) Glutathione oxidation and mitochondrial depolarization as mechanisms of nordihydroguaiaretic acid-induced apoptosis in lipoxygenase-deficient FL5.12 cells. *Toxicol. Sci. 53*, 77–83.

(17) Deshpande, V. S., and Kehrer, J. P. (2006) Oxidative stress-driven mechanisms of nordihydroguaiaretic acid-induced apoptosis in FL5.12 cells. *Toxicol. Appl. Pharmacol. 214*, 230–236.

(18) Fujimoto, N., Kohta, R., Kitamura, S., and Honda, H. (2004) Estrogenic activity of an antioxidant, nordihydroguaiaretic acid (NDGA). *Life Sci. 74*, 1417–1425.

(19) Lundberg, W. O., Halvorson, H. O., and Burr, G. O. (1944) The antioxidant properties of nordihydroguaiaretic acid. *Oil Soap 21*, 33–35.

(20) Oliveto, E. P. (1972) Nordihydroguaiaretic acid. A naturally occurring antioxidant. *Chem. Ind. 17*, 677–679.

(21) Ramasamy, S., Drummond, G. R., Ahn, J., Storek, M., Pohl, J., Parthasarathy, S., and Harrison, D. G. (1999) Modulation of expression of endothelial nitric oxide synthase by nordihydroguaiaretic acid, a phenolic antioxidant in cultured endothelial cells. *Mol. Pharmacol. 56*, 116–123.

(22) Kelly, M. R., Xu, J., Alexander, K. E., and Loo, G. (2001) Disparate effects of similar phenolic phytochemicals as inhibitors of oxidative damage to cellular DNA. *Mutat. Res. 485*, 309–318.

(23) Harper, A., Kerr, D. J., Gescher, A., and Chipman, J. K. (1999) Antioxidant effects of isoflavonoids and lignans, and protection against DNA oxidation. *Free Radical Res. 31*, 149–160.

(24) Koob, T. J. (2002) Biomimetic approaches to tendon repair. *Comp. Biochem. Physiol. A 133*, 1171–1192.

(25) Gooman, T., Grice, H. C., Becking, G. C., and Salem, F. A. (1970) A cystic neuropathy induced by nordihydroguaiaretic acid in the rat. *Lab. Invest. 23*, 93–107.

(26) Grice, H. C., Becking, G., and Gooman, T. (1968) Toxic properties of nordihydroguaiaretic acid. *Food Cosmet. Toxicol. 6*, 155–161.

(27) Lambert, J. D., Zhao, D., Meyers, R. O., Kuester, R. K., Timmermann, B. N., and Dorr, R. T. (2002) Nordihydroguaiaretic acid: hepatotoxicity and detoxification in the mouse. *Toxicon 40*, 1701–1708.

(28) Gordon, D. W., Rosenthal, G., Hart, J., Sirota, R., and Baker, A. L. (1995) Chaparral ingestion: The broadening spectrum of liver injury caused by herbal medications. *J. Am. Med. Assoc. 273*, 489–490.

(29) Koff, R. S. (1995) Herbal hepatotoxicity: Revisiting a dangerous alternative. *J. Am. Med. Assoc. 273*, 502.

(30) Batchelor, W. B., Heathcote, J., and Wanless, I. R. (1995) Chaparral-induced hepatic injury. *Am. J. Gastroenterol. 90*, 831–833.

(31) Katz, M., and Saibil, F. (1990) Herbal hapaptitis: subacute hepatic necrosis secondary to chaparral leaf. *J. Clin. Gastroenterol. 12*, 203–206.
(32) Clark, F., and Reed, R. (1992) Chaparral-induced toxic hepatitis-California and Texas, 1992. *J. Am. Med. Assoc. 268*, 3295–3296.
(33) Wagner, P., and Lewis, R. A. (1980) Interaction between activated nordihydroguaiaretic acid and deoxyribonucleic acid. *Biochem. Pharmacol. 29*, 3299–3306.
(34) Bolton, J. L., Acay, N. M., and Vukomanovic, V. (1994) Evidence that 4-allyl-*o*-quinones spontaneously rearrange to their more electrophilic quinone methides: potential bioactivation mechanism for the hepatocarcinogen safrole. *Chem. Res. Toxicol. 7*, 443–450.
(35) Iverson, S. L., Hu, L. Q., Vukomanovic, V., and Bolton, J. L. (1995) The influence of the *p*-alkyl substituent on the isomerization of *o*-quinones to *p*-quinone methides: potential bioactivation mechanism for catechols. *Chem. Res. Toxicol. 8*, 537–544.
(36) Thompson, D. C., Thompson, J. A., Sugumaran, M., and Moldeus, P. (1993) Biological and toxicological consequences of quinone methide formation. *Chem.-Biol. Interact. 86*, 129–162.
(37) Chichirau, A., Flueraru, M., Chepelev, L. L., Wright, J. S., Willmore, W. G., Durst, T., Hussain, H. H., and Charron, M. (2005) Mechanism of cytotoxicity of catechols and a naphthalenediol in PC12-AC cells: the connection between extracellular autoxidation and molecular electronic structure. *Free Radical Biol. Med. 38*, 344–355.
(38) Monks, T. J., Hanzlik, R. P., Cohen, G. M., Ross, D., and Graham, D. G. (1992) Quinone chemistry and toxicity. *Toxicol. Appl. Pharmacol. 112*, 2–16.
(39) O'Brien, P. J. (1991) Molecular mechanisms of quinone cytotoxicity. *Chem.-Biol. Interact. 80*, 1–41.
(40) Powis, G. (1987) Metabolism and reactions of quinoid anticancer agents. *Pharmacol. Ther. 35*, 57–162.
(41) Bolton, J. L., Pisha, E., Shen, L., Krol, E. S., Iverson, S. L., Huang, Z., van Breemen, R. B., and Pezzuto, J. M. (1997) The reactivity of *o*-quinones which do not isomerize to quinone methides correlates with alkycatechol-induced toxicity in human melanoma cells. *Chem.-Biol. Interact. 106*, 133–148.
(42) Jordan, R. T., and Allen, L. M. (1988) Pharmacologically active compositions of catecholic butanes with zinc. WO8801509, pp. 1–143.
(43) Lowry, O. H., Rosebrough, N. J., Farr, A. L., and Randall, R. J. (1951) *J. Biol. Chem. 193*, 265.
(44) Omura, T., and Sato, R. (1964) The carbon-monoxide-binding pigment of liver microsomes. II. Solubilization, purification, and properties. *J. Biol. Chem. 239*, 2379–2385.
(45) Perrin, D. D. and Dempsey, B. (1974) *Buffers for pH and Metal Ion Control*. Wiley, New York.
(46) Shen, L., Qiu, S., van Breemen, R. B., Zhang, F., Chen, Y., and Bolton, J. L. (1997) Reaction of the premarin metabolite 4-hydroxyequilenin semiquinone radical with 2′-deoxyguanosine: formation of unusual cyclic adducts. *J. Am. Chem. Soc. 119*, 11126–11127.
(47) Potter, D. W., Miller, D. W., and Hinson, J. A. (1986) Horseradish peroxidase-catalyzed oxidation of acetaminophen to intermediates that form polymers or conjugate with glutathione. *Mol. Pharmacol. 29*, 155–162.
(48) Potter, D. W., Miller, D. W., and Hinson, J. A. (1985) Identification of acetaminophen polymerization products catalyzed by horseradish peroxidase. *J. Biol. Chem. 260*, 12174–12180.
(49) Koob, T. J., and Hernandez, D. J. (2002) Material properties of polymerized NDGA-collagen composite fibers: development of biologically based tendon constructs. *Biomaterials 23*, 203–212.
(50) Herlinger, E., Jameson, R. F., and Linert, W. (1995) Spontaneous autoxidation of dopamine. *J. Chem. Soc., Perkin Trans. 1*, 259–263.
(51) Rinaldi, A. C., Porcu, M. C., Curreli, N., Rescigno, A., Finazzi-Agró, A., Pedersen, J. Z., Rinaldi, A., and Sanjust, E. (1995) Autoxidation of 4-methylcatechol: a model for the study of biosynthesis of copper amine oxidases quinoid cofactor. *Biochem. Biophys. Res. Commun. 214*, 559–567.
(52) Shen, L., Pisha, E., Huang, Z., Pezzuto, J. M., Krol, E. S., Alam, Z., van Breemen, R. B., and Bolton, J. L. (1997) Bioreductive activation of catechol estrogen-ortho-quinones: Aromatization of the B ring in 4-hydroxyequilenin markedly alters quinone formation and reactivity. *Carcinogenesis 18*, 1093–1101.
(53) Joslyn, M. A., and Branch, G. E. K. (1935) The kinetics of absorption of oxygen by catechol. *J. Am. Chem. Soc. 57*, 1779–1785.
(54) Roginsky, V., and Alegria, A. E. (2005) Oxidation of tea extracts and tea catechins by molecular oxygen. *J. Agric. Food Chem. 53*, 4529–4535.
(55) Schusler-van Hees, M. T., Beijersbergen van Henegouwen, G. M., and Stoutenberg, P. (1985) Autoxidation of catechol(amine)s. *Pharm. Weekbl. Sci. 7*, 245–251.
(56) Nebot, C., Moutet, M., Huet, P., Xu, J. Z., Yadan, J. C., and Chaudiere, J. (1993) Spectrophotometric assay of superoxide dismutase activity based on the activated autoxidation of a tetracyclic catechol. *Anal. Biochem. 214*, 442–451.
(57) Moridani, M. Y., Siraki, A., Chevaldina, T., Scobie, H., and O'Brien, P. J. (2004) Quantitative structure toxicity relationships for catechols in isolated rat hepatocytes. *Chem.-Biol. Interact. 147*, 297–307.
(58) Evans, D. C., Watt, A. P., Nicoll-Griffith, D. A., and Baillie, T. A. (2004) Drug-protein adducts: an industry perspective on minimizing the potential for drug bioactivation in drug discovery and development. *Chem. Res. Toxicol. 17*, 3–16.
(59) Ju, C., and Uetrecht, J. P. (2002) Mechanism of idiosyncratic drug reactions: reactive metabolite formation, protein binding and the regulation of the immune system. *Curr. Drug Metab. 3*, 367–377.

TX700205J

5. Nordihydroguaiaretic Acid Autoxidation Produces a Schisandrin-like Dibenzocyclooctadiene Lignan

Jennifer L. Billinsky and Ed S. Krol

Journal of Natural Products, 2008, *71* (9), pp 1612–1615

Publication Date (Web): August 2, 2008 (Note)

DOI: 10.1021/np8001354

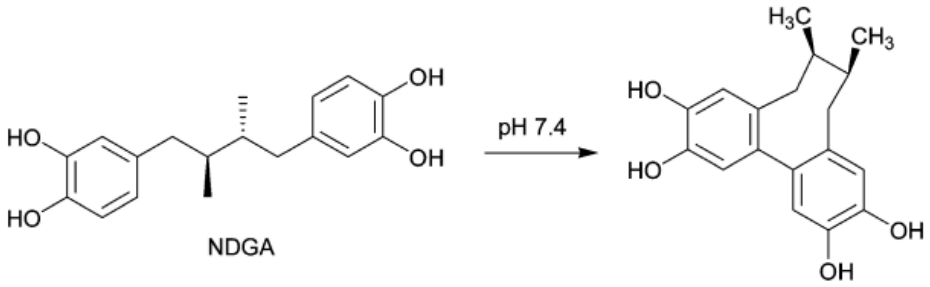

Notes

Nordihydroguaiaretic Acid Autoxidation Produces a Schisandrin-like Dibenzocyclooctadiene Lignan

Jennifer L. Billinsky[†] and Ed S. Krol*[,‡]

Graduate Toxicology Program, University of Saskatchewan, Saskatoon, SK Canada, and College of Pharmacy and Nutrition, University of Saskatchewan, Saskatoon, SK Canada

Received March 4, 2008

The lignan *meso*-nordihydroguaiaretic acid is known to undergo spontaneous oxidation in alkaline solution. In the presence of the trapping agent glutathione, the major oxidation products are consistent with the formation of a *meso*-nordihydroguaiaretic acid *ortho*-quinone. In the absence of a trapping agent however, the major oxidation product of *meso*-nordihydroguaiaretic acid in aqueous solution is a unique, stable schisandrin-like dibenzocyclooctadiene lignan that may be responsible for some of the biological effects of nordihydroguaiaretic acid.

Nordihydroguaiaretic acid (NDGA, masoprocol, **1**) (Figure 1) is a naturally occurring lignan from the creosote bush (*Larrea tridentata*). NDGA has been utilized in traditional healing practices for a wide range of ailments[1,2] and was licensed for use as a topical treatment for actinic keratosis (Actinex, Chemex Pharmaceuticals, Denver, CO). Use of NDGA for therapeutic purposes is currently limited due to reports of contact hypersensitivity,[3] nephrotoxicity,[4] hepatotoxicity,[5,6] and cytotoxicity.[5,7,8] It has been suggested that the toxicity is the result of oxidation to a reactive *ortho*-quinone species,[4] the presence of which we recently confirmed via trapping of NDGA *ortho*-quinones as glutathione (GSH) adducts.[9] NDGA has been shown to increase oxidized glutathione (GSSG) and lipid peroxidation levels in murine hematopoietic cells,[10] suggesting an increase in oxidative stress consistent with the formation of an *ortho*-quinone. There are numerous reports that NDGA can be unstable in aqueous media,[4,11−13] especially at elevated pH,[11,13] with a half-life of 3.1 h at pH 7.4.[9] NDGA, in the presence of O_2, has been reported to undergo conversion to an *ortho*-quinone,[12] or to an unspecified "activated NDGA", with a λ_{max} 286nm.[11] In this study we have isolated and identified the major non-GSH reactive product of NDGA autoxidation in aqueous solution and determined that NDGA forms a unique, stable nonquinone compound with a λ_{max} of 286 nm, suggesting it is the "activated NDGA" previously reported.[11]

NDGA was incubated at pH 7.4 in the absence of GSH, and HPLC was used to monitor the reaction. A mixture of products was observed and the reaction mixture was further analyzed by LC-MS (Figure 2). One of the LC-MS peaks was consistent with an *ortho*-quinone of NDGA that has undergone hydroxylation (t_R = 29 min, **3** ES-MS *m/z* 315 (100%) $[M - H]^-$). The ES-MS results for the 22 and 25 min peaks were consistent with either an *ortho*-quinone or *para*-quinone methide (ES-MS *m/z* 299 (100%) $[M - H]^-$), although previous studies suggested that *para*-quinone methide formation is unlikely.[9] Addition of GSH to the incubation mixture resulted in disappearance of both the 25 min and the 29 min peaks and the appearance of NDGA-SG adducts (data not shown). The major product, the 22 min peak (**4**), however was unaffected by the addition of GSH, suggesting it was not a quinone

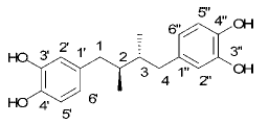

1

Figure 1. Nordihydroguaiaretic acid (NDGA).

species. The peak at 34 min was confirmed as being NDGA (**1**) by MS (ES-MS *m/z* 301 (100%) $[M - H]^-$) and comparison with an authentic standard.

Compound **4** was isolated and purified via reversed-phase flash column chromatography and was found to have an identical UV absorbance maximum (286 nm) to the previously unidentified autoxidation product of NDGA.[11] NDGA possesses a plane of symmetry, so that only half of the protons and carbons appear in the NMR spectrum. ^1H and ^{13}C NMR spectroscopic data for compound **4** indicate that distinct resonances are observed for all of the alkyl and aromatic protons. There are several pieces of NMR evidence to suggest that **4** is an intramolecular cyclization product of NDGA (Figure 3). Four singlets in the aromatic region corresponding to one proton each were observed (HMQC), suggesting that two of the aromatic protons of NDGA have been substituted due to the formation of a new carbon−carbon bond. A coupling reaction involving C-2′, C-2″, C-5′, or C-5″ of NDGA would result in splitting of the aromatic ^1H NMR signals. Our results suggest that coupling has occurred between the C-6′ and C-6″ positions of NDGA, which have previously been shown to be highly reactive.[9] A second piece of evidence comes from a COSY NMR experiment for **4**, where it was determined that only one of the CH_2 protons at C-7 is coupled to the adjacent CH proton at C-8 (this is also the case for the protons on C-7′ and C-8′), suggesting that one of the CH_2 protons is held at a 90° dihedral angle to the CH, a conformation that may be attained in an eight-membered ring. A compound that has cyclized between the aromatic C-6′ and C-6″ carbons of NDGA would result in the dibenzocyclooctadiene lignan **4**, as represented in Figure 4. As a result of the nonplanar eight-membered ring that is formed, compound **4** has no plane of symmetry and the NMR chemical shifts for all of the protons and carbon atoms of **4** are distinguishable. The aromatic protons at C-1 and C-9 of compound **4** (the numbering in NDGA **1** differs from that for the NDGA-derived dibenzocyclooctadiene lignan **4**; refer

* To whom correspondence should be addressed. Tel: (306) 966-2011. Fax: (306) 966-6377. E-mail: ed.krol@usask.ca.
† Graduate Toxicology Program.
‡ College of Pharmacy and Nutrition.

10.1021/np8001354 CCC: $40.75
Published on Web 08/02/2008

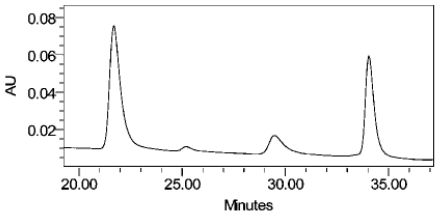

Figure 2. LC-MS-ES(−) (microbore column, see Experimental Section) for NDGA autoxidation products, pH 7.4, 37 °C. $t_R = 22$ min, *m/z* 299 $[M - H]^-$ (**4**); $t_R = 25$ min, *m/z* 299 $[M - H]^-$ (**2**); $t_R = 29$ min, *m/z* 315 $[M - H]^-$ (**3**); $t_R = 34$ min, *m/z* 301 $[M - H]^-$ (NDGA **1**).

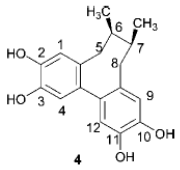

Figure 3. Structure of the NDGA-derived dibenzocyclooctadiene lignan **4**, the major NDGA autoxidation product at pH 7.4, 37 °C.

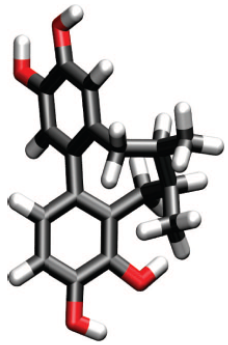

Figure 4. Representation of NDGA-derived dibenzocyclooctadiene lignan **4** in the *R*-biphenyl configuration from *meso*-NDGA **1**. This representation is based on NMR and CD data, after energy minimization in the MMFF94 force field using Spartan '06 (Wavefunction Inc., Irvine, CA). Image generated using VMD (Urbana, IL).

to Figures 1 and 3) were tentatively assigned from observed NOEs with H-5 and H-8, respectively. The ^{1}H and ^{13}C NMR results for the alkyl region were comparable to those of other dibenzocyclooctadiene lignans including gomisin J[14] and the (*R*,*R*)-tetramethoxy analogue of **4**.[15,16] A crystal structure reported for the (*R*,*R*)-tetramethoxy analogue of **4** indicates the phenyl rings are twisted about the biphenyl bond by an angle of 117.8°.[16] Compound **4**, determined by CD to be in the *R*-biphenyl configuration, displays a similar out-of-plane twist.

Similar coupling products have been prepared via oxidation of 4-methylcatechol with phenoloxidase,[17] and numerous synthetic dibenzocyclooctadiene lignans have been prepared from intramolecular cyclization reactions of matairesinol derivatives.[18−20] One possible mechanism for formation of dibenzocyclooctadiene lignan **4** from NDGA via a radical intermediate is suggested in Figure 5, although other radical and nonradical processes cannot be ruled out. This mechanism requires initial formation of phenoxy radicals at the 3′-OH and 3″-OH of NDGA. This diphenoxy radical of NDGA would undergo radical coupling of the carbon atoms *para* to the 3′- and 3″-OH of NDGA via the carbon-centered resonance forms (Figure 5).

A group of dibenzocyclooctadiene lignans known as schisandrins, isolated from *Schisandra chinensis*, have been studied for their potential therapeutic properties including the ability to protect against oxidative stress as antioxidants[21] or via enhancement of GSH synthesis;[22,23] the ability to inhibit P-glycoprotein[24] and multidrug resistance-associated protein 1;[25] and enhancement of apoptosis through caspase-9 activation.[26] In addition, schisandrin B is a substrate for murine CYP2E1,[27] and several schisandrins have been found to be CYP3A4 inhibitors.[28] The NDGA-derived dibenzocyclooctadiene lignan **4** is an analogue of the schisandrins and thus may also display similar biological activity. It is conceivable that the NDGA-derived dibenzocyclooctadiene lignan is also responsible for a portion of the biological activity of NDGA, especially if NDGA undergoing biological study is maintained under aerobic conditions for extended periods of time at pH 7.4 or higher.

We have observed that in the absence of GSH at pH 8.0, 37 °C, 50% of the NDGA is mainly converted to **4** after a 1 h incubation, with smaller amounts present as the *ortho*-quinone and hydroxylated *ortho*-quinone. In our microsomal incubations (pH 7.4, 37 °C) NDGA is preincubated for 5 min followed by a 60 min incubation, which is sufficient for measurable NDGA autoxidation to occur. NDGA is a known antioxidant[29] and a lipoxygenase inhibitor[2] and has been shown to inhibit P450[30] and suppress growth of breast cancer cells.[31] All of these systems incubate NDGA at or near pH 7.4, suggesting that at least some of the observed activity may be the result of the NDGA-derived dibenzocyclooctadiene lignan or an NDGA *ortho*-quinone. An *ortho*-quinone of NDGA would be expected to be involved in redox cycling or adduct formation with biological macromolecules,[9] whereas the dibenzocyclooctadiene lignan appears to be more stable and may be responsible for mediating biological processes associated with NDGA that are not necessarily associated with toxicity.

Extracts from Creosote bush containing NDGA used in traditional healing practices are typically prepared by boiling in water and then being either applied topically as a salve or paste or consumed as a tea (T. D. Johnson, personal communication). It is possible that the traditional extraction process may result in a significant conversion of NDGA- to NDGA-derived dibenzocyclooctadiene; however, this will require further investigation. An NDGA-derived dibenzocyclooctadiene lignan, in which the stereochemistry was not specified, has been screened by the National Cancer Institute (NSC 669349) in the United States and displays LD_{50} values in the μM range. In order to determine whether the NDGA-derived dibenzocyclooctadiene lignan **4** is responsible for the effects in the NCI study or any other biological activity associated with NDGA, it will be necessary to test the NDGA-derived dibenzocyclooctadiene lignan derived from *meso*-NDGA in a variety of *in vitro* systems. Of perhaps greater issue is that due to the rapid formation of the NDGA-derived dibenzocyclooctadiene lignan under conditions used for many *in vitro* studies, interlaboratory differences in incubation conditions for NDGA-dependent experiments could lead to significantly different results depending on the actual amount of NDGA- or NDGA-derived dibenzocyclooctadiene lignan present.

Experimental Section

General Experimental Procedures. ***Caution*****:** *NDGA is hazardous and should be handled carefully. meso*-Nordihydroguiairetic acid (NDGA) from *Larrea tridentata* was purchased from Sigma-Aldrich Co. (Madison, WI). Citric acid and K_2HPO_4 were purchased from Fisher Scientific (Ottawa, ON). HCl was purchased from BDH (Toronto, ON). All solvents were HPLC grade. Water was purified via a Millipore Milli-Q system (Mississauga, ON) with a Quantum EX cartridge.

UV spectra were recorded on an Agilent 8453 using Chem Station software. Negative electrospray mass spectra were obtained using an API Qstar XL with an Agilent 1100 HPLC (Saskatchewan Structural

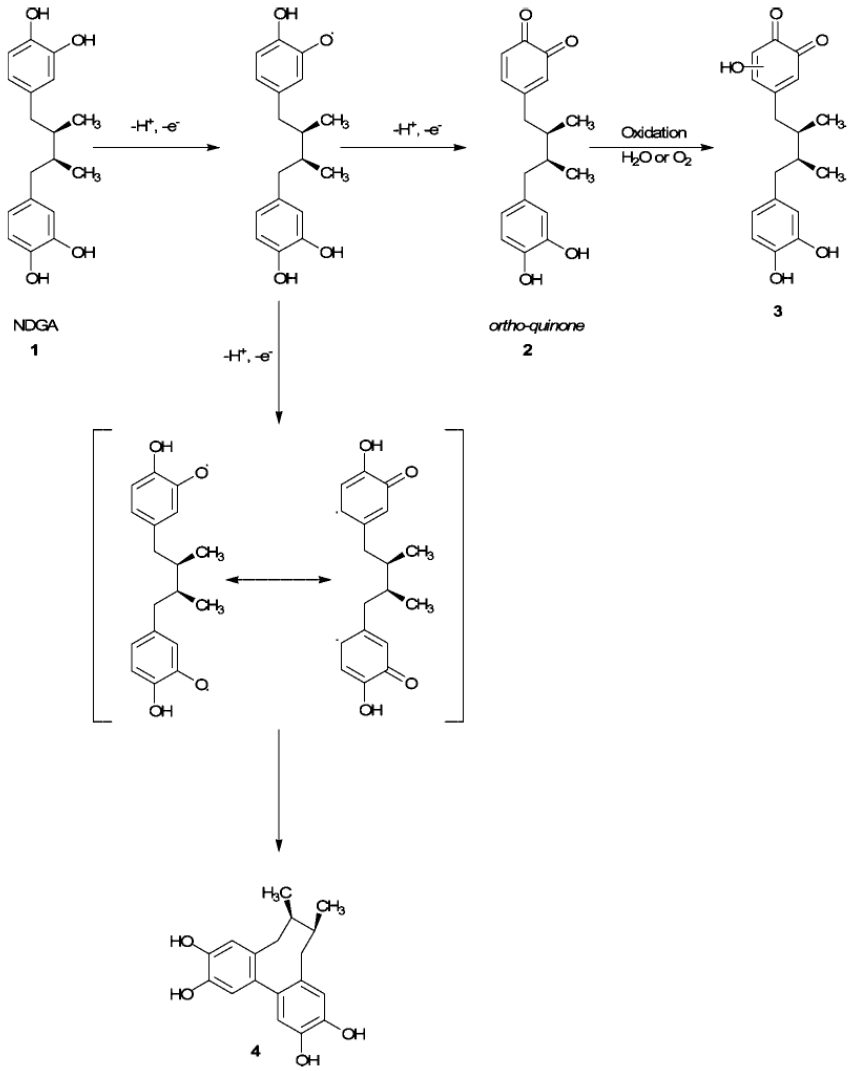

Figure 5. Possible reaction pathway for the formation of NDGA autoxidation products **3** and **4** in the absence of GSH.

Sciences Centre). NMR data were obtained on a Bruker AVANCE DPX-500 (Dept of Chemistry, University of Saskatchewan) operating at 500 and 125 MHz for proton and carbon, respectively, and the data analyzed using XWIN-NMR version 3.0. Residual signals from CD_3OD [3.30 ppm (^1H) and 49.0 ppm (^{13}C)] served as an internal standard. Programs for 2D experiments were available from the software package XWINNMR, provided by Bruker. The DEPT experiment together with 2D NMR experiments including COSY, HMQC, and NOESY experiments were performed with gradient pulses. CD data were obtained on an Applied Photophysics PiStar-180 spectrometer.

Autoxidation Incubation for ES-MS Analysis. A solution of NDGA in CH_3CN (20 mM) was added to 0.5 M pH 7.4 phosphate-citric acid buffer pre-equilibrated to 37 °C to give a final NDGA concentration of 0.1 mM. The reaction mixture was placed in a shaking water bath for 60 min, during which time the colorless solution became pink. The reaction was stopped by acidification to pH 1.5 with HCl. Autoxidation was not effected by light, as no difference was observed for dark control reactions. Aliquots of the supernatant (50 μL) were analyzed directly by electrospray LC-MS operating in the negative mode. An Allsphere ODS-2 microbore column (3 μm, 150 × 2.1 mm) operating at a flow rate of 0.2 mL/min was used to run a gradient elution. Solvent A: 0.1% formic acid/H_2O, solvent B: 0.1% formic acid/CH_3CN. An initial isocratic phase of 80% A for 2 min, decreased to 65% A over 38 min, isocratic for 1 min, and finally increased to 80% A over 1 min.

Synthesis of the NDGA Autoxidation Product. A solution of NDGA in CH_3CN (20 mM) was added to 0.5 M pH 8.5 phosphate-citric acid buffer pre-equilibrated to 37 °C to give a final NDGA concentration of 0.1 mM. The reaction mixture was placed in a shaking water bath for 90 min, during which time the colorless solution became pink. The reaction was stopped by acidification to pH 1.5 with HCl. The reaction mixture was concentrated *in vacuo* to yield a purple solid. The oxidation product was purified by C-18 flash column chromatography, using 70:30 H_2O/CH_3CN (v/v) containing 0.1%TFA, yielding an off-white solid.

(6*R*,7*S*)-2,3,10,11-Tetrahydroxy-6,7-dimethyl-5,6,7,8-tetrahydrodibenzo[*a*,*c*]cyclooctene (4): CD (*c* 0.62, CH_3OH) $[\theta]_{286}$ +15158.7; UV (CH_3CN) λ_{max} (log ϵ) 286 nm (3.87); ^1H NMR (CD_3OD, 500 MHz) δ 0.78 (3H, d, J = 6.9 Hz, CH_3-6), 0.99 (3H, d, J = 7.0 Hz, CH_3-7), 1.79 (1H,m, CH-7), 1.88 (1H, m, CH-6), 1.93 (1H, d, J = 13.2 Hz, CH_2-8b), 2.21 (1H, dd, J = 9.6, 13.2 Hz, CH_2-8a), 2.39 (1H,d, J =

13.5 Hz, CH_2-5b), 2.54 (1H, dd, $J = 7.5$, 13.5 Hz, CH_2-5a), 6.54 (1H, s, ArCH-9), 6.57 (1H, s, ArCH-1), 6.61 (1H, s), 6.63 (1H, s); ^{13}C NMR (CD_3OD, 125 MHz) δ 12.7 (CH_3-6), 22.2 (CH_3-7), 35.1 (C-6), 35.9 (C-8), 39.7 (C-5), 42.2 (C-7), 116.7, 117.3 (ArC-9), 117.6 (ArC-1), 119.9, 130.3, 133.7, 134.7, 135.8, 143.9, 144.1, 144.5, 145.6; ES-MS $t_R = 22$ min, negative ion electrospray-MS (80% CH_3CN with 0.1% formic acid), *m/z* 299 (100%) $[M - H]^-$); yield 16.2 mg, 54%.

Acknowledgment. This work was funded by HSURC, NSERC, and CFI. J.L.B. was a recipient of an NSERC PGS award. The authors wish to thank Dr. D. R. J. Palmer for help with generating the dibenzocyclooctadiene lignan image.

References and Notes

(1) Lambert, J. D.; Dorr, R. T.; Timmermann, B. *Pharm. Biol.* **2004**, *42*, 149–158.
(2) Arteaga, S.; Andrade-Cetto, A.; Cardenas, R. *J. Ethnopharmacol.* **2005**, *98*, 231–239.
(3) Olsen, E. A.; Abernethy, M. L.; Kulp-Shorten, C.; Callen, J. P.; Glazer, S. D.; Huntley, A.; McCray, M.; Monroe, A. B.; Tschen, E.; Wolf, J. E., Jr. *J. Am. Acad. Dermatol.* **1991**, *24*, 738–743.
(4) Grice, H. C.; Becking, G.; Gooman, T. *Food Cosmet. Toxicol.* **1968**, *6*, 155–161.
(5) Lambert, J. D.; Zhao, D.; Meyers, R. O.; Kuester, R. K.; Timmermann, B. N.; Dorr, R. T. *Toxicon* **2002**, *40*, 1701–1708.
(6) Grant, K. L.; Boyer, L. V.; Erdman, B. E. *Integr. Med.* **1998**, *1*, 83–87.
(7) Gooman, T.; Grice, H. C.; Becking, G. C.; Salem, F. A. *Lab. Invest.* **1970**, *23*, 93–107.
(8) Moridani, M. Y.; Siraki, A.; Chevaldina, T.; Scobie, H.; O'Brien, P. J. *Chem. Biol. Interact.* **2004**, *147*, 297–307.
(9) Billinsky, J. L.; Marcoux, M. R.; Krol, E. S. *Chem. Res. Toxicol.* **2007**, *20*, 1352–1358.
(10) Biswal, S. S.; Datta, K.; Shaw, S. D.; Feng, X.; Robertson, J. D.; Kehrer, J. P. *Toxicol. Sci.* **2000**, *53*, 77–83.
(11) Wagner, P.; Lewis, R. A. *Biochem. Pharmacol.* **1980**, *29*, 3299–3306.
(12) Jordan, R. T. Allen, L. M. Pharmacologically Active Compositions of Catecholic Butanes with Zinc. Int. Patent WO8801509, 1988.
(13) Yasumoto, K.; Yamamoto, A.; Mitsuda, H. *Agric. Biol. Chem.* **1970**, *34*, 1162–1168.
(14) Bhathena, S. J.; Ali, A. A.; Haudenschild, C.; Latham, P.; Ranich, T.; Mohamed, A. I.; Hansen, C. T.; Velasquez, M. T. *J. Am. Coll. Nutr.* **2003**, *22*, 157–164.
(15) Biftu, T.; Hazra, B. G.; Stevenson, R. *J. Chem. Soc., Perkin Trans. 1* **1979**, 2276–2281.
(16) Buckleton, J. S.; Cambie, R. C.; Clark, G. R.; Craw, P. A.; Rickard, C. E. F.; Rutledge, P. S.; Woodgate, P. D. *Aust. J. Chem.* **1988**, *41*, 305–324.
(17) Andersen, S. O.; Jacobsen, J. P.; Bojesen, G.; Roepstorff, P. *Biochim. Biophys. Acta* **1992**, *1118*, 134–138.
(18) Takeya, T.; Okubo, T.; Nishida, S.; Tobinaga, S. *Chem. Pharm. Bull.* **1985**, *33*, 3599–3607.
(19) Cambie, R. C.; Clark, G. R.; Craw, P. A.; Rutledge, P. S.; Woodgate, P. D. *Aust. J. Chem.* **1984**, *37*, 1775–1784.
(20) Kramer, B.; Averhoff, A.; Waldvogel, S. R. *Angew. Chem., Int. Ed.* **2002**, *41*, 2981–2982.
(21) Choi, Y. W.; Takamatsu, S.; Khan, S. I.; Srinivas, P. V.; Ferreira, D.; Zhao, J.; Khan, I. A. *J. Nat. Prod.* **2006**, *69*, 356–359.
(22) Chiu, P. Y.; Ko, K. M. *Biofactors* **2006**, *26*, 221–230.
(23) Chiu, P. Y.; Leung, H. Y.; Poon, M. K.; Mak, D. H.; Ko, K. M. *Mol. Cell. Biochem.* **2006**, *289*, 185–191.
(24) Pan, Q.; Lu, Q.; Zhang, K.; Hu, X. *Cancer Chemother. Pharmacol.* **2006**, *58*, 99–106.
(25) Li, L.; Pan, Q.; Sun, M.; Lu, Q.; Hu, X. *Life Sci.* **2007**, *80*, 741–748.
(26) Li, L.; Lu, Q.; Shen, Y.; Hu, X. *Biochem. Pharmacol.* **2006**, *71*, 584–595.
(27) Chiu, P. Y.; Leung, H. Y.; Poon, M. K.; Lee, S. S.; Ko, K. M. *Mol. Cell. Biochem.* **2006**, *293*, 87–92.
(28) Iwata, H.; Tezuka, Y.; Kadota, S.; Hiratsuka, A.; Watabe, T. *Drug Metab. Dispos.* **2004**, *32*, 1351–1358.
(29) Lundberg, W. O.; Halvorson, H. O.; Burr, G. O. *Oil Soap* **1944**, *21*, 33–35.
(30) Agarwal, R.; Wang, Z. Y.; Bik, D. P.; Mukhtar, H. *Drug Metab. Dispos.* **1991**, *19*, 620–624.
(31) Youngren, J. F.; Gable, K.; Penaranda, C.; Maddux, B. A.; Zavodovskaya, M.; Lobo, M.; Campbell, M.; Kerner, J.; Goldfine, I. D. *Breast Cancer Res. Treat.* **2005**, *94*, 37–46.

NP8001354

6. A Comparison Between Lignans From Creosote Bush and Flaxseed and Their Potential to Inhibit Cytochrome P450 Enzyme Activity

Jennifer Billinsky, Erin Boyd, Katherine Maloney, Ed Krol, Jane Alcorn.

Submitted for publication to Food and Chemical Toxicology.

Date submitted: July 9th 2009

Title: A comparison between lignans from creosote bush and flaxseed and their potential to inhibit cytochrome P450 enzyme activity

Jennifer Billinsky[1,2], Erin Boyd, Katherine Maloney[1], Ed Krol[1], Jane Alcorn[1*]

[1]College of Pharmacy and Nutrition, University of Saskatchewan, 110 Science Place, Saskatoon, SK, Canada, S7N 5C9
[2]Toxicology Graduate Program, University of Saskatchewan, 44 Campus Drive, Saskatoon, SK, Canada, S7N 5B3

*Corresponding author (Tel: (306) 966-6365, Fax: (306) 966-6377, e-mail: jane.alcorn@usask.ca)

Running title: Lignan inhibition of P450 enzyme activity

Keywords: lignans, creosote bush, flaxseed, P450 enzymes, inhibition, activation

- Supplementary figures which were not submitted for this manuscript publication can be found in Appendix A. These figures are referred to as Figure A.

1

[1] Abbreviations

16α-OH – 16α-hydroxytestosterone
ASECO – Anhydrosecoisolariciresinol
ED – Enterodiol
EL – Enterolactone
GSH - Glutathione
NDGA – Nordihydroguaiaretic acid
P450 – Cytochrome P450
SDG – Secoisolariciresinol diglucoside
SECO – Secoisolariciresinol

6.1 Abstract

Despite their structural similarity, the lignan of creosote bush has demonstrated toxicity associated with oral consumption while flaxseed lignans have no reported serious toxicity. The ability of lignans to cause either reversible or mechanism based inhibition of cytochrome P450 (P450) isoforms in rat hepatic microsomes was studied as a potential mechanism for this difference in toxicity potential. Neither creosote bush nor flaxseed lignan exhibited P450-mediated bioactivation, although previous reports do indicate bioactivation of creosote bush lignan to an ortho-quinone by a non P450-mediated mechanism. Both creosote bush and flaxseed lignans caused reversible inhibition of P450 enzyme activity that involved competitive or mixed-type inhibition. However, reversible inhibition was present at nonphysiologically relevant concentrations suggesting that the relevance of such interactions *in vivo* is limited. Interestingly, activation of cytochrome P450 isoforms was also observed at low lignan concentrations. Our data suggest that P450-mediated bioactivation or reversible inhibition cannot explain the differences in toxicity noted between the lignans of creosote bush and flaxseed. Whether non P450- mediated bioactivation of creosote bush lignan is responsible for the observed toxicity warrants further investigation.

6.2 Introduction

The popularity in natural product use I witness today arose from a growing public skepticism about taking "pharmaceutical chemicals" to treat illness. Such skepticism was supplanted by a public perception that "medications" from natural sources are safer to use and have similar efficacies as their pharmaceutical equivalents. The diverse assortment of natural products on the shelves of pharmacies, health food stores, and grocery stores attest to this enhanced public demand, but has compelled regulatory agencies to question the adequacy of the safety and efficacy data associated with the use of these products[10]. In the current regulatory environment, full realization of the wellness and therapeutic value of these natural products can only come about with more rigorous assessments of their safety and efficacy.

This is particularly true of natural products that contain lignans as the principal bioactive component. Interest in lignans continues to grow due to an increased awareness of their putative health benefits. One such product, Chaparral, contains lignans extracted from creosote bush. Creosote bush had centuries of traditional use by aboriginal peoples of the Southwestern United States as an effective natural medicine and was marketed as an extract of the plant in capsule form based on this historical medicinal value[106]. While traditional creosote bush use appears to be quite safe, chronic use of Chaparral led to reports of toxicity[33,35,106,107]. Nordihydroguaiaretic acid (NDGA) is the lignan of creosote bush, which is believed to be responsible for both the efficacious and toxic properties of Chaparral[27,31,41,162]. Wagner and Lewis 1980 previously reported that NDGA undergoes oxidation to "activated NDGA"[121]. Billinsky et al. 2008 suggest this "activated NDGA" is the result of an autoxidation process to a stable dibenzocyclooctadiene product of NDGA[163]. Whether this dibenzocyclooctadiene is present in traditional creosote bush products or is formed *in vivo* is not known.

The recent popularity of lignans from flaxseed, which are currently marketed as concentrated extracts of the principal plant lignan, secoisolariciresinol diglucoside (SDG), in products such as Brevail™ and Beneflax™, arises from recent promising clinical trial evidence of their chemopreventive and therapeutic properties for a variety of chronic diseases[93,94,164]. Following oral consumption, the glucose groups of SDG are cleaved to form the aglycone, secoisolariciresinol (SECO), which is further metabolized

to the mammalian lignans, enterodiol (ED) and enterolactone (EL), by colonic bacteria[54,55]. Flaxseed also contains smaller amounts of other lignans such as mataresinol, and lariciresinol. The presence of anhydrosecoisolariciresinol (ASECO) was reported in flaxseed[61]. However, its actual presence is questioned as the acid hydrolysis method used to extract and quantify lignans from flaxseed can convert SECO into ASECO [53]. Which lignan form mediates the putative health effects is not known, but little evidence of toxicity exists with their use, and most clinical trial data identifies their relative safety. Interestingly, a comparison of the structure of NDGA from creosote bush with the flaxseed lignan, SDG and its aglycone form, SECO, identifies remarkable structurally similarity, yet with obvious differences in their safety profiles (Figure 6.1).

Why lignan in Chaparral is associated with toxicity while lignans from flaxseed have limited reported toxicity may relate to differences in their ability to inhibit cytochrome P450 (P450) enzymes. Cytochrome P450 enzymes are the principal detoxification mechanisms of the body and mediate the elimination of a wide variety of drugs, phytochemicals, and environmental toxicants. Consequently, interactions involving P450 enzymes are widely reported in the literature. Such P450 enzyme interactions often involve P450 inhibition, which may proceed either through mechanism-based, irreversible interaction with a P450 enzyme or by a reversible competitive interaction between two substrates for the same P450. Both inhibition mechanisms represent common underlying mechanisms for toxicity associated with pharmaceutical products, phytochemicals and environmental toxicants[142].

Mechanism-based, irreversible inhibition of P450 usually follows from bioactivation by P450 to a reactive metabolite that, in turn, covalently binds to the enzyme (heme or apoprotein) and prevents further P450 activity[144]. Enzyme function is only restored with synthesis of new enzyme. Alternatively, the reactive metabolite may bind to other macromolecules (i.e. protein, nucleic acid) to inhibit their function or form a hapten leading to an immune response with toxicological outcomes[144]. Hence, P450-mediated bioactivation to reactive metabolites can represent an important mechanism of toxicity associated with natural product use. Reversible competitive interactions at the same P450 can also result in toxicity when natural products are present simultaneously with other chemicals whose metabolic clearance is predominantly dependent upon a

particular P450 enzyme[142]. Competitive interactions, then, may lead to the accumulation of a compound and eventual toxicity. Given the potential for significant adverse outcomes, evaluation of P450 inhibition is commonly investigated during standard safety assessments for drugs, environmental contaminants, and phytochemicals.

Our purpose was to determine whether mechanism-based, irreversible inhibition and/or reversible, competitive P450 inhibition might explain the differences in apparent toxicity between oral consumption of naturally occurring lignans from creosote bush, which have known toxicity, and flaxseed, which show relative safety. Additionally, such information is important to determine whether lignans present a significant concern with respect to their potential for P450-mediated interactions. As a proof-of-concept study, rat hepatic microsomal systems were employed to investigate the hypothesis that lignan from creosote bush undergoes P450-enzyme mediated bioactivation to form reactive metabolites while flaxseed lignans do not. Furthermore, I hypothesized that lignan from creosote bush inhibits P450 enzyme activity via mechanism-based and/or reversible inhibition mechanisms and that glutathione can attenuate the inhibition. The use of rat also supports current investigations in our laboratories concerning lignan efficacy and pharmacokinetics in rat models of hyperlipidemia and hyperglycemia[165]. Such investigations will make an invaluable contribution to our understanding of the safety of natural products containing lignan as the principal bioactive component.

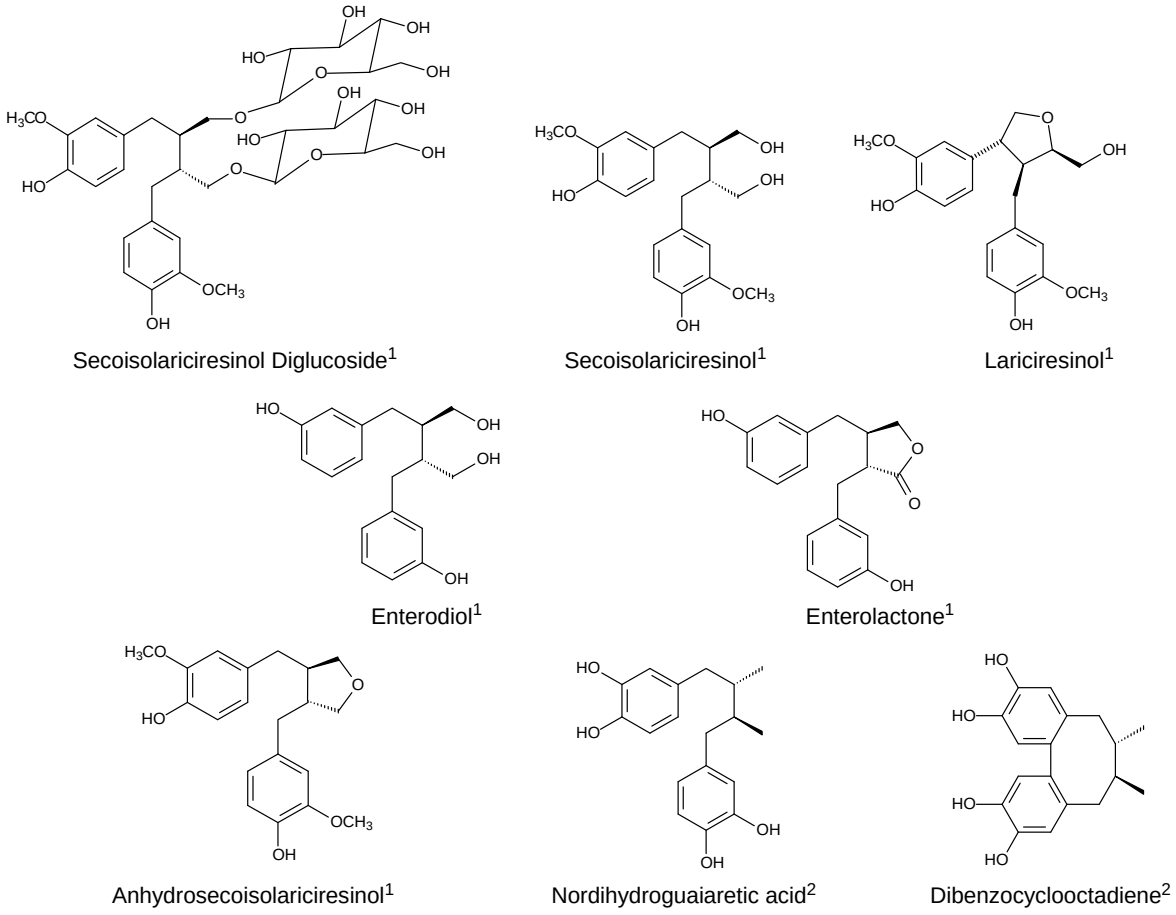

Figure 6.1: Structures of lignans derived from Flaxseed[1] and Creosote bush[2].

6.3 Methods

Chemicals

Acetaminophen, NADPH, trifluoroacetic acid, Folin and Ciocalteu's phenol reagent, testosterone, 6β-hydroxytestosterone, 2α-hydroxytestosterone, dimethoxyphenylacetone (DMPA), resorufin, resorufin methyl ether (methoxyresorufin), glutathione (GSH), nordihydroguaiaretic acid, enterodiol, enterolactone, and dimethylsulfoxide were purchased from Sigma-Aldrich Canada Ltd. (Oakville, ON). 16α-Hydroxytestosterone was purchased from Steraloids Inc. (Newport, RI). Silca gel 60 (230-400 mesh) was purchased from EMD Chemicals Inc. (Gibbstown, NJ). Secoisolariciresinol diglucoside (>95%) and secoisolariciresinol (>95%) (SECO) and were kind gifts from Agriculture and Agri-Food Canada, Saskatoon Research Centre (Dr. Alister Muir). Anhydrosecoisolariciresinol was synthesized from SECO. All other

chemicals were of the highest grade required for the experiments and solvents were high performance liquid chromatography grade. A MilliQ Synthesis (Millipore, Bedford, MA) water purification system provided purified deionized water.

Animals

Male Sprague-Dawley (SD) rats, 11 weeks old, were purchased from Charles River Laboratories, Inc. (Saint-Constant, PQ). Rats were housed in a temperature, humidity and 12 hour light-dark controlled facility and allowed a one-week acclimatization period during which time rats were fed standard laboratory rat chow *ad libitum* and had free access to water. All animal use and care was conducted in accordance with the Canadian Council on Animal Care and was approved by the University Committee on Animal Care and Supply at the University of Saskatchewan.

Synthesis of Anhydrosecoisolariciresinol

Secoisolariciresinol (SECO) (0.254 g, 0.702 mmol) was added to a 100 mL round bottom flask and dissolved in 30 mL of methanol. To the flask, 15 drops of concentrated HCl was added and the reaction mixture was refluxed at 60ºC for 20 hours at which time the reaction was quenched with 30 mL of water and extracted 3 times with ethyl acetate (40 mL). The organic layer was washed with 80 mL of sodium bicarbonate (0.6 M) and 80 mL of water and then dried with $MgSO_4$. The organic layer was filtered and dried to a volume of about 1 mL under vacuum. A normal phase silica gel flash column with 9:1 (dichloromethane:ethyl acetate) was used to purify anhydrosecoisolariciresinol (ASECO) to an off-white powder (0.0092 g, 0.268 mmol, 38% yield).

Preparation of Hepatic Microsomes

Rats (n=4) were anesthetized with isoflurane and a midline incision made to expose the abdominal cavity. A 20*g* 1 ¼" Terumo Surflo I.V. catheter was inserted into the portal vein, the vena cava was nicked to allow outflow, and the livers were perfused with room temperature phosphate buffered saline (PBS) for about 3 minutes to clear the liver of blood. Livers were excised, rinsed in PBS, and 6 g pieces were immediately flash frozen in liquid nitrogen and stored at -80°C until microsomal preparation.

Hepatic microsomes were prepared according to the method of Iba *et al*[159]. Briefly, 0.5 g of liver was homogenized in 2 mL cold homogenization buffer (50 mM

Tris buffer, 150 mM KCl, 0.1 mM dithiothreitol, 1 mM ethylenediamine tetracetic acid, 20% glycerol and 0.1 mM phenylmethylsulfonylfluoride) using potter-elvheim pestle and sleeve. The homogenate was transferred to a Beckman (Beckman Coulter Canada, Inc. Mississauga, ON) ultracentrifuge tube and spun in a Beckman L8-55 Ultracentrifuge at 9000×*g* for 30 minutes at 4°C. The supernatant was transferred into clean ultracentrifuge tubes and spun at 100 000×*g* for 30 minutes at 4°C. The pellet was washed with 2 mL 150 mM KCl then similarly spun for an additional 30 minutes at 4°C. The pellet was resuspended in 2 mL of 0.25 M sucrose solution and passed through a syringe with a 25×*g* needle. Microsomes were pooled (n = 4), partitioned into 500 µL aliquots in cryogenic microcentrifuge tubes (1.5 mL) and stored at -80°C until use.

Microsomal protein content was determined by the method of Lowry *et al*[160] using bovine serum albumin as the standard. Analysis was carried out on an Agilent 8453E UV-visible spectrophotometer using Chemstation software (Palo Alto, CA, USA). Absorbance was measured at 750 nm.

Hepatic Microsomal Incubation Experiments to Assess Formation of Reactive Intermediates

Microsomal incubation mixtures (1 mL) consisted of microsomal protein (1 nmol), $MgCl_2$ (5.0 mM), and 50 mM sodium phosphate buffer (pH 7.4). NDGA, SECO, or ASECO dissolved in DMSO was added to achieve a final concentration of 0.5 mM (final concentration of DMSO was <0.1%) and GSH dissolved in phosphate buffer was added to a final concentration of 1.0 mM or 5.0 mM. The mixture was pre-incubated in a shaking water bath set to 37°C for 5 min. NADPH (1 mM) was added to initiate the reaction. Control incubations included samples with no NADPH, heat-inactivated (95°C for 5 min) microsomes or no GSH. Incubations were carried out at 37°C in uncapped 12×75 mm glass culture tubes in a shaking water bath for 60 min. The reaction was terminated by chilling in an ice bath followed by subsequent addition of 50 µL of acetonitrile containing internal standard (2mM salicylamide). Samples were centrifuged at 20,000×*g* for 10 min on a Micromax Thermo IEC microcentrifuge. Aliquots of the supernatant (150 µL) were analyzed directly by HPLC (NDGA, SECO) or UPLC-MS (for ASECO where the analysis was conducted as a kind gift from Dr. Muir, Agriculture and Agri-Food Canada).

Hepatic Microsomal Incubation Experiments to Assess Cytochrome P450 Enzyme Inhibition

Inhibition of cytochrome P450 1A2, 2B, 2C11, and 3A2 by lignans was determined with assessment of P450 specific probe substrate metabolite pathways. The activities of CYP3A, 2B/2C11, 2C11 and 1A2 were monitored by measuring the formation of 6β-hydroxytestosterone, 16α-hydroxytestosterone, 2α-hydroxytestosterone, and resorufin formation, respectively. The lignans were first tested to identify possible mechanism-based inhibition of P450 enzymes. The microsomal protein concentration (0.5 mg/mL) and incubation time (15 min) were based upon conditions reported by Vuppugalla and Mehva [166] for the testosterone metabolites and 0.4 mg/mL with incubation time of 8 min according to Elbarbary et al.[167] for the resorufin assays, conditions that gave linear metabolite formation velocities.

Lignans at various concentrations were added to microsomal incubation mixtures (500 μL final volume for testosterone; 140 μL final volume for methoxyresorufin) containing microsomal protein (0.5 mg/mL for testosterone, 0.4 mg/mL for methoxyresorufin), $MgCl_2$ (5.0 mM for testosterone; 2.0 mM for methoxyresorufin), and potassium phosphate buffer (pH 7.4; 80 mM for testosterone; 50 mM for methoxyresorufin) and pre-incubated in a shaking water bath set to 37ºC for 5 min. Lignans were dissolved in DMSO (final concentration of DMSO was <0.1%), except for SDG and SECO, which were dissolved in phosphate buffer. NADPH (1 mM) was added to initiate the reactions, which were allowed to incubate for 0, 5, 10 or 20 minutes before the addition of specific P450 probe substrate. The final concentrations of testosterone and resorufin were 250 μM (but 50 uM for ED, EL and Dibenzocyclooctadiene) and 0.5 μM, respectively. The samples were incubated at 37ºC for 15 minutes following testosterone addition and 8 min following methoxyresorufin addition. The reaction was terminated by chilling in an ice bath and subsequent addition of 50 μL (testosterone) or 60 μL (methoxyresorufin) of ice cold acetonitrile containing internal standard (1 mM dimethylphenylacetone as the internal standard for SDG, or 100 μM acetaminophen as the internal standard for all other lignans for the testosterone assay). No internal standard was used for the methoxyresorufin assay. Samples were centrifuged at

20,000×*g* for 10 min (Micromax Thermo IEC). Aliquots of the supernatant (150 µL) were analyzed directly by HPLC. Control incubations contained either no NADPH or heat-inactivated (95°C for 5 min) microsomes. All reactions were performed in triplicate.

For assessment of lignan inhibition of P450 enzyme activity by reversible inhibition mechanisms, lignans at various concentrations were added to microsomal incubation mixtures as above. The probe substrates, testosterone and methoxyresorufin, were also added at various concentrations representing the approximate values of ½ K_M, K_M, $2K_M$ and the V_{Max} concentrations. The mixture was pre-incubated in a shaking water bath set to 37ºC for 5 min. NADPH (1 mM) was added to initiate the reactions, which were allowed to incubate for 15 minutes. The reaction was terminated and processed as above. Control incubations contained either no NADPH or heat-inactivated (95°C for 5 min) microsomes.

High Performance Liquid Chromatography Assays and Analysis of Resorufin

For NDGA and SECO microsomal incubations, 150 µL of microsomal suspension supernatants were injected onto a 250 × 4.6 mm Alltech ODS-2, 5 µm, C-18 column at a flow rate of 1.5 mL/min with detection wavelength monitored at 280 nm. The mobile phase consisted of A: Acetonitrile with 0.1% TFA and B: 0.1% TFA in water. For NDGA a gradient of 5% A for 3 min, increased to 20% A over 4 min, isocratic for 3 min, increased to 35% A over 26 min, increased to 90% A over 5 min and then held isocratic for 4 min was used. For SECO a gradient of 10% A for 5 min, increased to 40% A over 25 min, increased to 60% A over 10 min was used.

The analysis of the ASECO microsomal incubations was a kind gift from Agriculture and Agrifood Canada, Saskatoon, SK. A Synapt HDMS System Waters Acquity UPLC System with Waters Acquity PDA and Synapt Q-TOF in negative electrospray mode with Masslynx 4.1 software were used. Ten µL of microsomal suspension supernatants were injected onto a 50 × 2.1 mm, 1.7 µm, C-18 Waters BEH column at a flow rate of 0.6 mL/min with scanning UV detection from 200 – 400 nm. The mobile phase consisted of A: Acetonitrile and B: 1% FA in water. A gradient starting with 5% A, increased to 95% A over 2.6 min, and then decreased to 5% A over 2.08 min and held isocratic for 0.32 min was used.

The activities of CYP3A, 2B/2C11 and 2C11 were monitored by measuring the formation of 6β-, 16α- and 2α-hydroxytestosterone, respectively, by an HPLC assay of Pfeiffer and Metzler[168] with modifications. Briefly, 150 μL aliquots of microsomal incubation supernatants were injected onto a 250 × 4.6 mm Alltech ODS-2, 5 μm, C-18 analytical column with a 7.5 mm × 4.6 mm Allsphere ODS-2 C_{18} 5μm guard column at a flow rate of 1.0 mL/min with detection wavelength set at 240 nm. The mobile phase consisted of A: Acetonitrile with 0.1% trifluoroacetic acid (TFA) and B: 0.01% TFA in water. A gradient of 20% A increased to 25% A over 10 min, held isocratic for 5 min increased to 70% A over 10 min was used. Linear calibration curves were constructed from known concentrations of each testosterone metabolite (ranging from 0.4 to 25 μM) added to microsomal incubation suspensions (total volume 0.5 mL) containing heat-inactivated microsomes (95°C for 5 min) and 50 μL of the internal standard solution (1 mM dimethylphenylacetone as the internal standard for SDG, or 100 μM acetaminophen as the internal standard for all other lignans). Coefficients of determination were all greater than 0.999 and the relevant slope and y-intercept values were statistically different from zero ($p < 0.005$). Three quality control (QC) samples at 0.4, 1, and 10 μM were prepared independent of those used for the calibration curves and used as acceptance criteria for individual analysis runs. The calibration samples were processed as above and the supernatant was injected directly onto the analytical column for immediate HPLC analysis. Metabolite concentrations were calculated by interpolation from the linear calibration curve using measured metabolite to internal standard peak height ratios. Intra- and interday precision was <15% for each metabolite, respectively, and accuracy was within 15% of the nominal value for all testosterone metabolites. Quality control samples at three different concentrations in duplicate were randomly interspersed during the HPLC analysis and served as the acceptance criteria for a particular analysis.

The activity of CYP1A2 was monitored by measuring the formation of resorufin from methoxyresorufin using a 96-well fluorescence plate-reader method. A Biotek (Winooski, VT) Synergy HT plate reader with a built in plate shaker and chamber heater (37°C) was used to analyze the samples. Fluorescence detection employed an excitation wavelength of 530 nm and emission wavelength of 590 nm and Gen5 (version 1.00.14)

software was used to analyze the data. Linear calibration curves were constructed from known concentrations of resorufin (ranging from 5 to 200 nM) added to microsomal incubation suspensions (total volume 0.5 mL) containing heat-inactivated microsomes (95°C for 5 min) and metabolite concentrations in unknown samples (from which had the blank fluorescence values had been subtracted) interpolated from the standard curve. Coefficients of determination were all greater than 0.999 and the relevant slope and y-intercept values were statistically different from zero ($p < 0.005$). The intraday and interday accuracy fell within the allowable 15% variation. Quality control samples at 5, 30, and 150 nM in duplicate were randomly interspersed during the HPLC analysis and served as the acceptance criteria for a particular analysis.

Data and Statistical Analysis

For time and concentration dependant inhibition studies, the % inhibition of activity for each lignan concentration was plotted versus pre-incubation time using Microsoft Excel (Seattle, WA). The formation of metabolite was plotted against log inhibitor concentrations to estimate an apparent IC_{50} value when possible using a nonlinear regression analysis with GraphPad Prism 4.0. Otherwise, data was reported as a %inhibition from control (ratio of the rate of metabolism in the presence of lignan inhibitor relative to rate in the absence of lignan inhibitor). For reversible inhibition studies, the inverse of enzyme velocity versus inverse probe substrate concentration was plotted to generate Lineweaver-Burke plots using Microsoft Excel. All data is reported as mean ± CV (coefficient of variation).

6.4 Results

Cytochrome P450-Mediated Formation of Reactive Metabolites

Since SDG is unlikely absorbed due to the polar nature of the glycosidic groups, NDGA and SECO were investigated for their potential to undergo hepatic P450-mediated bioactivation to a reactive intermediate. ASECO was also examined as its structure is intermediate of NDGA and SECO. With respect to NDGA, Billinsky et al., 2007 had previously reported that NDGA underwent autoxidation and conversion via an *ortho*-quinone reactive intermediate to three glutathione (GSH) adducts[161]. Furthermore, in the absence of GSH NDGA autoxidation resulted in the formation of a novel

dibenzocyclooctadiene[163]. SECO was metabolized to lariciresinol both in the presence and absence of GSH and no GSH adducts were observed following microsomal incubations (data not shown).

For ASECO, all control experiments showed no product formation; however, in the presence of GSH a product peak in MS-ESI(-) with a *m/z* 648.19 $[M-H]^-$ was observed (data not shown). This mass is consistent with the formation of an ASECO-GSH adduct, which is likely derived from an ASECO *para*-quinone methide.

Mechanism-Based Inhibition of Cytochrome P450 Enzymes

To determine whether lignans result in mechanism-based inhibition of P450 enzymes initial experiments examined the extent of inhibition as a function of pre-incubation time and lignan concentration.

SDG did not cause mechanism-based inhibition of any P450 isoform at any concentration tested (Figure A1). The data also suggests that SDG does not cause reversible inhibition of P450 isoforms, as metabolite formation remained the same at pre-incubation time 0 at all SDG concentrations tested (Appendix A, Figure A1).

SECO did not cause significant inhibition of CYP1A2 (Figure A2a). SECO inhibited CYP3A in a concentration-dependent but not time-dependent manner suggesting that SECO is a reversible inhibitor of the three isoforms. Reversible inhibition is consistent with the lack of GSH adduct formation following microsomal incubation of SECO in the presence of GSH. However, at 2000 μM SECO inhibited 6β-, 16α- and 2α-hydroxytestosterone formation by only 36.2 ± 7.26%, 65.7 ± 8.36% and 64.4 ± 6.36%, respectively. Such concentrations are substantially greater than the levels anticipated under physiological conditions (25-100 μM)[169].

ASECO caused limited inhibition of CYP1A2, 2B, and 2C11 (Figure A3), with moderate inhibition of CYP3A at the highest concentration (100 μM) caused 49.2 ± 1.8% inhibition after 20 minutes preincubation. As with SDG and SECO, ASECO showed concentration-dependent but not time-dependant inhibition which suggests P450 inhibition by reversible mechanisms.

Enterodiol (ED) failed to inhibit P450 activity and rather caused activation of CYP1A2, 3A, 2B and 2C11 activity particularly at lower concentrations (Figure 6.2).

Although an apparent inhibition of CYP3A activity was observed after a 20 min pre-incubation (Figure 6.2b), control samples without ED showed a large %CV of 91.8% relative to the samples pre-incubated with ED for 20 min.

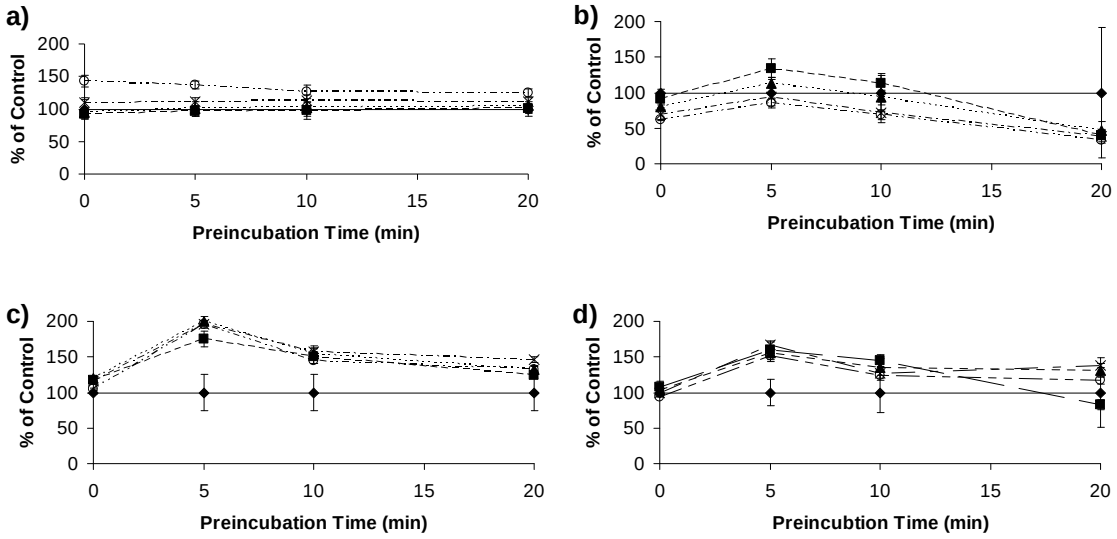

Figure 6.2: Cytochrome P450 enzyme activity (as percent of control) as a function of Enterodiol (ED) concentration and pre-incubation time. a) CYP1A2, b) CYP3A, c) CYP2B/2C11 and d) CYP2C11. Enterodiol (closed diamond = 0 μM; closed square = 50 μM; closed triangle = 100 μM; symbol 'x' = 250 μM; open circle = 500 μM) was pre-incubated in pooled male rat hepatic microsomes (n=4) for different time periods. At the end of each pre-incubation period, testosterone (50 μM) and methoxyresorufin (0.5 μM) was added and metabolite formation was determined after a 15 min and 8 min reaction time, respectively. Each point is the mean of 3 replicates ± percent coefficient of variation.

EL caused concentration-dependent, but not time-dependent, inhibition of CYP1A2 and only at high concentrations with 500 μM EL inhibiting CYP1A2 to 14.3 ± 23% that of control (Figure A4). EL also caused concentration-dependent inhibition of CYP3A. Interestingly, EL caused activation of 16α-hydroxytestosterone (16α-OH) formation, a metabolite pathway shared by CYP2B and CYP2C11. Given the ability of EL to inhibit 2α-OH formation, a pathway largely catalyzed by CYP2C11, increased 16α-OH formation may be due to activation of CYP2B activity by EL.

NDGA generally caused concentration-dependent but not time-dependent inhibition of all CYP isoforms (Figure A5). We anticipated that NDGA could be an

irreversible inhibitor given its ability to form a reactive *ortho*-quinone intermediate. Since this is an autoxidation process and not P450 catalyzed process, it appears that the *ortho*-quinone does not inhibit P450 in vitro[161,163]. Generally, marked inhibition was not observed until NDGA concentrations reached 100 μM or higher. At a pre-incubation time of 20 minutes and a concentration of 200 μM, NDGA inhibited CYP1A2, 2B/2C11 and 2C11 to 3.55 ± 12.0%, 21.2 ± 8.81% and 21.2 ± 9.37% of control, respectively. NDGA caused complete inhibition of formation of 6β-OH via CYP3A at pre-incubation time of 20 minutes and a concentration of 200 μM.

The NDGA dibenzocyclooctadiene did not cause significant inhibition of CYP2B/2C11 and did not cause time-dependant inhibition of any of the tested isoforms (Figure A5). The NDGA dibenzocyclooctadiene significantly inhibited CYP3A and CYP1A2 to 42.9 ± 3.6%, and 13.9 ± 4.3% of control, respectively, at 100 μM.

Reversible Inhibition of Cytochrome P450 Enzymes

To determine whether lignans inhibit specific P450 enzymes through reversible mechanisms, we monitored the metabolite formation of P450-probe substrates by rat hepatic microsomes in the presence of different concentrations of lignan and probe substrates. Since time- and concentration-dependent experiments indicated that SDG and ED were neither reversible nor irreversible inhibitors of P450 enzyme activity, we excluded SDG and ED from our evaluations for reversible inhibition. We estimated the % inhibition at each lignan concentration and when possible estimated the IC_{50} values to provide a measure of potency of the inhibition. Lineweaver-Burke plots were constructed to determine the mechanism of inhibition. HPLC results from lignan incubations indicated substrate depletion at a testosterone concentration of 25 μM, representing ½ Km for the substrate. Consequently, this concentration was not included in any of the graphical representations and analysis.

SECO caused a concentration-dependent decrease in 6β-OH formation, which is mediated by CYP3A (Figure 6.3a). A plot of 6β-OH formation (at K_M) as a function of the logarithmic concentration of SECO yielded an IC_{50} value of 373 μM (95% CI 266-523). A Lineweaver-Burke plot showed a pattern almost consistent with that of competitive inhibition, but the lines intersected in the upper right hand quadrant near the

y-axis (not shown). This suggests SECO inhibits CYP3A activity consistent with atypical Michaelis-Menten kinetics[170,171].

The formation of 16α-OH testosterone, representing CYP2B/2C11 activity, was largely unaffected by SECO at testosterone concentrations of 100 and 250 μM (Figure 6.3b). At 50 μM testosterone, SECO concentrations ≥50 μM increased the formation of 16α-OH testosterone. Since CYP2C11 activity was generally unaffected by SECO (Figure 6.3c), SECO-mediated activation of CYP2B likely explains the increased formation of 16α-OH testosterone. The percent of control activity of the various CYP isoforms tested at K_M, $2\times K_M$ and V_{Max} testosterone is summarized in Table 6.1.

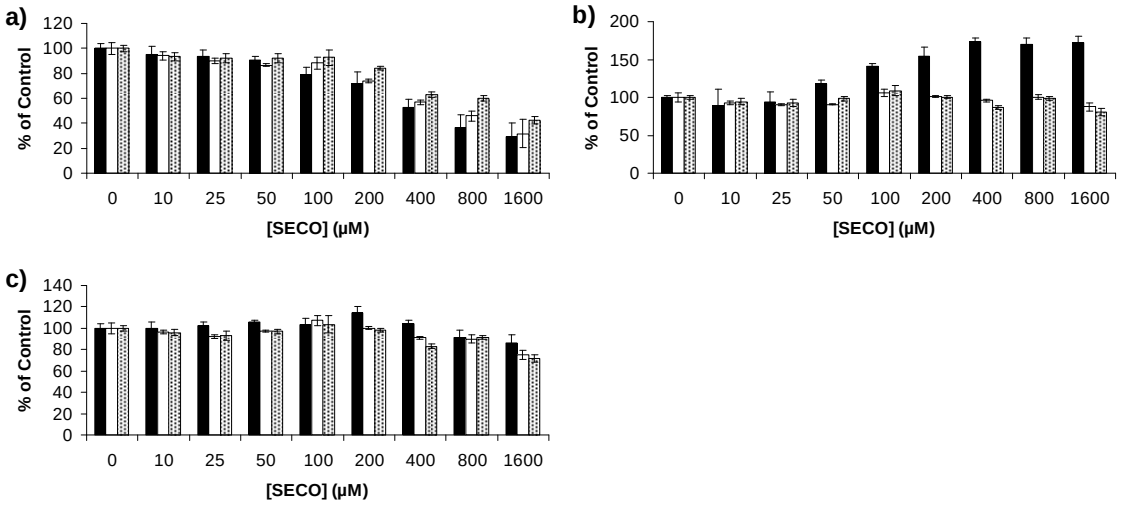

Figure 6.3: Secoisolariciresinol (SECO) concentration dependent inhibition of a) CYP3A, b) CYP2B/2C11 and c) CYP2C11 using testosterone (solid bar = 50 μM; open bar = 100 μM; stipled bar = 250 μM) as the probe substrate in incubation reactions (15 min) with pooled (n=4) male, rat liver microsomes. Each point represents the mean of 3 replicates ± percent coefficient of variation.

Table 6.1: The percent of control activity (mean ± % CV) for the formation of 6β-, 16α- and 2α-hydroxytestosterone (OHT) in pooled (n=4) rat liver microsomes by 50 and 1600 μM Secosiolariciresinol (SECO) at the K_M, 2×K_M and ~V_{Max} of testosterone.

	6β-OHT (CYP3A)		16α-OHT (CYP2B/2C11)		2α-OHT (CYP2C11)	
	Percent of Control Activity (mean ± % CV)		Percent of Control Activity (mean ± % CV)		Percent of Control Activity (mean ± % CV)	
Testosterone/ Methoxyresorufin	SECO 50 μM	SECO 1600 μM	SECO 50 μM	SECO 1600 μM	SECO 50 μM	SECO 1600 μM
K_M	90.7 ± 5.0	29.0 ± 11	117.5 ± 5.1	172 ± 8.1	106.1 ± 1.7	86.0 ± 7.6
$2K_M$	86.4 ± 1.1	31.8 ± 11	91.0 ± 0.5	87.4 ± 5.2	97.3 ± 0.5	75.0 ± 4.0
V_{Max}	91.9 ± 3.6	42.4 ± 3.1	98.4 ± 2.8	80.9 ± 5.2	97.1 ± 2.3	71.9 ± 3.3

Pre-incubation time- and concentration- dependant experiments showed that ASECO was not an inhibitor of CYP2B/2C11. Due to overlapping and unresolvable HPLC peaks, the inhibition of CYP2C11, measured by 2α-OH testosterone formation could not be assessed.

ASECO maximally inhibited CYP1A2 when methoxyresorufin concentration was at the K_M of the enzyme, with the greatest extent of inhibition occurring at 100 μM ASECO (70.8 ± 3.9% of control) (Figure 6.4a). Further increases in the extent of inhibition at higher ASECO concentrations was not observed, but this may be due to an inability to completely solubilize ASECO. ASECO generally caused a concentration-dependent inhibition of CYP3A at all testosterone concentrations, although the pattern of inhibition became inconsistent at ASECO concentrations beyond 100 μM, which may due to solubility issues (Figure 6.4b). The percent of control activity of the formation of resorufin and 6β-OH tested at K_M, $2\times K_M$ and V_{Max} of methoxyresorufin and testosterone is summarized in Table 5.2. A plot of the 6β-OH formation (at K_M) as a function of the logarithmic concentration of ASECO yielded an IC_{50} value of 36.4 μM (95% CI 21.9-60.3). The IC_{50} value for CYP1A2 inhibition was greater than 200 μM. A Lineweaver-Burke plot gave parallel lines, a pattern consistent with uncompetitive inhibition (not shown).

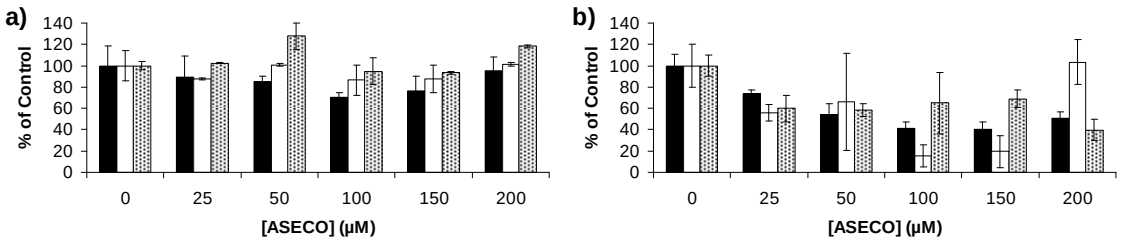

Figure 6.4: Anhydrosecoisolariciresinol (ASECO) concentration dependent inhibition of a) CYP1A2 and b) CYP3A using methoxyresorufin (solid bar = 0.5 μM; open bar = 1 μM; stipled bar = 2.5 μM) and testosterone (solid bar = 50 μM; open bar = 100 μM; stipled bar = 250 μM) as the probe substrates, respectively, in incubation reactions (15 min and 8 min, respectively) with pooled (n=4) male, rat liver microsomes. Each point represents the mean of 3 replicates ± percent coefficient of variation.

Table 6.2: The percent of control activity (mean ± % CV) for the formation of 6β-hydroxytestosterone (OHT) and resorufin in pooled (n=4) rat liver microsomes by 25 and 100 μM Anhydrosecosiolariciresinol (ASECO) at the K_M, 2×K_M and ~V_{Max} of testosterone or methoxyresorufin.

	Resorufin (CYP1A2)		6β-OHT (CYP3A)	
	Percent of Control Activity (mean ± % CV)		Percent of Control Activity (mean ± % CV)	
Testosterone/ Methoxyresorufin	ASECO 25 μM	ASECO 100 μM	ASECO 25 μM	ASECO 100 μM
K_M	89.6 ± 19.5	70.8 ± 3.9	74.0 ±3.5	40.9 ± 6.5
$2K_M$	87.5 ± 14.1	86.4 ± 14.0	55.5 ± 7.8	15.6 ± 10.2
V_{Max}	102.6 ± 3.8	94.7 ± 12.5	59.7 ± 12.2	65.2 ± 28.7

Enterolactone caused CYP2B/2C11 activation in time- and concentration-dependent experiments and thus was not examined for reversible inhibition of these enzymes. EL maximally inhibited CYP1A2 when methoxyresorufin concentration was at the K_M of the enzyme (Figure 6.5a). EL also caused a concentration-dependent decrease in resorufin formation at 2×K_M and V_{Max} methoxyresorufin concentrations (Figure 6.5a). At the Km of testosterone, EL did not inhibit CYP3A activity and at 500 μM EL, a 3-fold increase in metabolite formation was observed (Figure 6.5b). However, at 2×K_M and V_{Max} testosterone concentrations, EL generally caused a concentration-dependent decrease in CYP3A-mediated 6β-OH formation (Figure 6.5b). For CYP2C11, at the K_M of testosterone, EL generally increased the rate of 2α-OH formation at all EL concentrations. However, EL caused pronounced inhibition at 2×K_M and V_{Max} testosterone concentrations for the enzyme (Figure 6.5c). Plots of metabolite formation (at K_M) as a function of the logarithmic concentration of EL yielded an IC_{50} values of 441 μM (95% CI 115-1695), 72.9 μM (95% CI 54.0-98.2) (determined at the V_{Max} due to activation at K_M) and 104 μM (95% CI 85.7-127) (determined at the V_{Max} due to activation at K_M) for CYP1A2, CYP3A and CYP2C11, respectively. The percent of control activity of the various CYP isoforms tested at K_M, 2×K_M and V_{Max} of methoxyresorufin or testosterone is summarized in Table 6.3.

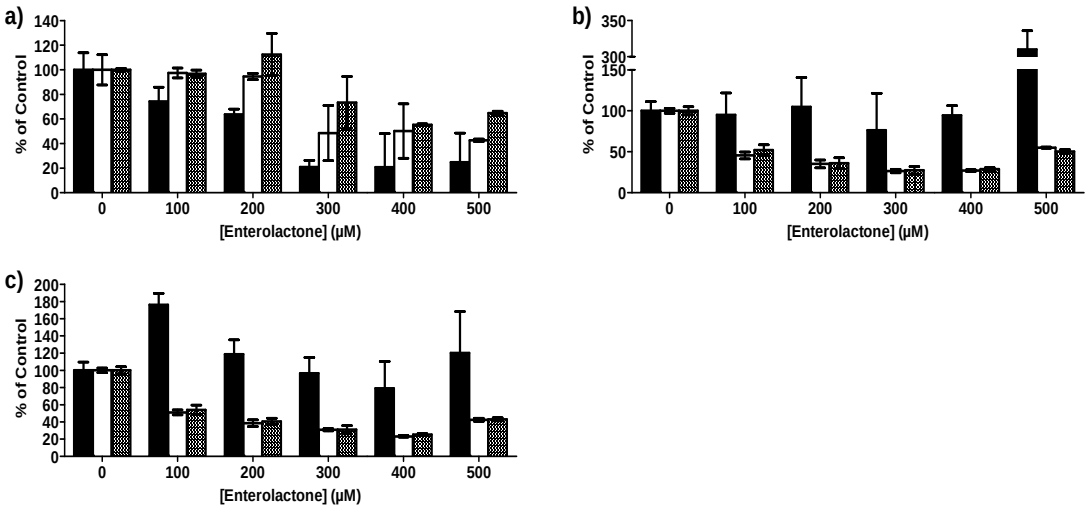

Figure 6.5: Enterolactone (EL) concentration dependent inhibition of a) CYP1A2, b) CYP3A and CYP2C11 using methoxyresorufin (solid bar = 0.5 µM; open bar = 1 µM; stipled bar = 2.5 µM) and testosterone (solid bar = 50 µM; open bar = 100 µM; stipled bar = 250 µM) as the probe substrates, respectively, in incubation reactions (15 min and 8 min, respectively) with pooled (n=4) male, rat liver microsomes. Each point represents the mean of 3 replicates ± percent coefficient of variation.

Table 6.3: The percent of control activity (mean ± % CV) for the formation of resorufin, and 6β-, 16α- and 2α-hydroxytestosterone (OHT) in pooled (n=4) rat liver microsomes by 100 and 500 μM Enterolactone (EL) at the K_M, 2×K_M and ~V_{Max} of methoxyresorufin or testosterone.

	Resorufin (CYP1A2)		6β-OHT (CYP3A)		16α-OHT (CYP2B/2C11)		2α-OHT (CYP2C11)	
	Percent of Control Activity (mean ± % CV)		Percent of Control Activity (mean ± % CV)		Percent of Control Activity (mean ± % CV)		Percent of Control Activity (mean ± % CV)	
Testosterone/ Methoxyresorufin	EL 100 μM	EL 500 μM	EL 100 μM	EL 500 μM	EL 100 μM	EL 500 μM	EL 100 μM	EL 500 μM
K_M	74.2 ± 13.8	24.7 ± 23.7	95.1 ± 26.8	309.9 ± 26.0	262.7 ± 17.1	302.5 ± 11.4	176.2 ± 13.2	120.2 ± 48.1
$2K_M$	97.4 ± 12.2	42.6 ±1.0	45.5 ± 4.2	55.0 ± 0.7	86.9 ± 1.8	61.9 ± 2.1	51.0 ± 2.9	42.4 ± 1.9
V_{Max}	96.7 ± 1.1	64.7 ± 1.6	52.0 ± 6.4	50.2 ± 2.3	75.4 ± 5.4	60.1 ± 2.7	53.9 ± 5.5	43.0 ± 1.7

Lineweaver-Burke plots were difficult to interpret for EL inhibition of CYP1A2, although the pattern was somewhat consistent with that of competitive inhibition, with the lines intersecting in the upper right hand quadrant (not shown). However, the pattern of the plots for CYP2C11 and CYP3A were consistent with noncompetitive inhibition by EL.

In general, NDGA caused a concentration-dependent decrease in CYP1A2, CYP3A, CYP2B and CYP2C11 activity (Figure 6.6). For CYP1A2, NDGA caused more prominent inhibition at the K_M of methoxyresorufin (Figure 6.6a), but for the CYP3A, CYP2B/2C11, and CYP2C11, NDGA caused most pronounced inhibition of testosterone metabolite formation at the V_{Max} for testosterone (Figure 6.6a, 6.6b, 6.6c). Furthermore, at the K_M of testosterone, NDGA increased the 16α- and 2α-hydroxylation of testosterone, index pathways for CYP2B/2C11 and CYP2C11, respectively. Activation of metabolism was more pronounced for 16α-OH formation. The IC_{50} values were calculated at the K_M of the substrate for CYP1A2 and CYP3A and at V_{Max} for testosterone for CYP2B/2C11 and CYP2C11, as activation was observed at the K_M for CYP2B/2C11 and CYP2C11. Plots of metabolite formation as a function of the logarithmic concentration of NDGA yielded IC_{50} values of 63.5 μM (95% CI 11.8-341), 97.3 μM (95% CI 49.6-191), 68.7 μM (95% CI 46.4-102) and 96.6 μM (95% CI 55.3-169) for CYP1A2, CYP3A, CYP2B/2C11 and CYP2C11, respectively. The percent of control activity of the various CYP isoforms tested at K_M, $2\times K_M$ and V_{Max} of methoxyresorufin or testosterone is summarized in Table 6.4.

Table 6.4: The percent of control activity (mean ± % CV) for the formation of resorufin, and 6β-, 16α- and 2α-hydroxytestosterone (OHT) in pooled (n=4) rat liver microsomes by 25 and 200 μM Nordihydroguaiaretic acid (NDGA) at the K_M, 2×K_M and ~V_{Max} of methoxyresorufin or testosterone.

	Resorufin (CYP1A2)		6β-OHT (CYP3A)		16α-OHT (CYP2B/2C11)		2α-OHT (CYP2C11)	
	Percent of Control Activity (mean ± % CV)		Percent of Control Activity (mean ± % CV)		Percent of Control Activity (mean ± % CV)		Percent of Control Activity (mean ± % CV)	
Testosterone/ Methoxyresorufin	NDGA 25 μM	NDGA 200 μM	NDGA 25 μM	NDGA 200 μM	NDGA 25 μM	NDGA 200 μM	NDGA 25 μM	NDGA 200 μM
K_M	84.1 ± 16.2	6.7 ± 13.5	81.8 ± 6.4	17.6 ± 11.7	158.3 ± 6.2	123.2 ± 8.8	118.0 ± 3.9	57.3 ± 8.6
$2K_M$	100.6 ± 1.7	17.9 ± 4.2	66.6 ± 1.8	12.4 ± 30.7	88.7 ± 4.5	42.2 ± 26.0	93.0 ± 2.9	37.5 ± 26.1
V_{Max}	109.1 ± 1.1	40.2 ± 7.9	63.6 ± 3.9	11.1 ± 3.5	79.8 ± 3.4	27.6 ± 0.3	88.7 ± 3.8	29.7 ± 0.1

Lineweaver-Burke plots for NDGA inhibition of CYP1A2 showed a pattern consistent with competitive inhibition, but with the lines intersecting in the upper right hand quadrant near the y-axis (not shown). For CYP3A the pattern was consistent with noncompetitive inhibition. For the CYP2B/2C11 and CYP2C11 pathways, the Lineweaver-Burke plots were more difficult to interpret. At higher NDGA concentrations, parallel lines suggested uncompetitive inhibition. However, activation of these pathways at the K_M of testosterone (Figure 6.6c and 6.6d) likely affected the overall pattern observed in these plots (not shown).

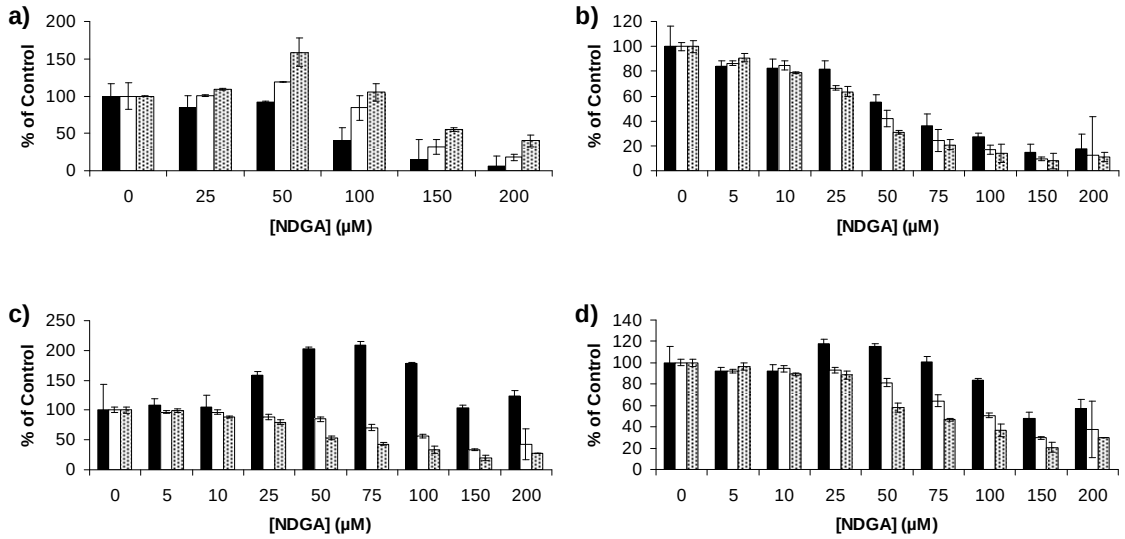

Figure 6.6: Nordihydroguaiaretic acid (NDGA) concentration dependent inhibition of a) CYP1A2, b) CYP3A c) CYP2B/2C11, and d) CYP2C11 using methoxyresorufin (solid bar = 0.5 μM; open bar = 1 μM; stipled bar = 2.5 μM) and testosterone (solid bar = 50 μM; open bar = 100 μM; stipled bar = 250 μM) as the probe substrates, respectively, in incubation reactions (15 min and 8 min, respectively) with pooled (n=4) male, rat liver microsomes. Each point represents the mean of 3 replicates ± percent coefficient of variation.

For NDGA dibenzocyclooctadiene, the activity of CYP2C11, as monitored by 2α-OH testosterone formation, could not be assessed, as the dibenzocyclooctadiene eluted at the same retention time as 2α-OH testosterone during the HPLC run. For CYP1A2, the dibenzocyclooctadiene caused more prominent inhibition at the K_M of methoxyresorufin (Figure 6.7a), but for CYP3A and CYP2B/2C11 slightly greater inhibition of testosterone metabolite formation at the testosterone V_{Max} was observed

(Figure 6.7b, 6.7c). At the V_{Max} of testosterone, dibenzocyclooctadiene concentrations of 50 to 150 µM increased the formation of resorufin, index pathways for CYP1A2 (Figure 6.7a). Dibenzocyclooctadiene did not cause significant inhibition of CYP2B/2C11 as evidenced by no substantial decrease in 16α-OH formation (Figure 6.7c). Plots of metabolite formation as a function of the logarithmic concentration of NDGA dibenzocyclooctadiene yielded an IC_{50} value of 36.8 µM (95% CI 25.3-53.6) for CYP3A. For CYP1A2, the data did not yield an interpretable due to extensive variation in the data. The percent of control activity of the various CYP isoforms tested at K_M, $2\times K_M$ and V_{Max} of methoxyresorufin or testosterone is summarized in Table 6.5.

Lineweaver-Burke plots for dibenzocyclooctadiene inhibition of CYP1A2 showed a pattern consistent with competitive inhibition, but with the lines intersecting in the upper right hand quadrant near the y-axis and for CYP3A the pattern was consistent with noncompetitive inhibition (not shown).

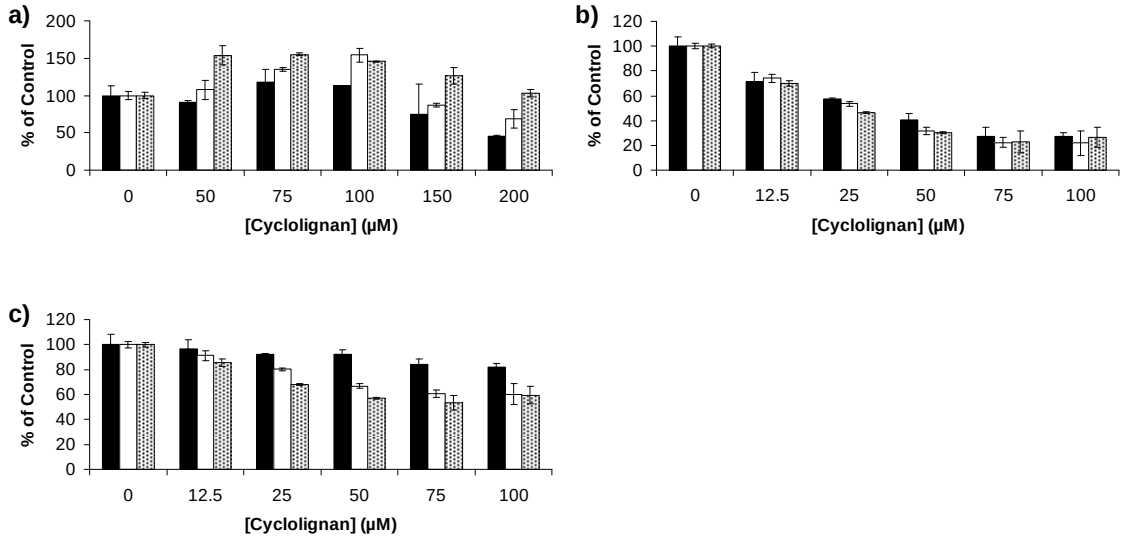

Figure 6.7: Dibenzocyclooctadiene concentration dependent inhibition of a) CYP1A2, b) CYP3A, and c) CYP2B/2C11 using methoxyresorufin (solid bar = 0.5 µM; open bar = 1 µM; stipled bar = 2.5 µM) and testosterone (solid bar = 50 µM; open bar = 100 µM; stipled bar = 250 µM) as the probe substrates, respectively, in incubation reactions (15 min and 8 min, respectively) with pooled (n=4) male, rat liver microsomes. Each point represents the mean of 3 replicates ± percent coefficient of variation.

Table 6.5: The percent of control activity (mean ± % CV) for the formation of resorufin, and 6β-, 16α- and 2α-hydroxytestosterone (OHT) in pooled (n=4) rat liver microsomes by 12.5, 50, 100 and 200 μM Dibenzocyclooctadiene (DIB) at the K_M, 2×K_M and ~V_{Max} of methoxyresorufin or testosterone

	Resorufin (CYP1A2)		6β-OHT (CYP3A)		16α-OHT (CYP2B/2C11)	
	Percent of Control Activity (mean ± % CV)		Percent of Control Activity (mean ± % CV)		Percent of Control Activity (mean ± % CV)	
Testosterone/ Methoxyresorufin	DIB 50 μM	DIB 200 μM	DIB 12.5 μM	DIB 100 μM	DIB 12.5 μM	DIB 100 μM
K_M	90.3 ± 2.5	45.3 ± 1.0	71.5 ± 7.4	26.9 ± 3.5	96.8 ± 7.0	82.0 ± 2.5
$2K_M$	107.4 ± 12.4	68.6 ± 12.1	74.0 ± 3.5	21.8 ± 10.0	91.3 ± 4.1	60.4 ± 8.2
V_{Max}	153.8 ± 12.7	103.4 ± 4.8	70.0 ± 2.2	26.4 ± 8.0	85.4 ± 2.9	59.6 ± 7.0

Inhibition of CYP1A2 by Nordihydroguaiaretic Acid in the Presence of Glutathione

The effect of adding GSH to microsomal incubations before the addition of NDGA was studied to determine whether GSH could attenuate inhibition at various time and inhibitor concentrations. GSH had little impact on NDGA inhibition of CYP1A2 activity (Figure A7). The calculated IC_{50} for NDGA in the presence and absence of GSH was 63.5 μM (95% CI 11.8-341) and 80.1 μM (95% CI 22.6-284), respectively, for CYP1A2. Interestingly, at 50 μM NDGA, GSH attenuated inhibition, and appeared to cause activation of CYP1A2 (Figure A8).

Summary of Inhibition of Rat CYP3A, CYP2B, CYP2C11 and CYP1A2 by Lignans

Table 6.6 summarizes the estimated IC_{50} values for lignan-mediated reversible inhibition different P450 isoforms. For lignans that failed to inhibit specific P450 isoforms the value reported represents the solubility limit for the respective lignan. Table 6.7 summarizes the type of reversible inhibition mechanism exhibited by each lignan for a particular P450 isoform.

Table 6.6: Summary of estimated lignan IC_{50} values (μM) (with 95% confidence intervals displayed in brackets) for CYP1A2, CYP3A, CYP2B/2C11 and CYP2C11. IC_{50} values were determined at probe substrate K_M, except where noted.

	CYP1A2	CYP3A	CYP2B/ CYP2C11	CYP2C11
Secoisolariciresinol	ND[a]	373 (266-523)	> 1600	> 1600
Anhydrosecoisolariciresinol	> 200	36.4 (21.9-60.3)	> 200	ND[b]
Enterolactone	441 (115-1695)	72.9[c] (54.0-98.2)	> 500	104[c] (85.7-127)
Nordihydroguaiaretic acid	63.5 (11.8-341)	97.3 (49.6-191)	68.7[c] (46.4-102)	96.6[c] (55.3-169)
Dibenzocyclooctadiene	ND[a]	36.8 (25.3-53.6)	ND[a]	ND[b]

ND = not determined
[a]No inhibition was observed at any lignan concentration
[b]Could not assess due to overlapping peak on high performance liquid chromatography
[c]IC_{50} assessed at V_{Max}

Table 6.7: Summary of the type of P450 enzyme inhibition caused by lignans of creosote bush and flaxseed.

	CYP1A2	CYP3A	CYP2B/ CYP2C11	CYP2C11
Secoisolariciresinol	NO	Competitive	NO[a]	NO
Anhydro-secoisolariciresinol	Un-competitive	Un-competitive	NO	NO
Enterolactone	Competitive	Non-competitive[a]	NO[a]	Non-competitive[a]
Nordihydroguaiaretic acid	Competitive	Non-competitive	Un-competitive[a]	Un-competitive[a]
Dibenzocyclooctadiene	Competitive	Non-competitive	NO	Could not assess

NO = No inhibition was observed
[a]Activation of P450 activity was observed.

6.4 Discussion

In our P450 enzyme inhibition studies with the lignans of creosote bush and flaxseed, none of the lignans evaluated caused mechanism-based inhibition of P450 activity. Most lignans exhibited reversible inhibition of several rat P450 enzymes that involved primarily competitive mechanisms, but sometimes showed inhibition more characteristic of noncompetitive or uncompetitive mechanisms. However, reversible inhibition of P450 activity occurred at concentrations unlikely achieved with usual lignan oral consumption levels. At concentrations consistent with therapeutic or beneficial effects of lignans, activation of CYP1A2 enzyme activity was observed with the creosote bush derived lignans. These data suggest a rather remote potential for significant interactions between the lignans and other P450 enzyme substrates through either reversible or mechanism-based enzyme inhibition mechanisms.

Cytochrome P450 enzyme interactions are commonly touted as a mechanism of toxicity[142,143]. In particular, bioactivation, or the metabolic activation of a compound to an electrophilic reactive intermediate, which subsequently undergoes covalent binding to

critical cellular macromolecules and interferes with their function, has long-standing recognition as a biochemical mechanism of organ toxicity[139-141]. Several examples exist of natural products undergoing P450-mediated bioactivation and irreversible P450 enzyme inhibition and hepatotoxicity[44,149,151,152,172]. Furthermore, natural products are known to result in significant interactions with coadministered therapeutic agents resulting in adverse effects or therapeutic failures[18,153,154]. With the growing interest in lignans for their health and wellness or therapeutic values, assessments of their safety are necessary to support their use.

Structural features of the lignans suggest their potential for oxidation to quinone derivatives, a class of compounds known to be electrophilic reactive intermediates[129,130]. Previous studies in our laboratory identified NDGA's (the major lignan of creosote bush) ability to undergo autoxidation to a reactive quinone species[161,163], whereas current studies indicate that SECO (the aglycone form of the major flaxseed lignan, SDG) underwent conversion to lariciresinol without formation of a stable reactive quinone intermediate. These studies, in conjunction with the growing interest in their use, compelled an investigation into their potential for mechanism-based inhibition and/or reversible inhibition of P450 isoforms. The use of *in vitro* microsomal systems for assessments of cytochrome P450 inhibition potential by drug candidates and natural products is a commonly employed technique to determine the likelihood for pharmacokinetic interactions resulting from P450 enzyme inhibition[143].

We examined the ability of creosote bush and flaxseed lignans to inhibit the activity of CYP3A, CYP2C and CYP1A2 enzymes as these isoforms are principally involved in the metabolism of drugs and other natural products on the market today. Our studies provided no evidence of mechanism-based inhibition of the P450 enzymes by either the lignans of creosote bush or flaxseed. The autoxidation of NDGA to a reactive intermediate in rat hepatic microsomes[161] did not result in the inactivation of P450 enzyme activity. These findings are not unexpected as the literature suggests ortho-quinones do not usually undergo adduct formation with cellular macromolecules, instead their damage is usually mediated through an increase in oxidative stress[128,173,174]. Although ortho-quinones may isomerize to para-quinone methides *in vivo*, a quinone derivative known to form covalent adducts with cellular macromolecules[134], this process

is unlikely to occur as NDGA is substituted at the benzylic carbon, which severely hinders the isomerization process[130].

Although our studies provide evidence of reversible inhibition of rat P450 enzyme activity by the lignans of creosote bush and flaxseed, such inhibition required rather high lignan concentrations. The principal creosote bush lignan, NDGA, and its autoxidation product, dibenzocyclooctadiene, inhibited CYP3A, CYP2B/2C11 and CYP1A2 activity suggesting that these lignans act as general reversible inhibitors of P450 activity. Although previous studies showed that in the presence of GSH NDGA is oxidized to NDGA-GSH adducts and prevents the formation of NDGA dibenzocyclooctadiene[163], inhibition of P450 activity was still observed. In the current experiments, addition of GSH to microsomal incubations before the addition of NDGA did not attenuate the inhibition of CYP1A2 caused by NDGA. These observations suggest that that GSH *in vivo* does not protect against reversible P450 inhibition by the creosote bush lignan, NDGA. Interestingly, at lower probe substrate concentrations, NDGA caused activation of CYP1A2 activity, while dibenzocyclooctadiene increased the metabolite formation of the index pathway for CYP2B/2C11. Although P450 enzyme activation has been observed for other compounds[143,175], the relevance of this phenomenon on *in vivo* metabolism is not known[143,176].

Reversible inhibition of P450 enzyme activity by the flaxseed lignans tended to show more specificity than the creosote bush lignans. The principal lignan present in flaxseed, SDG, failed to inhibit any P450 enzyme examined. This result was not unexpected given the physicochemical characteristics of SDG. Hydrophilic molecules tend not to be substrates for P450 enzymes and are primarily eliminated from the body via renal elimination mechanisms. Furthermore, studies have failed to detect systemic levels of SDG[177], suggesting that it is not absorbed from the gastrointestinal tract or undergoes extensive first pass metabolism prior to its appearance in the systemic circulation. Studies further suggest that this first-pass metabolism occurs at the gastrointestinal level, where the glucosidic groups of SDG are cleaved to produce the aglycone, SECO[57,178]. SECO is likely the flaxseed lignan form available for absorption following the oral consumption of flaxseed products[56,63].

Our data suggest SECO is a more specific inhibitor of P450 enzymes and causes a marked reduction in CYP3A activity only at high SECO concentrations. Our data also show that SECO activates CYP2B activity at lower probe substrate concentrations. We further examined the ability of an additional flaxseed lignan, ASECO, to inhibit P450 enzyme activity. Whether ASECO is present in flaxseed remains controversial as the identification of ASECO in flaxseed may be an artifact of the analytical techniques employed by Charlet *et al*[61]. Our lab has produced ASECO by acid hydrolysis of SECO using the same methods as Charlet *et al*, 2002[61]. Furthermore, ASECO could be formed during the isolation process for lignan enriched flaxseed products such as Beneflax™, and with oral consumption of flaxseed lignan products small amounts of ASECO could form within the acidic environment of the stomach. Such factors warranted an examination of ASECO's ability to inhibit P450 enzyme activity. ASECO inhibited CYP3A and CYP1A2 but had no affect on the index pathways for CYP2B/2C11 in the rat. In the presence of GSH, an adduct was formed that was consistent with a para-quinone methide[129,179]. Despite this observation, mechanism-based inhibition of P450 activity was not identified in our studies.

SDG (and SECO) is often referred to as the precursor for the enterolignans, ED and EL[56,57,177,178,180]. Much of the putative health benefits of flaxseed lignans are ascribed to the enterolignan forms, although definitive data for such assertions is lacking. Following oral consumption, SDG is converted to SECO, which further undergoes metabolism to ED and then to EL by colonic bacterial activity[56]. The literature reports significant systemic and urinary levels of EL and its conjugated forms[56,80] and much lower levels of ED suggesting that EL and ED are absorbed following their conversion within the gastrointestinal tract. This warranted an investigation of their potential to inhibit P450 enzyme activity. ED failed to inhibit any of the P450 index pathways evaluated in our study. On the other hand, EL inhibited CYP3A, CYP1A2, and CYP2C11 suggesting that, like NDGA, EL is a general reversible inhibitor of P450 enzymes. Interestingly, EL also activated the CYP2B/2C11 index pathway, the relevance of which is not known.

Lineweaver-Burke plots of the inhibition data suggest that lignans largely caused reversible inhibition via a combination of competitive, noncompetitive, and

uncompetitive mechanisms. The ability of lignans to activate P450 enzyme activity in the presence of low probe substrate concentrations for the P450 index pathways may account for the mixed type inhibition we observed[143]. Nonetheless, our *in vitro* results suggest that potential for pharmacokinetic interactions via inhibition of P450-mediated elimination by flaxseed lignans is extremely limited. Concentration at the P450 active site is a principal determinant of the potential for clinically relevant interactions[181]. Systemic levels reported in the literature suggest that lignan concentrations achieved at the P450 active site would be insufficient to cause significant inhibition. Even following oral consumption, when portal vein concentrations and hence, hepatic concentrations, of lignans are expected to be much greater than systemic levels, the competing phase II reactions (i.e. glucuronidation, sulfation)[182,183] would diminish the availability of lignans at the P450 enzyme active sites. The clinical use of lignans should not be associated with adverse outcomes resulting from inhibition of P450-mediated metabolism.

In conclusion, our data does not support the hypothesis that the differential toxicity between lignans of creosote bush and flaxseed may be due to differences in their capacity to undergo P450-mediated bioactivation to electrophilic reactive intermediates or reversible P450 enzyme inhibition. NDGA's autoxidation to a reactive quinone intermediate warrants further investigation as a possible mechanism associated with its known toxicity. Nonetheless, our *in vitro* data suggests the potential for inhibition of P450-mediated elimination of compounds by the lignans of creosote bush and flaxseed is limited. Their use for promotion of health and wellness or for therapeutic reasons should not be associated with adverse outcomes resulting from inhibition of P450-mediated metabolism. For the flaxseed lignans, our *in vitro* metabolism data is supported by the emerging clinical data on flaxseed lignan administration where no adverse effects have been reported as of yet. Such promising clinical trial data associated with the flaxseed lignans warrants further evaluations of their safety and efficacy, which remains a focus in our laboratory.

Conflict of interest statement

The authors declare that there are no conflicts of interest.

Acknowledgements

This study was performed with the assistance of NSERC and CFI grants. J.L.B. was the recipient of an NSERC Postgraduate Scholarship. The authors would like to thank Alister Muir from Agriculture and Agrifood Canada, Saskatoon for the kind gifts of SDG and SECO. In addition we thank Krista Thompson for running the UPLC-MS experiment.

7. GENERAL CONCLUSIONS AND FUTURE DIRECTIONS

7.1 General Conclusions

The overall aim of this dissertation was to investigate why the lignan NDGA, from the creosote bush, is associated with toxicity while the lignans from flaxseed are generally considered safe. Three objectives (Section 2.2) which each had a series of specific aims were executed using a variety of laboratory techniques to test the two hypotheses (Section 2.3), that NGDA and SECO can be oxidized to quinones in rat microsomal systems and also that lignans inhibit rat hepatic cytochrome P450 enzymes. The resulting conclusions drawn from the data obtained from the experiments for each of the thesis objectives is outlined below.

Objective 1 - Study the oxidation metabolism and bioactivation of Nordihydroguaiaretic acid and Secoisolariciresinol.

To accomplish the first objective, HPLC methods were developed to separate and purify oxidized metabolites of NDGA and SECO. NDGA and SECO were incubated in rat liver microsomes (RLM) in the presence and absence of GSH and the metabolites produced were identified using NMR and mass spectroscopy.

Despite being theoretically possible to undergo oxidation to both an *ortho*-quinone (o-Q) and a *para*-quinone methide (p-QM)[129,130], we demonstrated that NDGA only undergoes conversion to an o-Q in aqueous solution and at physiological pH and temperature. The o-Qs are known to be associated with toxicity and the production of o-Q reactive intermediates may be responsible for the hepatotoxicity caused by NDGA.

Three NDGA-GSH adducts, that were consistent with o-Q intermediates, were generated in the RLM experiments with GSH and were identified as one NGDA-GSH and two NDGA-GSH_2. Both control experiments (No NADPH added and heat inactivated microsomes) also generated the same metabolites in similar quantities, suggesting that CYP is only partially contributing to the metabolism of NDGA.

We did not find any evidence of p-QM formation in RLM. Although it is possible for o-Q to isomerize to p-QM *in vivo*, this process is unlikely to occur as NDGA is substituted at the benzylic carbon, which severely hinders the isomerization process[130].

While it was previously determined that NDGA undergoes CYP mediated metabolism[101], we have demonstrated that CYP metabolism only accounts for a small portion of NDGA's biological oxidation. Autoxidation is the main mechanism for NDGA oxidation in RLM[161]. Previous studies have been performed at biological pH and temperature, however considering that the half-life for NDGA in this range is 3.12 hours; it is possible that the biological effects produced by NDGA may be influenced by the o-Q as well.

Incubations of SECO in RLM in both the presence and absence of GSH indicated that SECO underwent conversion to lariciresinol without formation of a stable reactive quinone intermediate (submitted data from Chapter 6). Lariciresinol is formed by intramolecular cyclization of the aliphatic hydroxyl group on SECO with the distal benzylic carbon. The intramolecular cyclization of SECO to lariciresinol is believed to occur sufficiently rapidly, such that it out competes the formation of an intermolecular adduction between SECO and GSH. Secoisolariciresinol may be oxidized to a quinone methide intermediate before being converted into lariciresinol although further studies would have to be done to confirm this mechanism (Scheme 7.1).

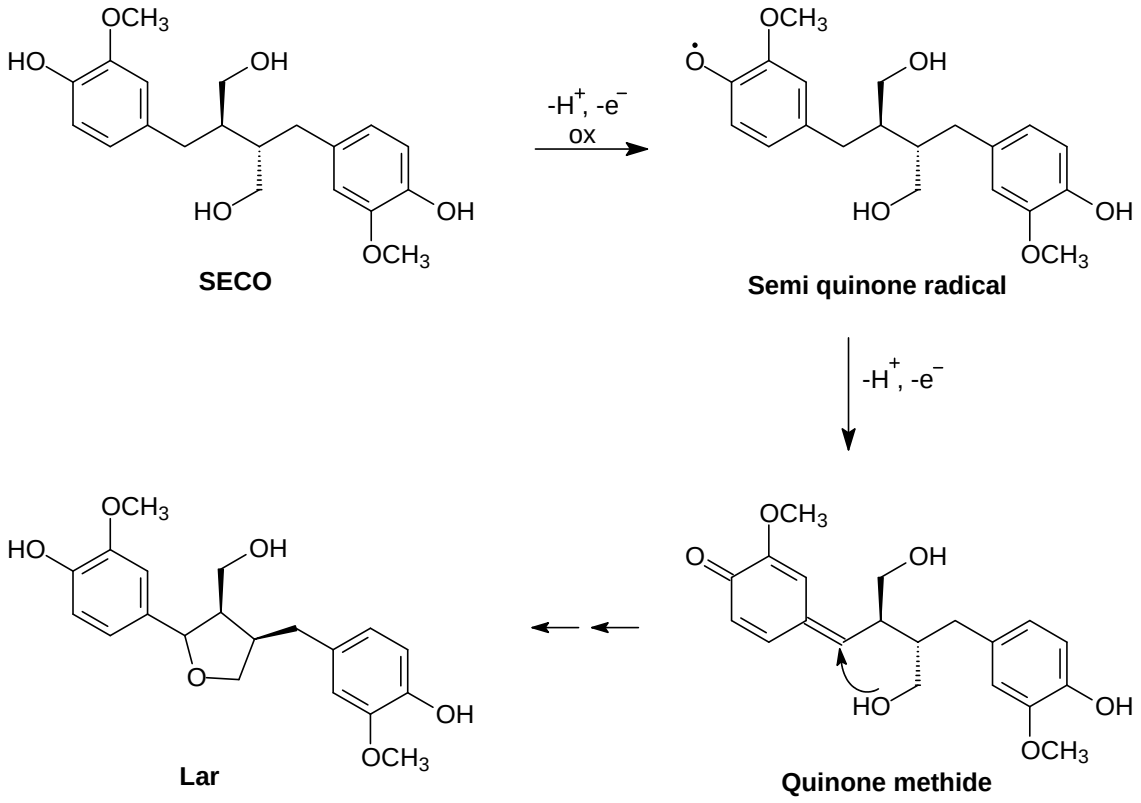

Scheme 7.1: Potential reaction scheme for the conversion of secoisolariciresinol (SECO) to lariciresinol (Lar) by cytochrome P450 enzymes in rat hepatic microsomes.

Objective 2 - Study the autoxidation of Nordihydroguaiaretic acid.

An HPLC method was developed to allow quantification of an NDGA autoxidation product. The stability of NDGA was investigated by measuring the loss of NDGA in aqueous phosphate-citric acid buffer over the range of pH 6.0 to 9.0 at 37ºC. A pH rate profile was generated and half-lives were calculated. NDGA undergoes base catalyzed autoxidation at 37ºC with a decreasing half-life with increasing pH level. The half-life of NDGA at physiologically relevant pH 7.4 is 3.12 hours[163].

Our previous studies demonstrated that nordihydroguaiaretic acid (NDGA) undergoes autoxidation in aqueous media under physiologically relevant conditions. Reports in the literature suggest that NDGA is unstable in aqueous media and that in the presence of molecular oxygen that NDGA may be converted to an ortho-quinone (o-Q)[31] or "activated NDGA"[121]. We aimed to determine the structurally identity of the NDGA autoxidation product in aqueous media.

When GSH was not present in the reaction mixture three products were generated. Two of the products were consistent with quinone formation and the third product was consistent with a quinone that had undergone hydroxylation.

Glutathione addition to the reaction mixture resulted in the disappearance of two of the products and subsequent appearance of two NDGA-GSH adducts. The third non-GSH reactive oxidation product was determined to be a unique, stable, schisandrin-like dibenzocyclooctadiene product that formed as a result of NDGA cyclization.

Nordihydroguaiaretic acid autoxidation in aqueous media in the presence of molecular oxygen leads to the formation of a novel schisandrin-like dibenzocyclooctadiene product which has a UV absorption maximum that is consistent with previous reports of "activated NDGA". NDGA is known to be an inhibitor of lipoxygenase[184] and CYP enzymes[102], experiments which are performed under conditions where NDGA can autoxidise to the dibenzocyclooctadiene. It may be possible that the effects previously ascribed to NDGA may actually be the result of o-Q intermediate or dibenzocyclooctadiene production.

Aboriginal preparations of creosote bush involve processes such as boiling the leaves for consumption as a tea or processing into a salve. It is conceivable that the preparations generated from creosote bush may contain amounts of NDGA-derived dibenzocyclooctadiene which may be responsible for some of the therapeutic effects of creosote bush.

Objective 3 - Study the inhibition of CYP isoforms 1A2, 2B, 2C11 and 3A by lignans.

An HPLC method and a fluorescence plate reader method were optimized to separate and quantify metabolites of P450-mediated testosterone and resorufin methyl ether metabolism, respectively, which would allow us to assess the inhibition of CYP isoforms 1A2, 2B, 2C11 and 3A by lignans.

In order to gain a better understanding of why the creosote bush lignan, nordihydroguaiaretic acid (NDGA) is toxic while flaxseed lignans are safe, we wanted to study the ability of lignans to undergo bioactivation in rat hepatic microsomes (RLM). We previously determined that NDGA undergoes bioactivation in RLM[161] but that SECO did not (submitted data, Chapter 6).

To add to our knowledge of how lignan structure can influence inhibition of CYP enzymes, we examined a number of lignans that are derived from both creosote bush and flaxseed. The lignans from creosote bush include NDGA and NDGA dibenzocyclooctadiene and the flaxseed lignans including secoisolariciresinol diglucoside (SDG), SECO, anhydrosecoisolariciresinol (ASECO), and enterodiol (ED) and enterolactone (EL), the mammalian lignans derived from SECO.

None of the lignans examined produced irreversible, mechanism-based inhibition of any of the P450 isoforms. Neither SDG nor ED caused reversible inhibition of the P450 examined however ED caused activation of all of the P450 isoforms studies at low concentrations. In addition, SECO, EL and NDGA caused activation of CYP3A and 2B/2C11 at low concentrations.

We postulated that the addition of the nucleophile GSH to RLM incubations, before the addition of lignan and substrate, would attenuate the inhibition of CYP1A2 by NDGA. GSH had little impact on NDGA inhibition of CYP1A2 activity however at 50 μM NDGA, GSH attenuated inhibition, and appeared to cause activation of CYP1A2 (submitted paper, Chapter 6).

Secoisolariciresinol, ASECO, EL, NDGA and the NDGA dibenzocyclooctadiene all caused reversible inhibition of P450 enzyme activity that involved either competitive or mixed-type inhibition. The relevance of the inhibition interactions *in vivo* is likely limited though, as the inhibition occurred at lignan concentrations which were greater than the anticipated physiologically relevant concentrations. We concluded that neither P450-mediated bioactivation nor reversible inhibition can explain the differences in toxicity noted between the lignans of creosote bush and flaxseed. There was no direct relationship between the structures of the lignans and the pattern of P450 inhibition or activation. Rather, the ability of NDGA to autoxidise and cause damage to tissues via covalent modification or generation of reactive oxygen species seems a more viable hypothesis.

7.2 Future Directions

The novel finding that NDGA autoxidizes to the NDGA dibenzocyclooctadiene under physiological *in vitro* conditions leads to a number of questions. Is it possible that either the o-Q intermediate or the autoxidized NDGA dibenzocyclooctadiene product is responsible for some of the activities which are currently associated with NDGA, such as lipoxygenase inhibition[184]? Could the creosote bush extraction processes used in traditional healing preparations lead to the formation of the NDGA dibenzocyclooctadiene? Is the NDGA dibenzocyclooctadiene causing the beneficial properties of the creosote bush, or is the NDGA dibenzocyclooctadiene responsible for the toxic properties associated with Chaparral consumption? Studies to investigate the lipoxygenase inhibition and chemopreventive properties in addition to the *in vitro* and animal *in vivo* use of the NDGA dibenzocyclooctadiene are warranted.

Secoisolariciresinol conversion to lariciresinol did not result in the formation of a stable quinone derived GSH adduct. It is possible that, based on the phenolic structure of SECO, that it could be oxidized to a p-QM before being directly converted to lariciresinol. However, further studies both NMR and perhaps electron paramagnetic resonance would need to be investigated to validate the process (Scheme 7.1).

Some of the lignans investigated caused activation of P450 enzymes. It is not clear whether the increase in P450 activity would occur *in vivo* or not. In order to further study the effect of the lignans on P450 enzymes and downstream consequences that this would have, animal dosing studies would be warranted.

Performing animal studies in rats would allow us to gather further information about potential for drug-natural product interactions. Livers could be analyzed for a number of different parameters such as enzyme induction, by measuring mRNA, protein levels and activity. Assessment as to whether any protein adducts have formed within the liver could also be measured which would indicate that reactive intermediate formation had occurred. In addition, measuring the levels of catalase and superoxide dismutase and levels of GSH and GSH reductase could generate further proof into whether oxidative stress is occurring in the liver due to formation of reactive intermediates.

8. REFERENCES

1. Morris, D. H. Flax - A Health and Nutrition Primer. 4th. 2007.
   Ref Type: Pamphlet

2. Health Canada . 2008. http://www.hc-sc.gc.ca/dhp-mps/prodnatur/index_e.html

3. Agriculture and Agri-Food Canada . 2007. http://www4.agr.gc.ca/AAFC-AAC/display-afficher.do?id=1171305207040&lang=e

4. Palozza,P., Moualla,S., & Krinsky,N.I. Effects of beta-carotene and alpha-tocopherol on radical-initiated peroxidation of microsomes. *Free Radic. Biol. Med.* **13**, 127-136 (1992).

5. Schatzkin,A., Mouw,T., Park,Y., Subar,A.F., Kipnis,V., Hollenbeck,A., Leitzmann,M.F., & Thompson,F.E. Dietary fiber and whole-grain consumption in relation to colorectal cancer in the NIH-AARP Diet and Health Study. *Am. J. Clin. Nutr.* **85**, 1353-1360 (2007).

6. Wayne,S.J., Neuhouser,M.L., Ulrich,C.M., Koprowski,C., Baumgartner,K.B., Baumgartner,R.N., McTiernan,A., Bernstein,L., & Ballard-Barbash,R. Dietary fiber is associated with serum sex hormones and insulin-related peptides in postmenopausal breast cancer survivors. *Breast Cancer Res. Treat.* (2007).

7. Fraser,M.L., Lee,A.H., & Binns,C.W. Lycopene and prostate cancer: emerging evidence. *Expert. Rev. Anticancer Ther.* **5**, 847-854 (2005).

8. Coleman,H. & Chew,E. Nutritional supplementation in age-related macular degeneration. *Curr. Opin. Ophthalmol.* **18**, 220-223 (2007).

9. FIM Rationale And Proposed Guidelines For The Nutraceutical Research & Education Act - NREA November 10-11 2002. 2002.
   http://www.fimdefelice.org/archives/arc.researchact.html

10. Natural Health Products Directorate. Natural Health Products Compliance Guide Version 2.1. 2007. http://www.hc-sc.gc.ca/dhp-mps/prodnatur/faq/question_consum-consom-eng.php
    Ref Type: Report

11. Health Canada . 2009. http://www.hc-sc.gc.ca/dhp-mps/prodnatur/legislation/docs/index-eng.php

12. Department of Justice Canada . 2009. http://laws.justice.gc.ca/en/ShowFullDoc/cr/SOR-2003-196///en

13. Health Canada . 2006. http://www.hc-sc.gc.ca/dhp-mps/prodnatur/faq/question_consum-consom-eng.php

14. Barnes,J., Anderson,L.A., & Phillipson,J.D. St John's wort (Hypericum perforatum L.): a review of its chemistry, pharmacology and clinical properties. *J. Pharm. Pharmacol.* **53**, 583-600 (2001).

15. Mannel,M. Drug interactions with St John's wort : mechanisms and clinical implications. *Drug Saf* **27**, 773-797 (2004).

16. Mueller,S.C., Majcher-Peszynska,J., Uehleke,B., Klammt,S., Mundkowski,R.G., Miekisch,W., Sievers,H., Bauer,S., Frank,B., Kundt,G., & Drewelow,B. The extent of induction of CYP3A by St. John's wort varies among products and is linked to hyperforin dose. *Eur. J. Clin. Pharmacol.* **62**, 29-36 (2006).

17. Spolarich,A.E. & Andrews,L. An examination of the bleeding complications associated with herbal supplements, antiplatelet and anticoagulant medications. *J. Dent. Hyg.* **81**, 67 (2007).

18. Yuan,C.S., Wei,G., Dey,L., Karrison,T., Nahlik,L., Maleckar,S., Kasza,K., Ang-Lee,M., & Moss,J. Brief communication: American ginseng reduces warfarin's effect in healthy patients: a randomized, controlled Trial. *Ann. Intern. Med.* **141**, 23-27 (2004).

19. Beckert,B.W., Concannon,M.J., Henry,S.L., Smith,D.S., & Puckett,C.L. The effect of herbal medicines on platelet function: an in vivo experiment and review of the literature. *Plast. Reconstr. Surg.* **120**, 2044-2050 (2007).

20. Goosen,T.C., Cillie,D., Bailey,D.G., Yu,C., He,K., Hollenberg,P.F., Woster,P.M., Cohen,L., Williams,J.A., Rheeders,M., & Dijkstra,H.P. Bergamottin contribution to the grapefruit juice-felodipine interaction and disposition in humans. *Clin. Pharmacol. Ther.* **76**, 607-617 (2004).

21. Liu,Y., Zhang,J.W., Li,W., Ma,H., Sun,J., Deng,M.C., & Yang,L. Ginsenoside metabolites, rather than naturally occurring ginsenosides, lead to inhibition of human cytochrome P450 enzymes. *Toxicol. Sci.* **91**, 356-364 (2006).

22. COLD-fX Website . 2008. http://www.cold-fx.ca/products-boost-immune-system.htm

23. Moss, G. P. Nomenclature of Lignans and Neolignans (IUPAC Recommendations 2000). Pure and Applied Chemistry 72[8], 1493-1523. 2000.

24. Lia,V.V., Confalonieri,V.A., Comas,C.I., & Hunziker,J.H. Molecular phylogeny of Larrea and its allies (Zygophyllaceae): reticulate evolution and the probable time of creosote bush arrival to North America. *Mol. Phylogenet. Evol.* **21**, 309-320 (2001).

25. Hyder,P.W., Fredrickson,E.L., Estell,R.E., Tellez,M., & Gibbens,R.P. Distribution and concentration of total phenolics, condensed tannins, and nordihydroguaiaretic acid (NDGA) in creosotebush (*Larrea tridentata)*. *Biochemical Systematics and Ecology* **30**, 912 (2002).

26. Downum,K.R., Dole,J., & Rodriguez,F. Nordihydroguaiaretic acid: inter- and intrapopulational variation in the Sonoran Desert Creosote Bush (Larrea Tridentata (Zygophyllaceae). *Biochemical Systematics and Ecology* **16**, 551-556 (1988).

27. Arteaga,S., Andrade-Cetto,A., & Cardenas,R. Larrea tridentata (Creosote bush), an abundant plant of Mexican and US-American deserts and its metabolite nordihydroguaiaretic acid. *J. Ethnopharmacol.* **98**, 231-239 (2005).

28. Vanharanta,M., Voutilainen,S., Lakka,T.A., van der,L.M., Adlercreutz,H., & Salonen,J.T. Risk of acute coronary events according to serum concentrations of enterolactone: a prospective population-based case-control study. *Lancet* **354**, 2112-2115 (1999).

29. Tyler,V.E. The Honest Herbal: A Sensible Guide to the Use of Herbs and Related Remedies. (The Haworth Press, Inc., Binghamton, NY; 1993).

30. Oliveto,E.P. Nordihydroguaiaretic Acid: A Naturally Occuring Antioxidant. *Chemistry and Industry* **2**, 677-679 (1972).

31. Grice,H.C., Becking,G., & Goodman,T. Toxic properties of nordihydroguaiaretic acid. *Food Cosmet. Toxicol.* **6**, 155-161 (1968).

32. Katz,M. & Saibil,F. Herbal hepatitis: subacute hepatic necrosis secondary to chaparral leaf. *J. Clin. Gastroenterol.* **12**, 203-206 (1990).

33. Gordon,D.W., Rosenthal,G., Hart,J., Sirota,R., & Baker,A.L. Chaparral ingestion. The broadening spectrum of liver injury caused by herbal medications. *JAMA* **273**, 489-490 (1995).

34. Koff,R.S. Herbal hepatotoxicity. Revisiting a dangerous alternative. *JAMA* **273**, 502 (1995).

35. Batchelor,W.B., Heathcote,J., & Wanless,I.R. Chaparral-induced hepatic injury. *Am. J. Gastroenterol.* **90**, 831-833 (1995).

36. Canadian Food Inspection Agency . 2005. 9-1-0008. http://www.inspection.gc.ca/english/corpaffr/recarapp/2005/20051222e.shtml

37. Herbs of Mexico . 2009. https://herbsofmexico.com/store/index.php?main_page=product_info&products_id=70

38. NZ Health.net . 2009. http://www.nzhealth.net.nz/herbs/chaparral.shtml

39. Rose Mountain Herbs . 2009. http://www.mountainroseherbs.com/learn/chaparral.php

40. All 4 Natural Health . 2009. http://www.all4naturalhealth.com/chaparral-herb.html

41. Lambert,J.D., Dorr,R.T., & Timmermann,B.N. Nordihydroguaiaretic Acid: A Review of Its Numerous and Varied Biological Activities. *Pharmaceutical Biology* **42**, 149-158 (2004).

42. Huang,R.C., Li,Y., Giza,P.E., Gnabre,J.N., Abd-Elazem,I.S., King,K.Y., & Hwu,J.R. Novel antiviral agent tetraglycylated nordihydroguaiaretic acid hydrochloride as a host-dependent viral inhibitor. *Antiviral Res.* **58**, 57-64 (2003).

43. Craigo,J., Callahan,M., Huang,R.C., & DeLucia,A.L. Inhibition of human papillomavirus type 16 gene expression by nordihydroguaiaretic acid plant lignan derivatives. *Antiviral Res.* **47**, 19-28 (2000).

44. Kent,U.M., Aviram,M., Rosenblat,M., & Hollenberg,P.F. The licorice root derived isoflavan glabridin inhibits the activities of human cytochrome P450S 3A4, 2B6, and 2C9. *Drug Metab Dispos.* **30**, 709-715 (2002).

45. Athar,M., Raza,H., Bickers,D.R., & Mukhtar,H. Inhibition of benzoyl peroxide-mediated tumor promotion in 7,12-dimethylbenz(a)anthracene-initiated skin of Sencar mice by antioxidants nordihydroguaiaretic acid and diallyl sulfide. *J. Invest Dermatol.* **94**, 162-165 (1990).

46. Nakadate,T., Yamamoto,S., Aizu,E., & Kato,R. Inhibition by lipoxygenase inhibitors of 7-bromomethylbenz[a]anthracene-caused epidermal ornithine decarboxylase induction and skin tumor promotion in mice. *Carcinogenesis* **10**, 2053-2057 (1989).

47. Olsen,E.A., Abernethy,M.L., Kulp-Shorten,C., Callen,J.P., Glazer,S.D., Huntley,A., McCray,M., Monroe,A.B., Tschen,E., & Wolf,J.E., Jr. A double-blind, vehicle-controlled study evaluating masoprocol cream in the treatment of actinic keratoses on the head and neck. *J. Am. Acad. Dermatol.* **24**, 738-743 (1991).

48. Epstein,E. Immunotherapy of warts with masoprocol cream. *Cutis* **59**, 287-289 (1997).

49. Morris,D.L. Essential nutrients and other functional compounds in flaxseed. *Nutrition Today* **36**, 159-162 (2001).

50. Flax Council of Canada . 2008. 10-1-0008. http://www.flaxcouncil.ca/english/index.php

51. Raffaelli,B., Hoikkala,A., Leppala,E., & Wahala,K. Enterolignans. *J. Chromatogr. B Analyt. Technol. Biomed. Life Sci.* **777**, 29-43 (2002).

52. Ford,J.D., Huang,K.S., Wang,H.B., Davin,L.B., & Lewis,N.G. Biosynthetic pathway to the cancer chemopreventive secoisolariciresinol diglucoside-hydroxymethyl glutaryl ester-linked lignan oligomers in flax (Linum usitatissimum) seed. *J. Nat. Prod.* **64**, 1388-1397 (2001).

53. Mazur,W., Fotsis,T., Wahala,K., Ojala,S., Salakka,A., & Adlercreutz,H. Isotope dilution gas chromatographic-mass spectrometric method for the determination of isoflavonoids, coumestrol, and lignans in food samples. *Anal. Biochem.* **233**, 169-180 (1996).

54. Rickard,S.E., Orcheson,L.J., Seidl,M.M., Luyengi,L., Fong,H.H., & Thompson,L.U. Dose-dependent production of mammalian lignans in rats and in vitro from the purified precursor secoisolariciresinol diglycoside in flaxseed. *J. Nutr.* **126**, 2012-2019 (1996).

55. Borriello,S.P., Setchell,K.D., Axelson,M., & Lawson,A.M. Production and metabolism of lignans by the human faecal flora. *J. Appl. Bacteriol.* **58**, 37-43 (1985).

56. Axelson,M., Sjovall,J., Gustafsson,B.E., & Setchell,K.D. Origin of lignans in mammals and identification of a precursor from plants. *Nature* **298**, 659-660 (1982).

57. Borriello,S.P., Setchell,K.D., Axelson,M., & Lawson,A.M. Production and metabolism of lignans by the human faecal flora. *J. Appl. Bacteriol.* **58**, 37-43 (1985).

58. Niemeyer,H.B., Honig,D.M., Kulling,S.E., & Metzler,M. Studies on the metabolism of the plant lignans secoisolariciresinol and matairesinol. *J. Agric. Food Chem.* **51**, 6317-6325 (2003).

59. Ford,J.D., Davin,L.B., & Lewis,N.G. Plant lignans and health: cancer chemoprevention and biotechnological opportunities. *Basic Life Sci.* **66**, 675-694 (1999).

60. Bakke,J.E. & Klosterman,H.J. A new diglucoside from flaxseed. *Proc. Natl. Acad. Sci. U. S. A* **10**, 18-22 (1956).

61. Charlet,S., Bensaddek,L., Raynaud,S., Gillet,F., Mesnard,F., & Fliniaux,M. An HPLC procedure for the quantification of anhydrosecoisolariciresinol. Application to the evaluation of flax lignan content. *Plant Physiology and Biochemistry* **40**, 225-229 (2002).

62. Liggins,J., Grimwood,R., & Bingham,S.A. Extraction and quantification of lignan phytoestrogens in food and human samples. *Anal. Biochem.* **287**, 102-109 (2000).

63. Nesbitt,P.D., Lam,Y., & Thompson,L.U. Human metabolism of mammalian lignan precursors in raw and processed flaxseed. *Am. J. Clin. Nutr.* **69**, 549-555 (1999).

64. Penalvo,J.L., Heinonen,S.M., Aura,A.M., & Adlercreutz,H. Dietary sesamin is converted to enterolactone in humans. *J. Nutr.* **135**, 1056-1062 (2005).

65. Heinonen,S., Nurmi,T., Liukkonen,K., Poutanen,K., Wahala,K., Deyama,T., Nishibe,S., & Adlercreutz,H. In vitro metabolism of plant lignans: new precursors of mammalian lignans enterolactone and enterodiol. *J. Agric. Food Chem.* **49**, 3178-3186 (2001).

66. Pietinen,P., Stumpf,K., Mannisto,S., Kataja,V., Uusitupa,M., & Adlercreutz,H. Serum enterolactone and risk of breast cancer: a case-control study in eastern Finland. *Cancer Epidemiol. Biomarkers Prev.* **10**, 339-344 (2001).

67. Ingram,D., Sanders,K., Kolybaba,M., & Lopez,D. Case-control study of phyto-oestrogens and breast cancer. *Lancet* **350**, 990-994 (1997).

68. Vanharanta,M., Voutilainen,S., Nurmi,T., Kaikkonen,J., Roberts,L.J., Morrow,J.D., Adlercreutz,H., & Salonen,J.T. Association between low serum enterolactone and increased plasma F2-isoprostanes, a measure of lipid peroxidation. *Atherosclerosis* **160**, 465-469 (2002).

69. Stattin,P., Adlercreutz,H., Tenkanen,L., Jellum,E., Lumme,S., Hallmans,G., Harvei,S., Teppo,L., Stumpf,K., Luostarinen,T., Lehtinen,M., Dillner,J., & Hakama,M. Circulating enterolactone and prostate cancer risk: a Nordic nested case-control study. *Int. J. Cancer* **99**, 124-129 (2002).

70. den,T., I, Keinan-Boker,L., Veer,P.V., Arts,C.J., Adlercreutz,H., Thijssen,J.H., & Peeters,P.H. Urinary phytoestrogens and postmenopausal breast cancer risk. *Cancer Epidemiol. Biomarkers Prev.* **10**, 223-228 (2001).

71. Sung,M.K., Lautens,M., & Thompson,L.U. Mammalian lignans inhibit the growth of estrogen-independent human colon tumor cells. *Anticancer Res.* **18**, 1405-1408 (1998).

72. Lin,X., Switzer,B.R., & Demark-Wahnefried,W. Effect of mammalian lignans on the growth of prostate cancer cell lines. *Anticancer Res.* **21**, 3995-3999 (2001).

73. Wang,C., Makela,T., Hase,T., Adlercreutz,H., & Kurzer,M.S. Lignans and flavonoids inhibit aromatase enzyme in human preadipocytes. *J. Steroid Biochem. Mol. Biol.* **50**, 205-212 (1994).

74. Welshons,W.V., Murphy,C.S., Koch,R., Calaf,G., & Jordan,V.C. Stimulation of breast cancer cells in vitro by the environmental estrogen enterolactone and the phytoestrogen equol. *Breast Cancer Res. Treat.* **10**, 169-175 (1987).

75. Prasad,K. Antioxidant Activity of Secoisolariciresinol Diglucoside-derived Metabolites, Secoisolariciresinol, Enterodiol, and Enterolactone. *Int. J. Angiol.* **9**, 220-225 (2000).

76. Neimeyer,H.B. & Metzler,M. Differences in the antioxidant activity of plant and mammalian lignans. *Journal of Food Engineering* **56**, 255-256 (2003).

77. Hu,C., Yuan,Y.V., & Kitts,D.D. Antioxidant activities of the flaxseed lignan secoisolariciresinol diglucoside, its aglycone secoisolariciresinol and the mammalian lignans enterodiol and enterolactone in vitro. *Food Chem. Toxicol.* **45**, 2219-2227 (2007).

78. Dean,B., Chang,S., Doss,G.A., King,C., & Thomas,P.E. Glucuronidation, oxidative metabolism, and bioactivation of enterolactone in rhesus monkeys. *Arch. Biochem. Biophys.* **429**, 244-251 (2004).

79. Jacobs,E. & Metzler,M. Oxidative metabolism of the mammalian lignans enterolactone and enterodiol by rat, pig, and human liver microsomes. *J. Agric. Food Chem.* **47**, 1071-1077 (1999).

80. Jacobs,E., Kulling,S.E., & Metzler,M. Novel metabolites of the mammalian lignans enterolactone and enterodiol in human urine. *J. Steroid Biochem. Mol. Biol.* **68**, 211-218 (1999).

81. Niemeyer,H.B., Honig,D., Lange-Bohmer,A., Jacobs,E., Kulling,S.E., & Metzler,M. Oxidative metabolites of the mammalian lignans enterodiol and enterolactone in rat bile and urine. *J. Agric. Food Chem.* **48**, 2910-2919 (2000).

82. Anderson,J.W., Johnstone,B.M., & Cook-Newell,M.E. Meta-analysis of the effects of soy protein intake on serum lipids. *N. Engl. J. Med.* **333**, 276-282 (1995).

83. Prasad,K., Mantha,S.V., Muir,A.D., & Westcott,N.D. Reduction of hypercholesterolemic atherosclerosis by CDC-flaxseed with very low alpha-linolenic acid. *Atherosclerosis* **136**, 367-375 (1998).

84. Arjmandi,B.H., Khan,D.A., Juma,S., Venkatesh,S., Sohn,E., Wei,L., & Derman,R. Whole flaxseed consumption lowers serum LDL-cholesterol and lipoprotein(a) concentrations in postmenopausal women. *Nutrition Research* **18**, 1203-1214 (1998).

85. Patade,A., Devareddy,L., Lucas,E.A., Korlagunta,K., Daggy,B.P., & Arjmandi,B.H. Flaxseed reduces total and LDL cholesterol concentrations in Native American postmenopausal women. *J. Womens Health (Larchmt.)* **17**, 355-366 (2008).

86. Stuglin,C. & Prasad,K. Effect of Flaxseed Consumption on Blood Pressure, Serum Lipids, Hemopoietic System and Liver and Kidney Enzymes in Healthy Humans. *Journal of Cardiovascular Pharmacology and Therapeutics* **10**, 23-27 (2005).

87. Prasad,K. Reduction of serum cholesterol and hypercholesterolemic atherosclerosis in rabbits by secoisolariciresinol diglucoside isolated from flaxseed. *Circulation* **99**, 1355-1362 (1999).

88. Jenkins,D.J., Kendall,C.W., Vidgen,E., Agarwal,S., Rao,A.V., Rosenberg,R.S., Diamandis,E.P., Novokmet,R., Mehling,C.C., Perera,T., Griffin,L.C., & Cunnane,S.C. Health aspects of partially defatted flaxseed, including effects on serum lipids, oxidative measures, and ex vivo androgen and progestin activity: a controlled crossover trial. *Am. J. Clin. Nutr.* **69**, 395-402 (1999).

89. Rhee,Y. & Brunt,A. Pilot study: Flaxseed Supplementation Was Effective in Lowering Serum Glucose and Triacylglycerol in Glucose Intolerant People. *Journal of the American Nutraceutical Association* **9**, 28-34 (2006).

90. Pan,A., Sun,J., Chen,Y., Ye,X., Li,H., Yu,Z., Wang,Y., Gu,W., Zhang,X., Chen,X., Demark-Wahnefried,W., Liu,Y., & Lin,X. Effects of a flaxseed-derived lignan supplement in type 2 diabetic patients: a randomized, double-blind, cross-over trial. *PLoS. ONE.* **2**, e1148 (2007).

91. Demark-Wahnefried,W., Robertson,C.N., Walther,P.J., Polascik,T.J., Paulson,D.F., & Vollmer,R.T. Pilot study to explore effects of low-fat, flaxseed-supplemented diet on proliferation of benign prostatic epithelium and prostate-specific antigen. *Urology* **63**, 900-904 (2004).

92. Hemmings,S.J., Westcott,N., Muir,A., & Czechowicz,D. The effects of dietary flaxseed on the Fischer 344 rat: II. Liver gamma-glutamyltranspeptidase activity. *Cell Biochem. Funct.* **22**, 225-231 (2004).

93. Pan,A., Sun,J., Chen,Y., Ye,X., Li,H., Yu,Z., Wang,Y., Gu,W., Zhang,X., Chen,X., Demark-Wahnefried,W., Liu,Y., & Lin,X. Effects of a flaxseed-derived lignan supplement in type 2 diabetic patients: a randomized, double-blind, cross-over trial. *PLoS. ONE.* **2**, e1148 (2007).

94. Zhang,W., Wang,X., Liu,Y., Tian,H., Flickinger,B., Empie,M.W., & Sun,S.Z. Dietary flaxseed lignan extract lowers plasma cholesterol and glucose concentrations in hypercholesterolaemic subjects. *Br. J. Nutr.* **99**, 1301-1309 (2008).

95. Brevail . 2008. http://www.brevail.com/index.html

96. Lundberg,W.O., Halvorson,H.O., & Burr,G.O. The Antioxidant Properties of Nordihydroguaiaretic Acid. *Oil and Soap* **21**, 33-35 (1944).

97. Ramasamy,S., Drummond,G.R., Ahn,J., Storek,M., Pohl,J., Parthasarathy,S., & Harrison,D.G. Modulation of expression of endothelial nitric oxide synthase by nordihydroguaiaretic acid, a phenolic antioxidant in cultured endothelial cells. *Mol. Pharmacol.* **56**, 116-123 (1999).

98. Goodman,T., Grice,H.C., Becking,G.C., & Salem,F.A. A cystic nephropathy induced by nordihydroguaiaretic acid in the rat. Light and electron microscopic investigations. *Lab Invest* **23**, 93-107 (1970).

99. Robison,T.W., Sevanian,A., & Forman,H.J. Inhibition of arachidonic acid release by nordihydroguaiaretic acid and its antioxidant action in rat alveolar macrophages and Chinese hamster lung fibroblasts. *Toxicol. Appl. Pharmacol.* **105**, 113-122 (1990).

100. Sahu,S.C., Ruggles,D.I., & O'Donnell,M.W. Prooxidant activity and toxicity of nordihydroguaiaretic acid in clone-9 rat hepatocyte cultures. *Food Chem. Toxicol.* **44**, 1751-1757 (2006).

101. Lambert,J.D., Zhao,D., Meyers,R.O., Kuester,R.K., Timmermann,B.N., & Dorr,R.T. Nordihydroguaiaretic acid: hepatotoxicity and detoxification in the mouse. *Toxicon* **40**, 1701-1708 (2002).

102. Agarwal,R., Wang,Z.Y., Bik,D.P., & Mukhtar,H. Nordihydroguaiaretic acid, an inhibitor of lipoxygenase, also inhibits cytochrome P-450-mediated monooxygenase activity in rat epidermal and hepatic microsomes. *Drug Metab Dispos.* **19**, 620-624 (1991).

103. Lewis,D.F.V. Guide to Cytochromes P450: Structure and Function. (Routledge, UK,2009).

104. Zamora,J.M., Mora,E.C., & Parish,E.J. A comparison of the cytotoxicity of nordihydroguaiaretic acid and its derivatives. *Journal of the Tennessee Academy of Science* **67**, 77-80 (1992).

105. Im,J.Y. & Han,P.L. Nordihydroguaiaretic acid induces astroglial death via glutathione depletion. *J. Neurosci. Res.* **85**, 3127-3134 (2007).

106. Clark,F. & Reed,R. Chaparral-Induced Toxic Hepatitis- California and Texas, 1992. *JAMA* **268**, 3295-3298 (1992).

107. Grant,K.L., Boyer,L.V., & Erdman,B.E. Case Report- Chaparral-Induced Hepatotoxicity. *Integrative Medicine* **1**, 83-87 (1998).

108. Biswal,S.S., Datta,K., Shaw,S.D., Feng,X., Robertson,J.D., & Kehrer,J.P. Glutathione oxidation and mitochondrial depolarization as mechanisms of nordihydroguaiaretic acid-induced apoptosis in lipoxygenase-deficient FL5.12 cells. *Toxicol. Sci.* **53**, 77-83 (2000).

109. Deshpande,V.S. & Kehrer,J.P. Oxidative stress-driven mechanisms of nordihydroguaiaretic acid-induced apoptosis in FL5.12 cells. *Toxicol. Appl. Pharmacol.* **214**, 230-236 (2006).

110. Culver,C.A., Michalowski,S.M., Maia,R.C., & Laster,S.M. The anti-apoptotic effects of nordihydroguaiaretic acid: inhibition of cPLA(2) activation during TNF-induced apoptosis arises from inhibition of calcium signaling. *Life Sci.* **77**, 2457-2470 (2005).

111. Zavodovskaya,M., Campbell,M.J., Maddux,B.A., Shiry,L., Allan,G., Hodges,L., Kushner,P., Kerner,J.A., Youngren,J.F., & Goldfine,I.D. Nordihydroguaiaretic acid (NDGA), an inhibitor of the HER2 and IGF-1 receptor tyrosine kinases, blocks the growth of HER2-overexpressing human breast cancer cells. *J. Cell Biochem.* **103**, 624-635 (2008).

112. Meyer,G.E., Chesler,L., Liu,D., Gable,K., Maddux,B.A., Goldenberg,D.D., Youngren,J.F., Goldfine,I.D., Weiss,W.A., Matthay,K.K., & Rosenthal,S.M. Nordihydroguaiaretic acid inhibits insulin-like growth factor signaling, growth, and survival in human neuroblastoma cells. *J. Cell Biochem.* **102**, 1529-1541 (2007).

113. Blecha,J.E., Anderson,M.O., Chow,J.M., Guevarra,C.C., Pender,C., Penaranda,C., Zavodovskaya,M., Youngren,J.F., & Berkman,C.E. Inhibition of IGF-1R and lipoxygenase by nordihydroguaiaretic acid (NDGA) analogs. *Bioorg. Med. Chem. Lett.* **17**, 4026-4029 (2007).

114. Tang,D.G., La,E., Kern,J., & Kehrer,J.P. Fatty acid oxidation and signaling in apoptosis. *Biol. Chem.* **383**, 425-442 (2002).

115. Tong,W.G., Ding,X.Z., & Adrian,T.E. The mechanisms of lipoxygenase inhibitor-induced apoptosis in human breast cancer cells. *Biochem. Biophys. Res. Commun.* **296**, 942-948 (2002).

116. Yu,Y.U., Kang,S.Y., Park,H.Y., Sung,S.H., Lee,E.J., Kim,S.Y., & Kim,Y.C. Antioxidant lignans from Machilus thunbergii protect CCl4-injured primary cultures of rat hepatocytes. *J Pharm. Pharmacol.* **52**, 1163-1169 (2000).

117. La,E., Kern,J.C., Atarod,E.B., & Kehrer,J.P. Fatty acid release and oxidation are factors in lipoxygenase inhibitor-induced apoptosis. *Toxicol. Lett.* **138**, 193-203 (2003).

118. Mikuni,M., Yoshida,M., Hellberg,P., Peterson,C.A., Edwin,S.S., Brannstrom,M., & Peterson,C.M. The lipoxygenase inhibitor, nordihydroguaiaretic acid, inhibits ovulation and reduces leukotriene and prostaglandin levels in the rat ovary. *Biol. Reprod.* **58**, 1211-1216 (1998).

119. Sinnott. Nontoxic Extract of Larrea Tridenta and Method of Making Same. 726686[5837252]. 1998.
Ref Type: Patent

120. Jordan, R. T. and Allen, L. M. Pharmacologically active compositions of catecholic butanes with zinc. [WO8801509], 1-143. 1988.
Ref Type: Patent

121. Wagner,P. & Lewis,R.A. Interaction between activated nordihydroguaiaretic acid and deoxyribonucleic acid. *Biochem. Pharmacol.* **29**, 3299-3306 (1980).

122. Boyle,M.A. Personal Nutrition. (Wadsworth/Thomson Learning,2001).

123. Wanasundara,P.K. & Shahidi,F. Process-induced compositional changes of flaxseed. *Adv. Exp. Med. Biol.* **434**, 307-325 (1998).

124. Cunnane,S.C., Ganguli,S., Menard,C., Liede,A.C., Hamadeh,M.J., Chen,Z.Y., Wolever,T.M., & Jenkins,D.J. High alpha-linolenic acid flaxseed (Linum usitatissimum): some nutritional properties in humans. *Br. J. Nutr.* **69**, 443-453 (1993).

125. Kulling,S.E., Jacobs,E., Pfeiffer,E., & Metzler,M. Studies on the genotoxicity of the mammalian lignans enterolactone and enterodiol and their metabolic precursors at various endpoints in vitro. *Mutat. Res.* **416**, 115-124 (1998).

126. Hemmings,S.J. & Barker,L. The effects of dietary flaxseed on the Fischer 344 rat: I. Development, behaviour, toxicity and the activity of liver gamma-glutamyltranspeptidase. *Cell Biochem. Funct.* **22**, 113-121 (2004).

127. Collins,T.F., Sprando,R.L., Black,T.N., Olejnik,N., Wiesenfeld,P.W., Babu,U.S., Bryant,M., Flynn,T.J., & Ruggles,D.I. Effects of flaxseed and defatted flaxseed meal on reproduction and development in rats. *Food Chem. Toxicol.* **41**, 819-834 (2003).

128. Monks,T.J., Hanzlik,R.P., Cohen,G.M., Ross,D., & Graham,D.G. Quinone chemistry and toxicity. *Toxicol. Appl. Pharmacol.* **112**, 2-16 (1992).

129. Bolton,J.L., Acay,N.M., & Vukomanovic,V. Evidence that 4-allyl-o-quinones spontaneously rearrange to their more electrophilic quinone methides: potential bioactivation mechanism for the hepatocarcinogen safrole. *Chem. Res. Toxicol.* **7**, 443-450 (1994).

130. Iverson,S.L., Hu,L.Q., Vukomanovic,V., & Bolton,J.L. The influence of the p-alkyl substituent on the isomerization of o- quinones to p-quinone methides: potential bioactivation mechanism for catechols. *Chem. Res. Toxicol.* **8**, 537-544 (1995).

131. Thompson,D.C., Thompson,J.A., Sugumaran,M., & Moldeus,P. Biological and toxicological consequences of quinone methide formation. *Chem Biol. Interact.* **86**, 129-162 (1993).

132. Moridani,M.Y., Cheon,S.S., Khan,S., & O'Brien,P.J. Metabolic activation of 3-hydroxyanisole by isolated rat hepatocytes. *Chem Biol Interact.* **142**, 317-333 (2003).

133. Bolton,J.L., Wu,H.M., & Hu,L.Q. Mechanism of isomerization of 4-propyl-o-quinone to its tautomeric p- quinone methide. *Chem. Res. Toxicol.* **9**, 109-113 (1996).

134. Powis,G. Metabolism and reactions of quinoid anticancer agents. *Pharmacol. Ther.* **35**, 57-162 (1987).

135. Zhang,Y., Gaikwad,N.W., Olson,K., Zahid,M., Cavalieri,E.L., & Rogan,E.G. Cytochrome P450 isoforms catalyze formation of catechol estrogen quinones that react with DNA. *Metabolism* **56**, 887-894 (2007).

136. Tajima,K., Yamamoto,K., & Mizutani,T. Formation of a glutathione conjugate from butylated hydroxytoluene by rat liver microsomes. *Biochem. Pharmacol.* **34**, 2109-2114 (1985).

137. Thompson,D., Constantin-Teodosiu,D., Egestad,B., Mickos,H., & Moldeus,P. Formation of glutathione conjugates during oxidation of eugenol by microsomal fractions of rat liver and lung. *Biochem. Pharmacol.* **39**, 1587-1595 (1990).

138. Williams,D.A. & Lemke,T.L. Foye's Principles of Medicinal Chemistry. (Lippincott Williams & Wilkins,2002).

139. Miller,E.C. & Miller,J.A. The Presence and Significance of Bound Aminoazo Dyes in the Livers of Rats Fed p-Dimethylaminoazobenzene. *Cancer Research* 468-480 (1947).

140. Mitchell,J.R., Jollow,D.J., Potter,W.Z., Davis,D.C., Gillette,J.R., & Brodie,B.B. Acetaminophen-induced hepatic necrosis. I. Role of drug metabolism. *J. Pharmacol. Exp. Ther.* **187**, 185-194 (1973).

141. Masubuchi,N., Makino,C., & Murayama,N. Prediction of in vivo potential for metabolic activation of drugs into chemically reactive intermediate: correlation of in vitro and in vivo generation of reactive intermediates and in vitro glutathione conjugate formation in rats and humans. *Chem. Res. Toxicol.* **20**, 455-464 (2007).

142. Fowler,S. & Zhang,H. In vitro evaluation of reversible and irreversible cytochrome P450 inhibition: current status on methodologies and their utility for predicting drug-drug interactions. *AAPS. J.* **10**, 410-424 (2008).

143. Stresser,D.M., Blanchard,A.P., Turner,S.D., Erve,J.C., Dandeneau,A.A., Miller,V.P., & Crespi,C.L. Substrate-dependent modulation of CYP3A4 catalytic activity: analysis of 27 test compounds with four fluorometric substrates. *Drug Metab Dispos.* **28**, 1440-1448 (2000).

144. Kalgutkar,A.S., Obach,R.S., & Maurer,T.S. Mechanism-based inactivation of cytochrome P450 enzymes: chemical mechanisms, structure-activity relationships and relationship to clinical drug-drug interactions and idiosyncratic adverse drug reactions. *Curr. Drug Metab* **8**, 407-447 (2007).

145. Lin,J.H. & Lu,A.Y. Inhibition and induction of cytochrome P450 and the clinical implications. *Clin. Pharmacokinet.* **35**, 361-390 (1998).

146. Masubuchi,Y. & Horie,T. Toxicological significance of mechanism-based inactivation of cytochrome p450 enzymes by drugs. *Crit Rev. Toxicol.* **37**, 389-412 (2007).

147. Zhang,Z.Y. & Wong,Y.N. Enzyme kinetics for clinically relevant CYP inhibition. *Curr. Drug Metab* **6**, 241-257 (2005).

148. Shou,M., Lin,Y., Lu,P., Tang,C., Mei,Q., Cui,D., Tang,W., Ngui,J.S., Lin,C.C., Singh,R., Wong,B.K., Yergey,J.A., Lin,J.H., Pearson,P.G., Baillie,T.A., Rodrigues,A.D., & Rushmore,T.H. Enzyme kinetics of cytochrome P450-mediated reactions. *Curr. Drug Metab* **2**, 17-36 (2001).

149. He,K., Iyer,K.R., Hayes,R.N., Sinz,M.W., Woolf,T.F., & Hollenberg,P.F. Inactivation of cytochrome P450 3A4 by bergamottin, a component of grapefruit juice. *Chem. Res. Toxicol.* **11**, 252-259 (1998).

150. Usia,T., Watabe,T., Kadota,S., & Tezuka,Y. Metabolite-cytochrome P450 complex formation by methylenedioxyphenyl lignans of Piper cubeba: mechanism-based inhibition. *Life Sci.* **76**, 2381-2391 (2005).

151. Surh,Y.J. & Lee,S.S. Capsaicin, a double-edged sword: toxicity, metabolism, and chemopreventive potential. *Life Sci.* **56**, 1845-1855 (1995).

152. Johnson,B.M., Qiu,S.X., Zhang,S., Zhang,F., Burdette,J.E., Yu,L., Bolton,J.L., & van Breemen,R.B. Identification of novel electrophilic metabolites of piper methysticum Forst (Kava). *Chem. Res. Toxicol.* **16**, 733-740 (2003).

153. Dietz,B. & Bolton,J.L. Botanical dietary supplements gone bad. *Chem. Res. Toxicol.* **20**, 586-590 (2007).

154. Kupiec,T. & Raj,V. Fatal seizures due to potential herb-drug interactions with Ginkgo biloba. *J. Anal. Toxicol.* **29**, 755-758 (2005).

155. Evans,D.C., Watt,A.P., Nicoll-Griffith,D.A., & Baillie,T.A. Drug-protein adducts: an industry perspective on minimizing the potential for drug bioactivation in drug discovery and development. *Chem. Res. Toxicol.* **17**, 3-16 (2004).

156. Akiyama,K., Maruyama,M., Yamauchi,S., Nakashima,Y., Nakato,T., Tago,R., Sugahara,T., Kishida,T., & Koba,Y. Antimicrobiological activity of lignan: effect of benzylic oxygen and stereochemistry of 2,3-dibenzyl-4-butanolide and 3,4-dibenzyltetrahydrofuran lignans on activity. *Biosci. Biotechnol. Biochem.* **71**, 1745-1751 (2007).

157. Fujisawa,S., Atsumi,T., Kadoma,Y., & Sakagami,H. Antioxidant and prooxidant action of eugenol-related compounds and their cytotoxicity. *Toxicology* **177**, 39-54 (2002).

158. Moridani,M.Y., Siraki,A., Chevaldina,T., Scobie,H., & O'Brien,P.J. Quantitative structure toxicity relationships for catechols in isolated rat hepatocytes. *Chem. Biol. Interact.* **147**, 297-307 (2004).

159. Iba,M.M., Soyka,L.F., & Schulman,M.P. Characteristics of the liver microsomal drug-metabolizing enzyme system of newborn rats. *Mol. Pharmacol.* **13**, 1092-1104 (1977).

160. Lowry,O.H., Rosebrough,N.J., Farr,A.L., & Randall,R.J. Protein measurement with the Folin phenol reagent. *J. Biol. Chem.* **193**, 265-275 (1951).

161. Billinsky,J.L., Marcoux,M.R., & Krol,E.S. Oxidation of the lignan nordihydroguaiaretic acid. *Chem. Res. Toxicol.* **20**, 1352-1358 (2007).

162. Moore,M. Medicinal Plants of the Desert and Canyon West. (Museum of New Mexico Press, Sante Fe, New Mexico; 1989).

163. Billinsky,J.L. & Krol,E.S. Nordihydroguaiaretic acid autoxidation produces a schisandrin-like dibenzocyclooctadiene lignan. *J. Nat. Prod.* **71**, 1612-1615 (2008).

164. Hallund,J., Tetens,I., Bugel,S., Tholstrup,T., & Bruun,J.M. The effect of a lignan complex isolated from flaxseed on inflammation markers in healthy postmenopausal women. *Nutr. Metab Cardiovasc. Dis.* **18**, 497-502 (2008).

165. Felmlee,M.A., Woo,G., Simko,E., Krol,E.S., Muir,A.D., & Alcorn,J. Effects of the flaxseed lignans secoisolariciresinol diglucoside and its aglycone on serum and hepatic lipids in hyperlipidaemic rats. *Br. J. Nutr.* 1-9 (2009).

166. Vuppugalla,R. & Mehvar,R. Enzyme-selective effects of nitric oxide on affinity and maximum velocity of various rat cytochromes P450. *Drug Metab Dispos.* **33**, 829-836 (2005).

167. Elbarbry,F.A., McNamara,P.J., & Alcorn,J. Ontogeny of hepatic CYP1A2 and CYP2E1 expression in rat. *J. Biochem. Mol. Toxicol.* **21**, 41-50 (2007).

168. Pfeiffer,E. & Metzler,M. Effect of bisphenol A on drug metabolising enzymes in rat hepatic microsomes and precision-cut rat liver slices. *Arch. Toxicol.* **78**, 369-377 (2004).

169. Hu,C., Yuan,Y.V., & Kitts,D.D. Antioxidant activities of the flaxseed lignan secoisolariciresinol diglucoside, its aglycone secoisolariciresinol and the mammalian lignans enterodiol and enterolactone in vitro. *Food Chem. Toxicol.* **45**, 2219-2227 (2007).

170. Folk,J.E., Wolff,E.C., Schirmer,E.W., & Ornfield,J. The kinetics of carboxypeptidase B activity. III. Effects of alcohol on the peptidase and esterase activities; kinetic models. *J. Biol. Chem.* **237**, 3105-3109 (1962).

171. Atkins,W.M. Non-Michaelis-Menten kinetics in cytochrome P450-catalyzed reactions. *Annu. Rev. Pharmacol. Toxicol.* **45**, 291-310 (2005).

172. Zhou,S., Koh,H.L., Gao,Y., Gong,Z.Y., & Lee,E.J. Herbal bioactivation: the good, the bad and the ugly. *Life Sci.* **74**, 935-968 (2004).

173. Chichirau,A., Flueraru,M., Chepelev,L.L., Wright,J.S., Willmore,W.G., Durst,T., Hussain,H.H., & Charron,M. Mechanism of cytotoxicity of catechols and a naphthalenediol in PC12-AC cells: the connection between extracellular autoxidation and molecular electronic structure. *Free Radic. Biol. Med.* **38**, 344-355 (2005).

174. O'Brien,P.J. Molecular mechanisms of quinone cytotoxicity. *Chem. Biol. Interact.* **80**, 1-41 (1991).

175. Lasker,J.M., Huang,M.T., & Conney,A.H. In vitro and in vivo activation of oxidative drug metabolism by flavonoids. *J. Pharmacol. Exp. Ther.* **229**, 162-170 (1984).

176. Houston,J.B. & Kenworthy,K.E. In vitro-in vivo scaling of CYP kinetic data not consistent with the classical Michaelis-Menten model. *Drug Metab Dispos.* **28**, 246-254 (2000).

177. Kuijsten,A., Arts,I.C., Vree,T.B., & Hollman,P.C. Pharmacokinetics of enterolignans in healthy men and women consuming a single dose of secoisolariciresinol diglucoside. *J. Nutr.* **135**, 795-801 (2005).

178. Thompson,L.U., Robb,P., Serraino,M., & Cheung,F. Mammalian lignan production from various foods. *Nutr. Cancer* **16**, 43-52 (1991).

179. Awad,H.M., Boersma,M.G., Boeren,S., van Bladeren,P.J., Vervoort,J., & Rietjens,I.M. The regioselectivity of glutathione adduct formation with flavonoid quinone/quinone methides is pH-dependent. *Chem. Res. Toxicol.* **15**, 343-351 (2002).

180. Bambagiotti-Alberti,M., Coran,S.A., Ghiara,C., Giannellini,V., & Raffaelli,A. Revealing the mammalian lignan precursor secoisolariciresinol diglucoside in flax seed by ionspray mass spectrometry. *Rapid Commun. Mass Spectrom.* **8**, 595-598 (1994).

181. Bjornsson,T.D., Callaghan,J.T., Einolf,H.J., Fischer,V., Gan,L., Grimm,S., Kao,J., King,S.P., Miwa,G., Ni,L., Kumar,G., McLeod,J., Obach,R.S., Roberts,S., Roe,A., Shah,A., Snikeris,F., Sullivan,J.T., Tweedie,D., Vega,J.M., Walsh,J., & Wrighton,S.A. The conduct of in vitro and in vivo drug-drug interaction studies: a Pharmaceutical Research and Manufacturers of America (PhRMA) perspective. *Drug Metab Dispos.* **31**, 815-832 (2003).

182. Axelson,M. & Setchell,K.D. Conjugation of lignans in human urine. *FEBS Lett.* **122**, 49-53 (1980).

183. Dean,B., Chang,S., Doss,G.A., King,C., & Thomas,P.E. Glucuronidation, oxidative metabolism, and bioactivation of enterolactone in rhesus monkeys. *Arch. Biochem. Biophys.* **429**, 244-251 (2004).

184. Yasumoto,K., Yamamoto,A., & Mitsuda,H. Studies on Soybean Lipoxygenase. 4. Effect of Phenolic Antioxidants on Lipoxygenase Reaction. *Agricultural and biological chemistry* **34**, 1162-1168 (1970).

APPENDIX A – Supplementary figures for "A Comparison Between Lignans From Creosote Bush and Flaxseed and Their Potential to Inhibit Cytochrome P450 Enzyme Activity"

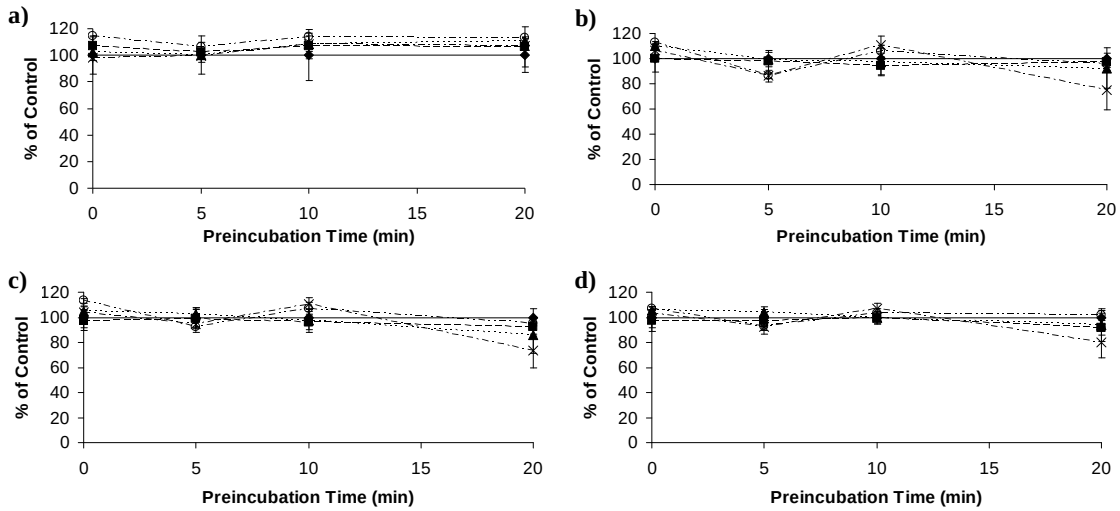

Figure A1: Cytochrome P450 enzyme activity (as percent of control) as a function of Secoisolariciresinol diglucoside (SDG) concentration and pre-incubation time. a) CYP1A2, b) CYP3A, c) CYP2B/2C11 and d) CYP2C11. Secoisolariciresinol diglucoside (closed diamond = 0 µM; closed square = 100 µM; closed triangle = 250 µM; symbol 'x' = 500 µM; open circle = 2000 µM) was pre-incubated in pooled male rat hepatic microsomes (n=4) for different time periods. At the end of each pre-incubation period, testosterone (250 µM) and methoxyresorufin (0.5 µM) was added and metabolite formation was determined after a 15 min and 8 min reaction time, respectively. Each point is the mean of 3 replicates ± percent coefficient of variation.

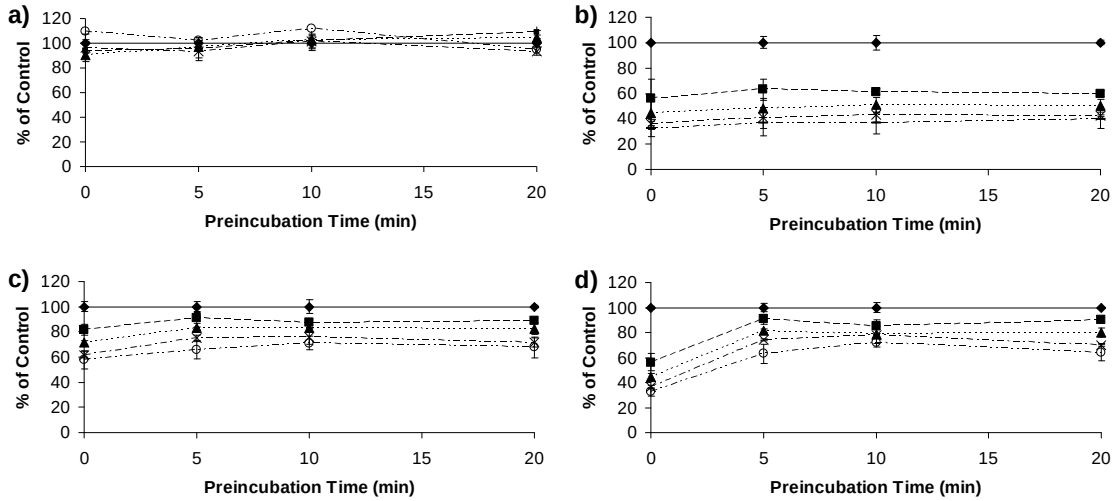

Figure A2: Cytochrome P450 enzyme activity (as percent of control) as a function of Secoisolariciresinol (SECO) concentration and pre-incubation time. a) CYP1A2, b) CYP3A, c) CYP2B/2C11 and d) CYP2C11. Secoisolariciresinol (closed diamond = 0 µM; closed square = 500 µM; closed triangle = 1000 µM; symbol 'x' = 1500 µM; open circle = 2000 µM) was pre-incubated in pooled male rat hepatic microsomes (n=4) for different time periods. At the end of each pre-incubation period, testosterone (250 µM) and methoxyresorufin (0.5 µM) was added and metabolite formation was determined after a 15 min and 8 min reaction time, respectively. Each point is the mean of 3 replicates ± percent coefficient of variation.

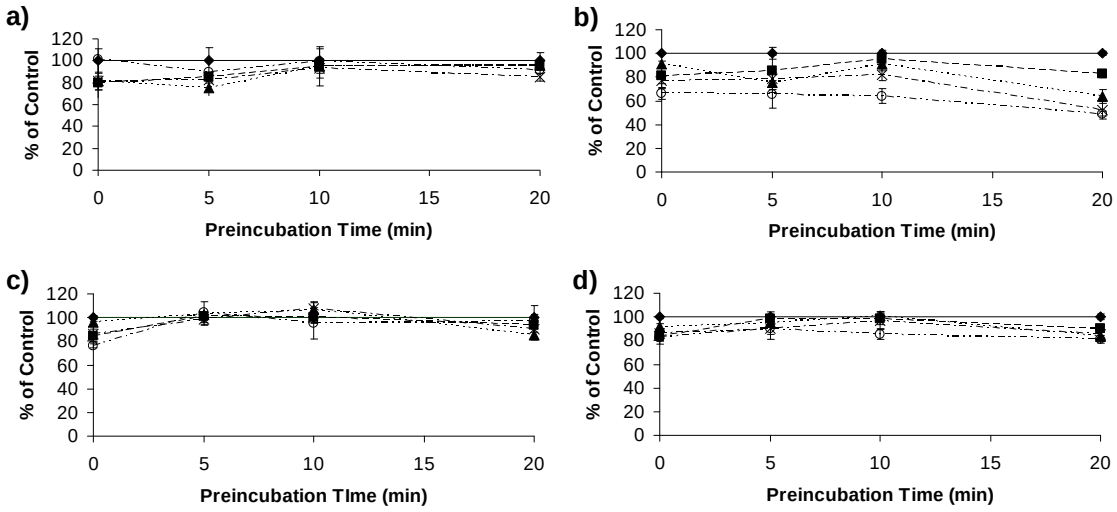

Figure A3: Cytochrome P450 enzyme activity (as percent of control) as a function of Anhydrosecoisolariciresinol (ASECO) concentration and pre-incubation time. a) CYP1A2, b) CYP3A, c) CYP2B/2C11 and d) CYP2C11. Anhydrosecoisolariciresinol (closed diamond = 0 µM; closed square = 1 µM; closed triangle = 10 µM; symbol 'x' = 50 µM; open circle = 100 µM) was pre-incubated in pooled male rat hepatic microsomes (n=4) for different time periods. At the end of each pre-incubation period, testosterone (250 µM) and methoxyresorufin (0.5 µM) was added and metabolite formation was determined after a 15 min and 8 min reaction time, respectively. Each point is the mean of 3 replicates ± percent coefficient of variation.

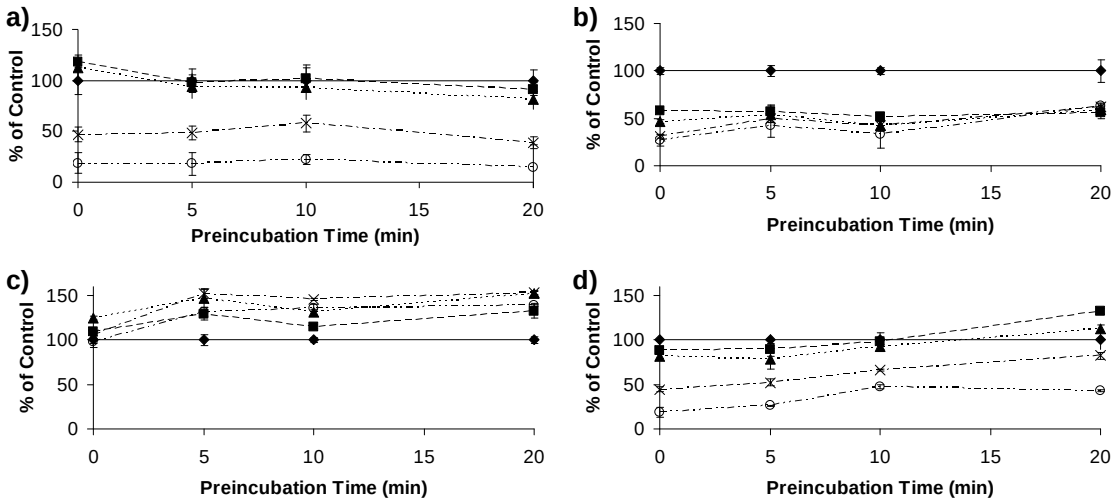

Figure A4: Cytochrome P450 enzyme activity (as percent of control) as a function of Enterolactone (EL) concentration and pre-incubation time. a) CYP1A2, b) CYP3A, c) CYP2B/2C11 and d) CYP2C11. Enterolactone (closed diamond = 0 μM; closed square = 50 μM; closed triangle = 100 μM; symbol 'x' = 250 μM; open circle = 500 μM) was pre-incubated in pooled male rat hepatic microsomes (n=4) for different time periods. At the end of each pre-incubation period, testosterone (50 μM) and methoxyresorufin (0.5 μM) was added and metabolite formation was determined after a 15 min and 8 min reaction time, respectively. Each point is the mean of 3 replicates ± percent coefficient of variation.

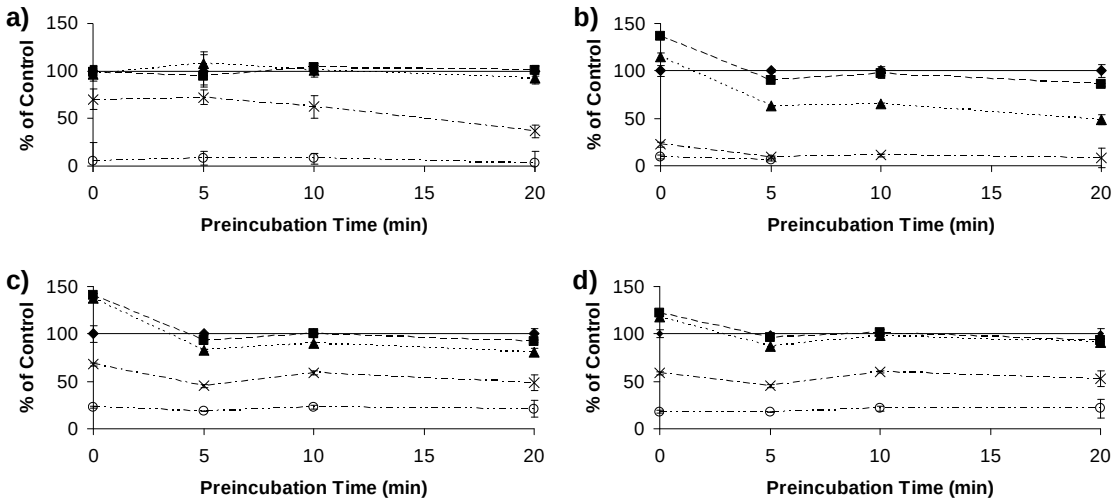

Figure A5: Cytochrome P450 enzyme activity (as percent of control) as a function of Nordihydroguaiaretic acid (NDGA) concentration and pre-incubation time. a) CYP1A2, b) CYP3A, c) CYP2B/2C11 and d) CYP2C11. Nordihydroguaiaretic acid (closed diamond = 0 μM; closed square = 1 μM; closed triangle = 10 μM; symbol 'x' = 100 μM; open circle = 200 μM) was pre-incubated in pooled male rat hepatic microsomes (n=4) for different time periods. At the end of each pre-incubation period, testosterone (250 μM) and methoxyresorufin (0.5 μM) was added and metabolite formation was determined after a 15 min and 8 min reaction time, respectively. Each point is the mean of 3 replicates ± percent coefficient of variation.

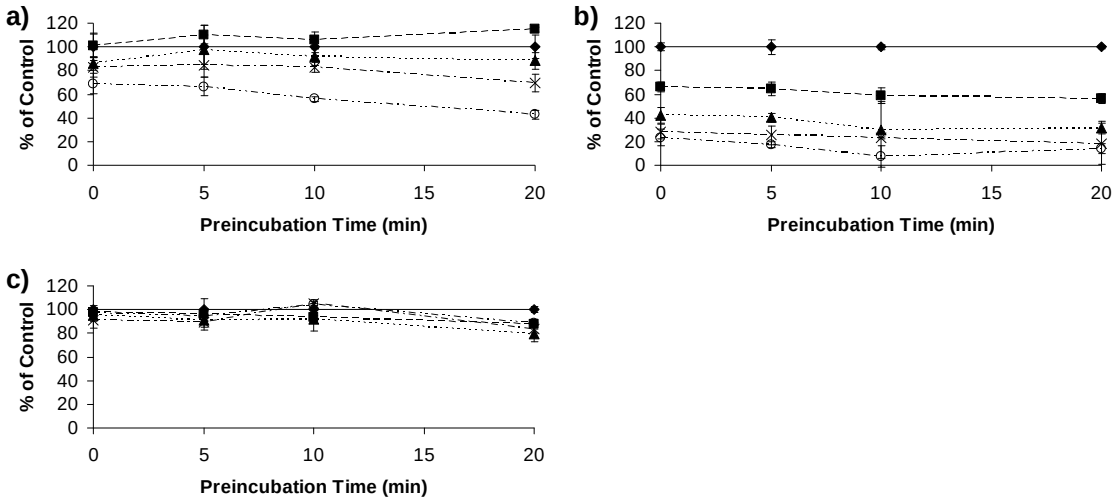

Figure A6: Cytochrome P450 enzyme activity (as percent of control) as a function of Dibenzocyclooctadiene concentration and pre-incubation time. a) CYP1A2, b) CYP3A and CYP2B/2C11. Dibenzocyclooctadiene (closed diamond = 0 µM; closed square = 25 µM; closed triangle = 50 µM; symbol 'x' = 75 µM; open circle = 100 µM) was pre-incubated in pooled male rat hepatic microsomes (n=4) for different time periods. At the end of each pre-incubation period, testosterone (50 µM) and methoxyresorufin (0.5 µM) was added and metabolite formation was determined after a 15 min and 8 min reaction time, respectively. Each point is the mean of 3 replicates ± percent coefficient of variation.

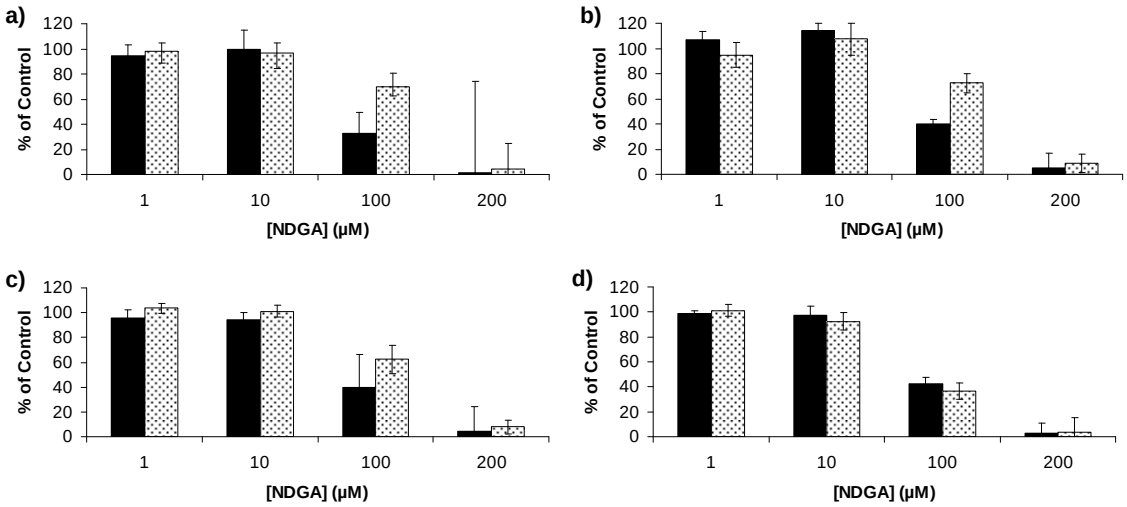

Figure A7: CYP1A2 enzyme activity (as percent of control) as a function of Nordihydroguaiaretic acid (NDGA) concentration in the presence of glutathione performed at various pre-incubation times. a) 0 min, b) 5 min, c) 10 min and d) 20 min. Nordihydroguaiaretic acid (solid bar) or Nordihydroguaiaretic acid and 500 µM glutathione (stipled bar) was pre-incubated in pooled male rat hepatic microsomes (n=4) for different time periods. Glutathione was present before initiation of the reaction. At the end of each pre-incubation period methoxyresorufin (0.5 µM) was added and metabolite formation was determined after an 8 min reaction time. Each point is the mean of 3 replicates ± percent coefficient of variation.

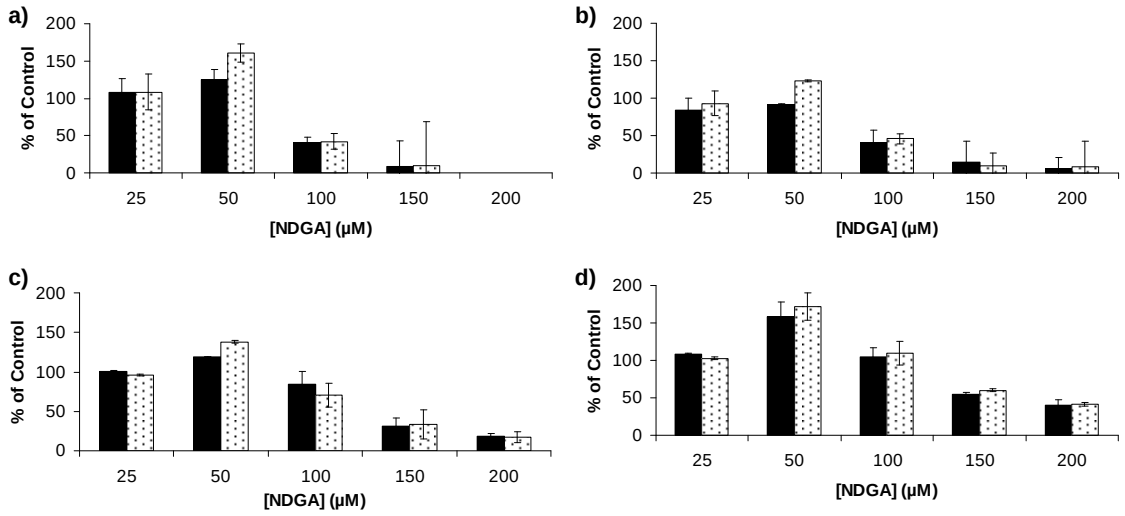

Figure A8: Nordihydroguaiaretic acid (NDGA) concentration dependent inhibition of CYP1A2 in the presence (solid bar) and absence (stipled bar) of 500 µM glutathione using methoxyresorufin as the probe substrate in incubation reactions (8 min) with pooled (n=4) male, rat liver microsomes. Graphs represent methoxyresorufin concentrations of: a) 0.25 µM, b) 0.5 µM, c) 1.0 µM and d) 2.5 µM. Each point represents the mean of 3 replicates ± percent coefficient of variation.

APPENDIX B – Permissions to use previously published papers from Chapters 4 and 5

AMERICAN CHEMICAL SOCIETY LICENSE
TERMS AND CONDITIONS
Sep 04, 2009

This is a License Agreement between Jennifer L Billinsky ("You") and American Chemical Society ("American Chemical Society") provided by Copyright Clearance Center ("CCC"). The license consists of your order details, the terms and conditions provided by American Chemical Society, and the payment terms and conditions.

All payments must be made in full to CCC. For payment instructions, please see information listed at the bottom of this form.

License Number	2262180290441
License Date	Sep 04, 2009
Licensed content publisher	American Chemical Society
Licensed content publication	Chemical Research in Toxicology
Licensed content title	Oxidation of the Lignan Nordihydroguaiaretic Acid
Licensed content author	Jennifer L. Billinsky et al.
Licensed content date	Sep 1, 2007
Volume number	20
Issue number	9
Type of Use	Thesis/Dissertation
Requestor type	Not specified
Format	Print
Portion	Full article
Author of this ACS article	Yes
Order reference number	
Title of the thesis / dissertation	Oxidative Metabolism and Cytochrome P450 Enzyme Inhibition Potential of Creosote Bush and Flaxseed Lignans
Expected completion date	Sep 2009
Estimated size(pages)	127

Billing Type	Invoice
Billing Address	430 Stone Court Saskatoon, SK S7M 4J2 Canada
Customer reference info	
Total	0.00 USD

Terms and Conditions

AMERICAN CHEMICAL SOCIETY LICENSE TERMS AND CONDITIONS

Sep 04, 2009

This is a License Agreement between Jennifer L Billinsky ("You") and American Chemical Society ("American Chemical Society") provided by Copyright Clearance Center ("CCC"). The license consists of your order details, the terms and conditions provided by American Chemical Society, and the payment terms and conditions.

All payments must be made in full to CCC. For payment instructions, please see information listed at the bottom of this form.

License Number	2262180501751
License Date	Sep 04, 2009
Licensed content publisher	American Chemical Society
Licensed content publication	Journal of Natural Products
Licensed content title	Nordihydroguaiaretic Acid Autoxidation Produces a Schisandrin-like Dibenzocyclooctadiene Lignan
Licensed content author	Jennifer L. Billinsky et al.
Licensed content date	Sep 1, 2008
Volume number	71
Issue number	9
Type of Use	Thesis/Dissertation
Requestor type	Not specified
Format	Print
Portion	Full article
Author of this ACS article	Yes
Order reference number	
Title of the thesis / dissertation	Oxidative Metabolism and Cytochrome P450 Enzyme Inhibition Potential of Creosote Bush and Flaxseed Lignans

Expected completion date	Sep 2009
Estimated size(pages)	127
Billing Type	Invoice
Billing Address	430 Stone Court Saskatoon, SK S7M 4J2 Canada
Customer reference info	
Total	0.00 USD